

ACTIVE SOUND QUALITY CONTROL: DESIGN TOOLS AND AUTOMOTIVE APPLICATIONS

Promotoren:
Prof. dr. ir. Paul Sas
Prof. dr. ir. W. Desmet

Proefschrift voorgedragen tot
het behalen van het doctoraat
in de ingenieurswetenschappen

door

**Leopoldo Pisanelli Rodrigues
DE OLIVEIRA**

2009D07

July 2009



KATHOLIEKE UNIVERSITEIT LEUVEN
FACULTEIT INGENIEURSWETENSCHAPPEN
DEPARTEMENT WERKTUIGKUNDE
AFDELING PRODUCTIETECHNIEKEN,
MACHINEBOUW EN AUTOMATISERING
Celestijnenlaan 300B, 3001 Heverlee (Leuven), Belgium

ACTIVE SOUND QUALITY CONTROL: DESIGN TOOLS AND AUTOMOTIVE APPLICATIONS

Jury:
Prof. dr. ir. Dirk Vandermeulen (voorzitter)
Prof. dr. ir. Paul Sas
Prof. dr. ir. Wim Desmet
Prof. dr. ir. Jan Swevers
Prof. dr. ir. Gerrit Vermeir
dr. ir. Herman Van der Auweraer (LMS Intl.)
Prof. dr. ir. Bert Roozen (TU Eindhoven)
Prof. Tit. Paulo S. Varoto (EESC-USP)

Proefschrift voorgedragen tot
het behalen van het doctoraat
in de ingenieurswetenschappen
door

**Leopoldo Pisanelli Rodrigues
DE OLIVEIRA**

ISBN 978-94-6018-064-4
D/2009/7515/47
UDC 534.83

July 2009

© Katholieke Universiteit Leuven
Faculteit Toegepaste Wetenschappen
Arenbergkasteel, B-3001 Heverlee (Leuven), Belgium

Alle rechten voorbehouden. Niets uit deze uitgave mag worden verveelvoudigd en/of openbaar gemaakt worden door middel van druk, fotokopie, microfilm, elektronisch of op welke andere wijze ook zonder voorafgaandelijke schriftelijke toestemming van de uitgever.

All rights reserved. No part of this publication may be reproduced in any form, by print, photoprint, microfilm or any other means without written permission from the publisher.

D/2009/7515/47
ISBN 978-94-6018-064-4
UDC 534.83

Preface

Living in Belgium for four and half years has been a life-changing experience, but to highlight the special moments and acknowledge everyone, you should allow me to go back to January 2002: Maíra had just graduated and I was half way on my Masters, when she got the opportunity to go for a 6-month internship at Daimler in Stuttgart. That would be the longest we stayed apart. However, a certain conference seemed the ideal excuse for me to visit her in Germany and get to know the venue of ISMA. I was so happy when the paper was accepted and I got the go ahead to go to Europe for the first time. We both went to ISMA2002, unaware that Leuven would be our home for four and a half years! That year, in Leuven, there were about ten Brazilians, among which Prof. Rogerio Pirk, who I have to thank for introducing me to the conference chairman, Prof. Paul Sas, who took some of his time during the conference, to talk to me and my Brazilian promoter Prof. Paulo Varoto about me going for a PhD in Leuven.

Things were just great, Maíra was coming back to Brazil, I was wrapping up my dissertation and, naturally, applying for a Brazilian scholarship to start my PhD in Leuven by mid-2003. Only thing thou, the assessor from CNPq did not think that was a good plan and denied my proposal. Determined to stay in the academia, I started my doctoral program in the Engineering School of São Carlos, the same faculty where I graduated as a Mechanical Engineer and got my MSc, under the same promoter, Prof. Varoto, with whom I had been working for more than five years back then, and who I thank for all these years of guidance and support. Varoto introduced me to the word of Vibration Testing and Modal Analysis, he involved me not only in work directly related to my research track, but basically with everything that was going on in the Dynamics Lab. at that time; I had the chance to test from steel beams to aircraft wings, from hermetic compressors to truck

chassis and civil structures, and for that I have to thank him a lot. He also made it possible for me to come to my first international conference, IMAC 2001, where we met Prof. Sas who gave us a CD with some ISMA proceedings, actually starting this whole process!

Eventually, thanks to a bilateral agreement firmed between the University of São Paulo, my home university, and the Katholieke Universiteit Leuven, I could apply again for a full PhD in Leuven. The first round was held in USP, to select the pre-candidates that would, in time, be evaluated by the International Office of the K.U.Leuven. At this point, I would like to thank Prof. Maria do Carmo Calijuri, Dean of EESC-USP, who handed in person my registration for the Brazilian round, making sure it was accepted in due time. Also thanks to Mrs Deisemara N. da Silva from the International Relations Office - USP. My special thanks go to the International Office staff of the K.U.Leuven, in particular to Prof. Paul De Boeck, Mrs Marie-Thérèse Deloddere, Mrs Hilde Nijs, Mr Edmundo Guzman and Mr Robert Geivers. Thank you all for the effort you put on keeping and improving this program, and for granting me the scholarship which made it possible to pursue this dream.

When arriving in Leuven we were faced with the challenge of finding decent and affordable residence in late Spetember. Thanks to Mrs Joske Vettenburg, now retired, we ended up having the unique experience of living very close to a lovely couple, older than us in age, but younger in spirit, who learned us a lot about the Belgium way of living, eating, drinking, gardening, . . . Jan and Lieve Dequeker, thank you!

Although I'm naming everyone, I'm afraid I will skip the friends list, just to avoid forgetting someone's name; better, I will thank all the good friends we made in Leuven, who made our time there so nice and unforgettable by organizing happy-hours, PMA-weekends, Christmas and new-year receptions, having us for dinner, coming home for dinner, watching movies with pizza or going to the cinema, going for a drink in Leuven or visiting a brewery, sitting together at Alma or during coffee break, bringing sandwiches on Friday, going to wedding parties, inviting us for Zolder, giving us tickets for Zolder, getting through the Sint Sixtus phone reservation system, sharing the office(s), sharing a room in a conference, a table later on in some fancy jazz-club (and paying the bill), spending new years eve together, asking for help on their new house, inviting for BBQ on their new house, playing football on Thursdays (even thou it was just once), inviting us for a farewell

dinner at home when it was actually a surprise at the city centre with a whole lot of you guys

My gratitude goes to the PMA staff, in special to Mrs Lieve Notré, Mrs Karin Dewit, Mrs Carine Coosemans, Mrs Ann Letelier, Mrs Regine Vanswijgenhoven and Mr Jan Thielemans, always prompt to help with our silly questions, strange requests, hotel and tickets reservations, licenses, etc.

I would like to express my heartfelt gratitude to my promoters, Prof. Paul Sas, who I have mentioned already, and Prof. Wim Desmet, who I had the pleasure to meet in 2004. What a privilege it was to work with both of you. In my first months at PMA, the feeling was that one couldn't avoid but learning, just by attending meetings and listening to you. Paul, you have been a raw model of researcher, team leader and kart driver to me; Wim, I can only dream to have a fraction of your talent when dealing with people, guiding a group, motivating your team mates and drinking beer. I would also like to thank you both for involving me in two European projects, very much in line with my research track and that allowed me to meet so many people and work together with other companies and universities during my PhD; I believe it really made the difference. Thanks also for the incentive in working closer to LMS International, it has been challenging and motivating to work with some bright people there and to see their interest in this work.

In this context, I would like to thank Dr. Herman Van der Auweraer and Dr. Karl Janssens, a non-exhaustive list of people I had the privilege working with at LMS, but probably the ones I worked longer and closely together. It has been a pleasure to work with you. Your role on the success of this PhD is greater than you imagine and the only thing I can hope for, is that our relation can go on after this.

My thanks further go to Prof. Jan Swevers and Prof. Gerrit Vemeir that followed my work from the beginning; your constructive comments helped improving this manuscript and the work as a whole. Prof. Swevers, I would also like to thank you for the other occasions, either guiding Master students, which was a good deal of learning for me, or having a laugh on Friday afternoons during happy-hour. Prof. Bert Roozen, thank you for accepting taking part in this jury committee and for your valuable comments during my preliminary defence.

Neste momento, não posso deixar de agradecer a meus pais, Abílio e Vera. A saudade foi grande, mas a certeza do amor e apoio incondicional de vocês sempre me deram forças. Obrigado pela criação que me deram, pelos valores Cristãos e por incentivar sempre meus estudos. Obrigado também aos meus irmãos queridos, Caco e Gi, pelo carinho de vocês. Foi difícil ficar tanto tempo longe de vocês, dos seus momentos de conflito e de alegria, e de ter vivido tantas coisas que gostaria de ter dividido com vocês; mas saibam que sempre estiveram no meu coração.

Maíra, thank you very much for believing in this dream. It is easy to look back now and realize it was worth enduring all the hard moments I left unwritten here, the *saudade* we felt from those we loved most, from our friends in Brazil and everything that made our journey harder. Thank you very much for being my best friend, my lover, my co-worker, my co-author, my co-pilot, for reading my drafts, shortening my mails, waking me up in the morning, . . . love of my life, thanks for being there, always!

Leopoldo Pisanelli R. de Oliveira
July, 2009

Abstract

Active control is a potential solution to cope with the steadily increasing requirements for noise reduction in the mobility industry. Cavity noise reduction, as encountered in aircraft cabins and vehicle interiors, are typical examples. However, not only noise reduction is pursued, but rather an improvement on the appreciation of the perceived noise by the occupants. The first requirement, therefore, is to assess the control efficiency taking human perception into account, e.g. by means of psychoacoustic metrics. A further step involves the design of dedicated control schemes for sound quality improvement. This thesis proposes simulation procedures for the design and optimization of vibro-acoustic systems and their embedded controllers. With the aid of a real-time engine sound simulator and a vehicle mockup, the evaluation of the optimal control performance by means of SQ metrics is assessed. Experimental validation of passive and optimal systems are also reported, which attests the added value of the proposed design procedure. It is shown that the use of standard control strategies can improve sound quality, although it is not always guaranteed. Also, a novel active sound quality controller is presented. This adaptive scheme is capable of equalizing, rather than only reducing, selected harmonic components of the disturbance sound. Results show large order-level reductions for stationary excitation, which allow a comfortable margin for equalization. Due to its improved convergence speed, this adaptive controller can handle non-stationary disturbances with limited loss in performance.

Beknopte Samenvatting

Actieve regeling is een potentiële oplossing om het hoofd te bieden aan de gestaag toenemende eisen voor geluidsonderdrukking in de voertuig-industrie. Geluidsonderdrukking in holtes, zoals die in vliegtuigcabines en voertuiginterieurs voorkomen, is een typisch voorbeeld. Niet alleen geluidsonderdrukking wordt nagestreefd, maar ook een verbetering van de appreciatie van het waargenomen geluid en een reductie van de geluidshinder voor de inzittenden. De eerste eis is daarom de beoordeling van de regel-efficiëntie die de menselijke perceptie in acht moet nemen, bijvoorbeeld door middel van psycho-akoestische statistieken. Een volgende stap betreft het ontwerp van specifieke regelschema's voor de verbetering van geluidskwaliteit. Dit proefschrift stelt simulatieprocedures voor, voor het ontwerp en de optimalisatie van een vibro-akoestisch systeem en zijn geïntegreerde regelaars. De evaluatie van optimale regeling op de prestaties wordt beoordeeld door middel van SQ maatstaven met behulp van een real-time motorgeluidsimulator en een proefmodel van een voertuig. Experimentele validatie van passieve en optimale systemen, die de toegevoegde waarde van de voorgestelde ontwerpprocedure verklaart, wordt hier ook vermeld. Het is gebleken dat het gebruik van standaard regelstrategieën de geluidskwaliteit kan verbeteren, maar dit is niet altijd gegarandeerd. Een nieuwe actieve geluidskwaliteitsregelaar wordt hier ook voorgesteld. Dit adaptieve systeem is niet alleen in staat harmonisch geselecteerde componenten van het storend geluid te verminderen, maar ook om deze af te vlakken. Voor stationaire excitatie tonen de resultaten grote verminderingen aan van de niveaus van de orders, waardoor een comfortabele marge voor afvlakking ontstaat. Vanwege de verbeterde convergentiesnelheid kan de regelaar omgaan met niet-stationaire storingen met een beperkt verlies aan performantie.

Table of contents

Acknowledgements	I
Abstract	V
Beknopte Samenvatting	VII
Table of contents	VIII
1 Introduction	1
1.1 The research goals	8
1.2 Active control of noise and the mobility industry	8
1.2.1 Successful market applications of ANC	9
1.2.2 Active control in the automotive sector	12
1.2.3 Recent challenges in automotive sound control	19
1.3 Sound quality and active control	20
1.4 Requirements for smart-system development	25
1.5 Contributions	30
1.6 Thesis structure	31
1.7 Conclusions	33
2 A state-space modelling approach for active structural acoustic control	35
Abstract	37
1. Introduction	38
2. Modelling Procedure	39
2.1 Vibro-acoustic modelling	42
2.2 Reduced State-Space formulation	47
2.3 SAP model	49

3. Results	51
3.1 Passive results	52
3.2 ASAC Simulation	53
4. Summary and Conclusions	60
Acknowledgements	61
References	61
3 Concurrent mechatronic design approach for active control of cavity noise	65
Abstract	67
1. Introduction	68
2. Fully Coupled Vibro-Acoustic Modelling Approach	70
2.1. From vibro-acoustic FE to state-space formulation	71
2.2. Experimental Validation	82
2.3. Inclusion of sensor and actuators pairs (SAP) models	83
3. Concurrent Mechatronic Design of Active Systems	87
4. Conclusions and Future Work	96
Acknowledgements	96
Bibliography	97
4 Active sound quality control of engine induced cavity noise	103
Abstract	105
1. Introduction	106
2. ASAC simulation scheme and experimental validation	107
2.1 From vibro-acoustic FE to state-space model	108
2.2 Control strategy: collocated velocity feedback	111
2.3 Passive and active system experimental validation	113
3. Sound quality assessment	116
3.1 Specific Loudness and Zwicker Loudness	116
3.2 Roughness and Modulation Index	117
4. Results	121
5. Conclusions	126
Acknowledgements	127
Bibliography	127

5 Active control of engine noise transmitted into cavities: simulation, experimental validation and sound quality assessment	131
Abstract	133
1. Introduction	134
2. Control Strategies	135
3. ASAC simulation scheme	137
4. Experimental Validation	139
4.1 Feedback control	141
4.2 Adaptive feedforward control	143
5. Conclusions and Future Work	146
Acknowledgements	147
References	147
6 NEX-LMS: a novel adaptive control scheme for sound quality control	149
Abstract	151
1. Introduction	152
2. Novel adaptive algorithm for sound quality control: NEX-LMS	153
3. Controller implementation	158
4. Results	162
5. Conclusions	165
Acknowledgements	166
Bibliography	167
7 Conclusions and future developments	171
7.1 Main achievements	171
7.2 General conclusions	172
7.3 Future developments	174
Bibliography	177
Curriculum Vitae	193
List of Publications	195

Chapter 1

Introduction

In the beginning was the word

St. John 1:1

As beings that rely strongly on their visual sense, people often take the role of sound for granted in their daily lives; even though acoustic communication is one of the fundamental prerequisites for the existence of human society.

Besides being often undermined by sense of vision, which takes up more space in the brain, hearing provides the reason and the means for one of the most intriguing forms of art: *music*. Intriguing, because it has the power, like no other, to evoke emotions and stimulate our imagination, probably due to the positioning of the hearing system in the brain, which is physically closer to the areas that control pain, pleasure, motivation, i.e., basic emotions. This close relation between hearing and emotions is not only noticeable with music, but rather with everyday acoustic stimuli, such as those from home appliances (Jurč and Jiríček, 2005) or vehicle noise (Vastfjäll et al., 2002).

In engineering, when approaching a new problem, one tends to use standard tools in order to model, simplify and describe it in a systemic way. As far as sound is concerned, one of the most used measures of volume is the sound pressure level (SPL) either in decibels (dB) or in its filtered forms dB(A), dB(B), dB(C), etc.; or even, if more detailed

information about its frequency content is needed, frequency spectra or time-frequency plots are used. Figures 1(a) and (b) depict the time history and the frequency spectrum of a pressure signal, respectively. The analysis of these two plots reveals a repetitive and quite tonal behaviour of this signal; however, not much about human appreciation can be concluded. A time-frequency plot (Fig. 1c) reveals how frequency components are spread over time with a certain pattern, but arguably, just a very experienced person could predict its nature. Finally, Fig. 1(d) reveals the real nature of that pressure signal, but again, only a person trained in reading this ‘medieval time-frequency diagram’ can anticipate how it would feel like to actually hear it. It is trying to explain how acoustic stimuli correlates to hearing sensations, that the multidisciplinary field of psychoacoustics developed in the late 1960’s (Zwicker and Fastl, 1999). Practical applications are usually less subjective than scaling the level of appreciation of a piece of music, but enough, so that time or frequency analysis of pressure fluctuations do not suffice. In fact, in most engineering applications, the important issue is improving acoustic comfort (CALM II Network, 2004) rather than preventing hearing damage, or even, assuring that resulting sound reflects some of the product’s desirable attributes (Penne, 2004; Bras-sow and Clapper, 2005).

The branch of acoustics that relates human perception (psychoacoustics) with the physics of sound generation and transmission (vibroacoustics) is often referred to as sound quality (SQ). Several approaches to SQ are present and, as a relatively new and rather case-dependent research area, the combination and extension of existing techniques as well as new ones are often being proposed. Three groups of SQ evaluation tools are jury tests, objective metrics and its combinations in predictor models. These different tools are selected, depending on the phase in which the SQ issue is tackled (Van der Auweraer and Wyck-aert, 2004):

SQ analysis: to identify the temporal and/or spectral structures that confer a certain quality to a sound stimulus. It often involves modifications of the original sound and a subjective evaluation (jury test) to determine the main contributors and allow target setting for that family of stimuli.

SQ trouble-shooting: to identify the underlying physical phenomena responsible for the sound quality aspect of interest, allowing

an engineering solution. It can use the knowledge base developed in the SQ analysis step, by isolating the relevant SQ aspects and proper metrics to assess the effect of design changes.

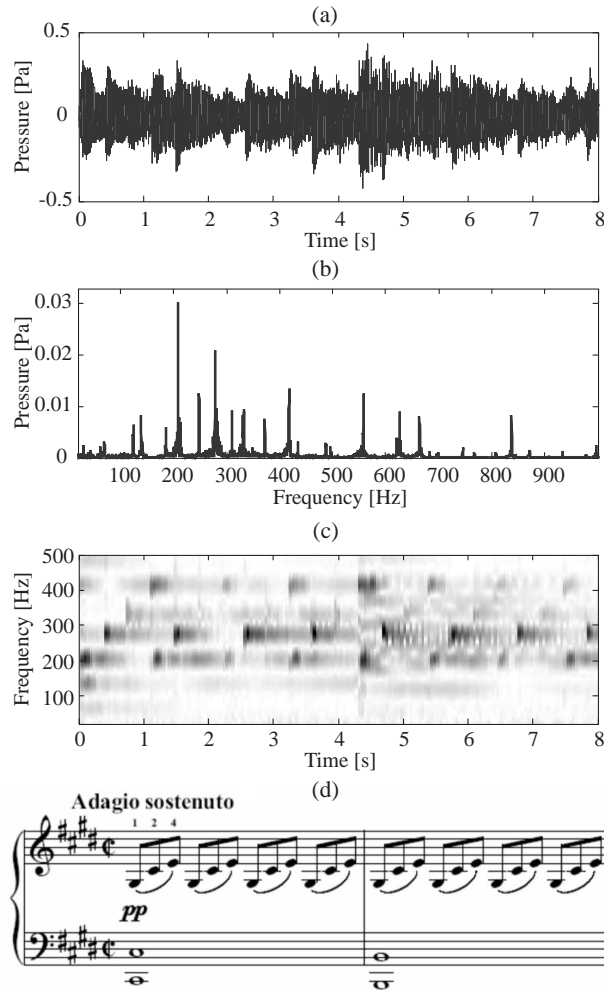


FIGURE 1: Several representations of the first bars on Beethoven's sonata Op.27 No.2: (a) time domain, (b) frequency domain, (c) time-frequency plot and (d) music score

SQ engineering: to address the sound quality issue, either by reducing annoyance or improving the desired quality aspects.

SQ control: to achieve the desired SQ target settings by means of active control. This is the last step in SQ engineering, where product development has evolved to the point of including active solutions in the early design stages, allowing the proper assessment of tradeoffs between passive and active solutions.¹

In the last decade the attention on SQ increased significantly, which is reflected in research as well as practical applications, not only in the automotive sector but also in home appliances, entertainment, communication, etc. In a recent publication, Fastl (2005) analyzes the recent developments in SQ evaluation, which he divides in two main branches: emission and immission (Fig. 2).

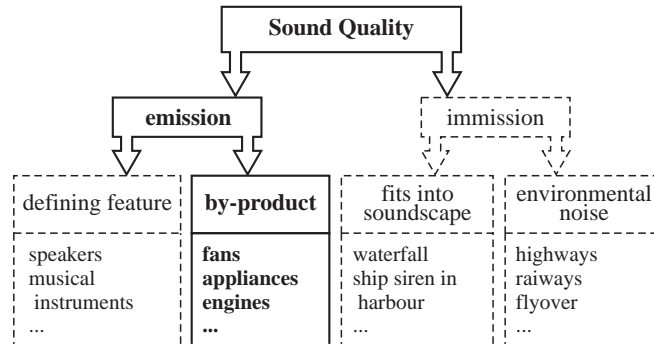


FIGURE 2: Branches of SQ evaluation: (—) focus of the present work and (- -) other branches

While emission is related to sound radiated from the product or process under study, immission refers to environmental soundscapes, where the generating sources are not under study but rather the sound field as a whole. Taking the emission branch, loudspeakers and musical instruments are primarily sound sources from which one expects

¹This phase does not belong to the original list (Van der Auweraer and Wyckaert, 2004) but is added here for the sake of completeness, as it summarizes the purpose of this work. This subject is treated in more details in section 1.4

the best possible sound quality. On the other hand, most products and processes generate sound as a by-product, as it is the case of electric motors, engines, gear boxes in vehicles and wind turbines, rolling tyres, etc.; while some can be annoying and undesirable, others can evoke desirable feeling that reflects the brand identity (Penne, 2004; Mori et al., 2005; Brassow and Clapper, 2005). In fact, a message conveyed through sound can have a strong effect, as humans tend to react emotionally to auditory stimuli (Vastfjäll et al., 2002).

Probably, the first to realize the importance of consumer product's sound to their positioning on the market was the automotive industry, about 30 year ago. American, European and Japanese companies had driven more and more resources to sound treatment, isolation and powertrain design, not only to reduce noise and improve comfort, but also to create and consolidate a sound identity, very much related to the exterior and interior engine sound. During the late 1980's, the Americans for example, had foreseen the evolution in noise, vibration and harshness (NVH) would change the sound of their cars such that the noise perceived by customers would sound like music (Saha, 2007). Vehicle SQ has improved in the past decades, but it is an overstatement to compare it to music. More recently, however, the concept of *music analogy* was developed (Fastl, 2002; Fridrich, 2005) preaching that instead of leaving for a large group of potential customers to define what is a *good sound* (in a conventional jury test), a small group of specialized SQ-engineers should take this decision; a role closer to the conductor of an orchestra, who takes the decision on how a piece of music should be played rather than the audience. This expert panel then uses their subjective classifications together with objective SQ metrics to set design/modification requirements for present/new products. Fridrich (2005) claims that this approach brings faster and more accurate results.

Beyond the analysis and the assessment of SQ design targets, what is pursued in this thesis are procedures for the design of active systems that take the human perception into account. NVH solutions have gone a long way since engines were bolted straight onto car bodies but, in order to achieve optimized design solutions with well-balanced tradeoffs, the NVH group has to be allowed earlier in the design process. The sound characteristics of a vehicle prototype need to be assessable even when only virtual prototypes are available, which is technically possible with the state-of-the-art virtual prototyping tools. However,

research on auralization of interior vehicle noise is relatively recent, strongly dependent on measured data from previous (similar) cases and not yet fully capable of supporting the specific aspects related to advanced materials, actuator and sensor dynamics and control (Van der Auweraer et al., 2006).

The successful development of new products, therefore, relies on the capability of assessing the performance of conceptual design alternatives in an early design phase. In recent years, major progress was made hereto, based on the extensive use of virtual prototyping. The state-of-the-art in computer aided engineering (CAE) techniques which can be used for the analysis of time-harmonic acoustic problems is presented by Pluymers et al. (2007). An overview is given, with automotive interior noise applications, on recently investigated extensions and enhancements to enlarge the application range of different techniques. The efficiency of present CAE techniques allows the use of optimization, e.g., in improving the NVH characteristics of a full-scale engine (Junhong and Jun, 2006) or a vehicle body (Donders et al., 2007). The novelty on this framework is to account for the human perception when defining product performance criteria (Mori et al., 2005; Berckmans et al., 2008).

In addition, active control has shown the potential to enhance system dynamic performance which allows lighter and improved products. Research done in the last years on smart materials and control concepts has led to practical applications with promising results for the automotive industry (Hurlebaus and Gaul, 2006). In order to make the step to the design of active sound quality control (ASQC), the control schemes, along with appropriate simulation procedures, need to become an integral part of the product development process (Van der Auweraer et al., 2007). In other words, this requires:

- (i) the product performance metrics to be based on human perception attributes and
- (ii) the simulation models to support active control design.

The proposed solution is summarised in the block diagram in Fig 3, which depicts a general scheme for real-time auralization of active systems. The success of this approach requires the multiple-input/multiple-output (MIMO) vibro-acoustic system model to be accurate enough, to provide SQ-equivalent pressure responses and, yet,

compact enough to allow real-time simulation. Ideally, sensor and actuator models should be included independently, such that the vibro-acoustic system modelling and reduction does not have to be repeated for each possible configuration. In this way, different sensors and actuators types, configuration and positioning can be evaluated with minimal computational effort. The loads, typically forces on engine mountings, suspension bushings, etc., can come either from measurements or simulation. All of these features can be relaxed, depending on the demands, e.g., simulating in real-time might not be crucial at an early stage when non-detailed conceptual ideas are matchmarked; sensor/actuators dynamics can also be negligible during a initial sensitivity analysis for sensor/actuator positioning; etc.

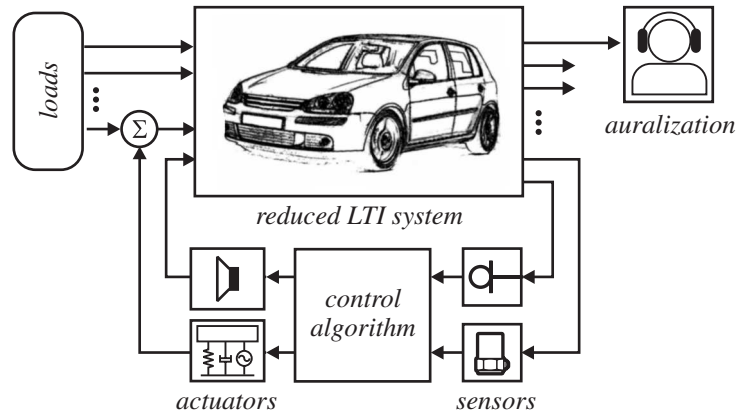


FIGURE 3: Block diagram for smart-system auralization

The remainder of this chapter is organized as follows: The research goals are described in the next section. Section 1.2 presents a short history of active control in the automotive industry and addresses the fact that, despite the academic success of active control applications, they are not often seen in vehicle applications. The role of SQ in the mobility sector is addressed in Section 1.3, where the link between SQ and active control is also drawn. In Section 1.4, the motivation and requirements for proper smart systems modelling/simulation methodologies are highlighted. State-of-the-art design concepts and their relation with active control and SQ are discussed. The thesis contributions

are listed in Section 1.5 and the thesis structure is presented in Section 1.6.

1.1 The research goals

The work presented in this thesis focusses on design procedures for active control systems with the aim of improving the perceived sound quality. Applications can range from home appliances to aerospace, but special attention is drawn to automotive applications. The main objective is to propose simulation methodologies to computer aid the design of active solutions for NVH and SQ problems.

Most design or trouble shooting decisions aimed at the improvement of SQ are based on the evaluation of different solutions by means of jury tests. This is a rather empirical and time consuming methodology. Therefore, an important aspect for bringing human perception earlier in the design phase, which would potentially improve product quality and its perception, is narrowing the gap between design changes and its effect on the resulting product SQ. In other words, most of the developments on this field have been focussed on experimental analysis techniques; the challenge now resides in developing and improving predictive SQ tools for both, passive and active design.

Therefore, the goal of this thesis is to:

- (i) simulate and optimize smart structures at component and system level, which require compact and accurate active system representations;
- (ii) assess the effect of design modifications on SQ targets, also if smart materials are involved. In this case, the earlier such assessment is enabled, the better real tradeoffs can be evaluated;
- (iii) achieve a pre-defined SQ design target by means of active control.

1.2 Active control of noise and the mobility industry

This section presents a short history of the use of active control in the mobility industry. To have a complete overview of all past and current applications is practically impossible; however, what is discussed

here are: (i) successful market applications, (ii) the academic success of active noise control (ANC) and active structural acoustic control (ASAC), and its contrasting struggle to reach the automotive market and (iii) recent challenges in automotive sound control.

1.2.1 Successful market applications of ANC

Noise cancelling headsets are, undoubtedly, the most successful application of ANC and one of the oldest (Simshauser and Hawley, 1955). In this application, the secondary actuator (Fig. 4) can be placed close to the sensor, allowing feedback control (Carme, 1987; Gan and Kuo, 2007), although feedforward is also used (Sas and Van Laere, 1988). Linear time invariant as well as adaptive schemes are used in both, feedback and feedforward implementations. Currently, several brands offer a wide range of products, as from €30 to €300 in the amateur range and up to €1000 for professional (aircraft/helicopter pilots) use.

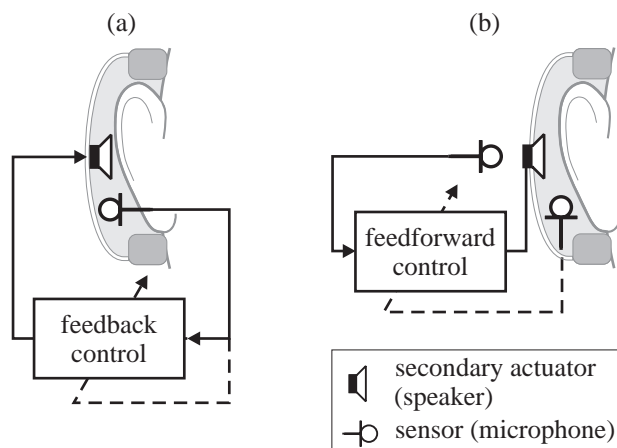


FIGURE 4: Active headset control schemes: (a) feedback and (b) feedforward

Another family of successful applications is the control of noise in ducts, such as, air-conditioning, industrial ventilation systems and engine exhausts.

Some of the first academic demonstrators came out during the 1950's (Olson, 1953, 1956), when analog electronics allowed the implementation of the concepts enunciated by Lord Rayleigh and patented by Lueg (1932). However, the outburst of work on the subject only came later, mainly due to a technology breakthrough: the use of adaptive digital controllers (Kido, 1975). It is the application of digital signal processing that has made the implementation of useful active noise control systems possible (Elliott and Nelson, 1993).

Most of the success of ANC in ducts and headsets is due to the relative simplicity inherent to those applications (Park et al., 2002). In the case of ducts, for example, one can assume one-dimensional wave propagation, which allows the use of a single secondary source (Nelson and Elliot, 1992). As a result, laboratory setups are also easy to built, with assured boundary conditions, which motivates its use for benchmarking new control implementations, as suggested by the following selected references from the past five years (Zhou et al., 2008; Jones et al., 2007; Barrault et al., 2007; Sun and Meng, 2006; Martin et al., 2004).

As far as automotive applications are concerned, active mufflers can perform as well as their passive counterparts, with the advantage of offering less resistance to the gas flow, which results in a smaller back pressure, hence, a more efficient engine operation (Boonen, 2003; Fohr et al., 2002). The main impediment for mass-production is cost; usual materials used in ANC would not withstand the harsh environment

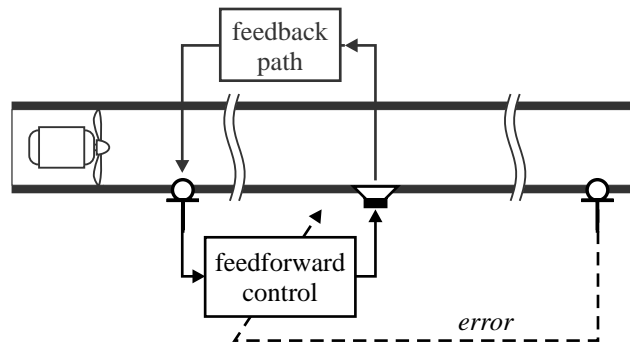


FIGURE 5: Adaptive feedforward control in a duct

imposed by the hot and corrosive exhaust gasses, therefore the development of special hardware is needed. Gradually, OEMs seem to better understand the flexibility and added value offered by smart systems and, after the necessary product development and robustness assessment, might eventually realize it as a commercial product (Maguire, 2008).

Environmental concern has grown over the years and a rather sensitive area is aviation. With residential areas ever growing closer to the airports, together with air-traffic, community awareness of aircraft ground operations (take-off, climbing, approach and landing) has increased. The factors that shape community perception, ranging from ‘acceptable’ to ‘annoying’, are discussed in (Whitten, 1972). More than 35 year latter, the subject is still of much concern (Berckmans et al., 2008). Although still incipient, active control can have an important role in this field, e.g., with active chevrons that prioritize noise reduction during take-off and landing and fuel economy during cruise (Mabe, 2008).

So far, most of the research focus on active control for aircrafts has been on internal noise reduction. The most common applications are in turbo-prop aircrafts, as the interior sound field in such planes is primarily affected by tonal noise with high SPL, which relates to the blade pass frequency (BPF) and its harmonics. In military applications, the level of noise can reach up to 150dB or 100dB(A) in semi-enclosed loading areas (Kochan et al., 2008).

The first ANC system operational in a propeller aircraft was implemented on an Avro BAe748 aircraft (Elliott, 1990). In this paper, theoretical results (with a simplified cylindrical model) are compared with measured flight data, which shows that, provided a certain degree of correlation between the internal/external acoustic load and the measured propeller BPF reference signal, the implemented feedforward principle would work. The system was set-up to minimize the sum of squared pressures at 32 microphone positions (estimated potential energy) with 16 loudspeakers. The system targeted the BPF (88 Hz) and its second harmonic, achieving 14db and 4dB reduction, respectively. These results involve local reductions of up to 35 dB, but the spatial extent of these high-level reductions is shown to be considerably smaller for the second harmonic frequency.

Followed by this first implementation, other commercial aircrafts implemented ANC solutions, such as the SAAB 340 and 2000, Bom-

bardier Dash 8 and Challenger 604, Beechcraft 1900D, etc. (Ross, 1982; Elliott, 1990; Sas, 2004). In military aircrafts ANC is still preferred, as it, when compared to passive solutions, presents superior weight and noise reduction performance at low frequency (Kochan et al., 2008).

1.2.2 Active control in the automotive sector

Despite the considerable amount of papers being published on ANC and ASAC, one of the reasons that makes it difficult to trace back the evolution of automotive applications is the lack of publications on this subject, as indicated by Dehandschutter (1997). The automotive industry is very much innovation- and technology-driven; consequently, research results are submitted for patenting rather early and are often immature if compared to later publications Guicking (1996). On their review of automotive applications, Mackay and Kenchington (2004) admit that client confidentiality prevents most mature results from being published. In fact, recent advances in the field, very much related to the theme of this thesis, are ongoing but not often reported on open literature (Kronast, 2007), probably due to company confidentiality issues.

Although it is the main focus of many research projects and publications (including those comprising Chapters 2 to 6 of this thesis), sound is just a vehicle by-product. As a result, for quite some time, NVH has been aiming at reducing sound pressure levels. Indeed, active control might not be the most cost effective solution for automotive noise reduction (Sano et al., 2002), which is debateable as a thorough comparison of active and passive integrated design, addressing the proper tradeoffs involved, is yet to be made (Maguire, 2008).

The primary features of a vehicle are transport and safety. Therefore, the introduction of microcontrollers in the automotive sector is thanks, first, to electronic fuel injection (EFI), followed by anti-lock braking systems (ABS), traction control and, more recently, dynamic stability control (DSC), active and semi-active suspension (see Fig. 6 and Table. 1).

The implementation of these systems require the installation of dedicated sensors and actuators (Table 1) and stimulated the development of automotive microcontrollers. By the late 1990's, shared engine/transmission control units employed 16- or 32-bit processors with up to 512KB of ROM and 64KB of RAM, running at 50 ~ 100Hz (Happian-Smith, 2002; Braess and Seiffert, 2005). Figure 7 shows a

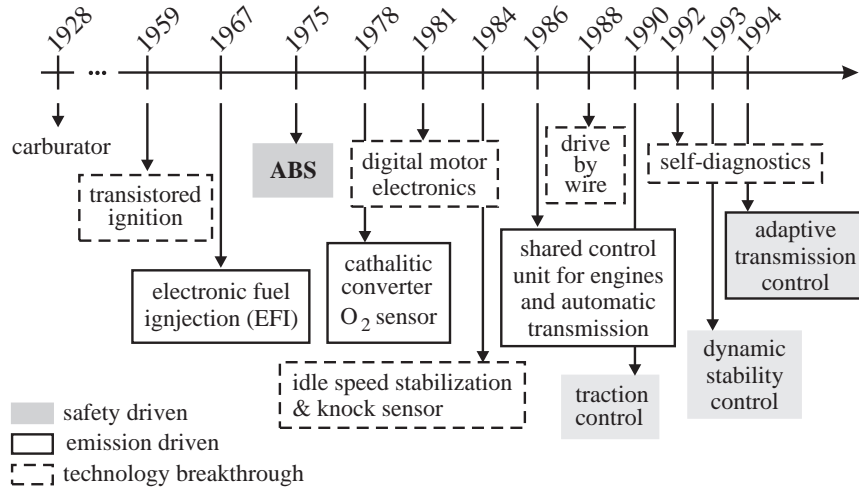


FIGURE 6: Significant milestones in automotive design (after Braess and Seiffert 2005)

complete powertrain control unit, integrating, a.o., engine management and transmission control. These controllers are programmable, e.g. in C++ and accept commands such as table look-up and interpolate (Happian-Smith, 2002), which is now used to set ignition timing, but can also be useful for sound quality control, where the reference for the desired sound amplitude is other than zero (see Section 1.3). For the sake of comparison, the controllers reported on Chap. 3 to 6 were implemented on a dSPACE 1006, with a 2.6GHz processor, 1MB L2 cache, 256MB local- and 128 MB global-memory. Besides needing more processing power and memory, ANC applications do not share the same reliability requirements as the aforementioned applications, i.e., in the event of a malfunction, the ANC system could simply be shut down without compromising the occupant's safety.

Active and semi-active suspension applications are finding their way into mass-production vehicles. As some of these applications can run on a few hundred Hertz frequency sample, part of the required hardware is already on-board, mostly due to ABS and ESC technology (see Table 1). An active suspension (e.g., with electromagnetic shock absorbers) has a wider range of applications and, in principle, can perform better

TABLE 1: Examples of sensors and actuators in automotive closed-loop control systems

controller	indirect controlled variable	sensors	actuators
EFI	air/fuel rate	lambda sensor (O ₂ sensor)	fuel injector
knocking	(diesel engine) knock	accelerometer	ignition coil switch transistor
ABS	wheelslip	magnetic proximity	break piston solenoid valve
DSC	vehicle attitude	yaw sensor, steering angle	same as ABS
active and semi-active suspension	pitch, roll, bounce	accelerometer, LVDT	electromagnetic or hydraulic actuators, solenoid valve

than a semi-active one. On the other hand, semi-active suspensions are inherently stable, less complex and commercially available, either with a magnetorheological fluid or solenoid valves to change the damper restriction.

Swevers et al. (2007) proposes a control structure for the on-line tuning of semi-active suspensions. The fact that the design/implementation of such control strategy does not require a model of either the vehicle or the shock absorber, makes it quite attractive for industrial application. However, when evaluating the controller performance, they are faced with the lack of objective criteria for assessing ride comfort. In a way, it resembles the evaluation of the acoustic performance in dB, which, as mentioned before, can be misleading. To cope with that, a rather new term is emerging which is analogous to sound quality: *vibration quality* (Jay, 2007), that is regarded as a possible continuation to this thesis (see Section 7.3). The assessment of a

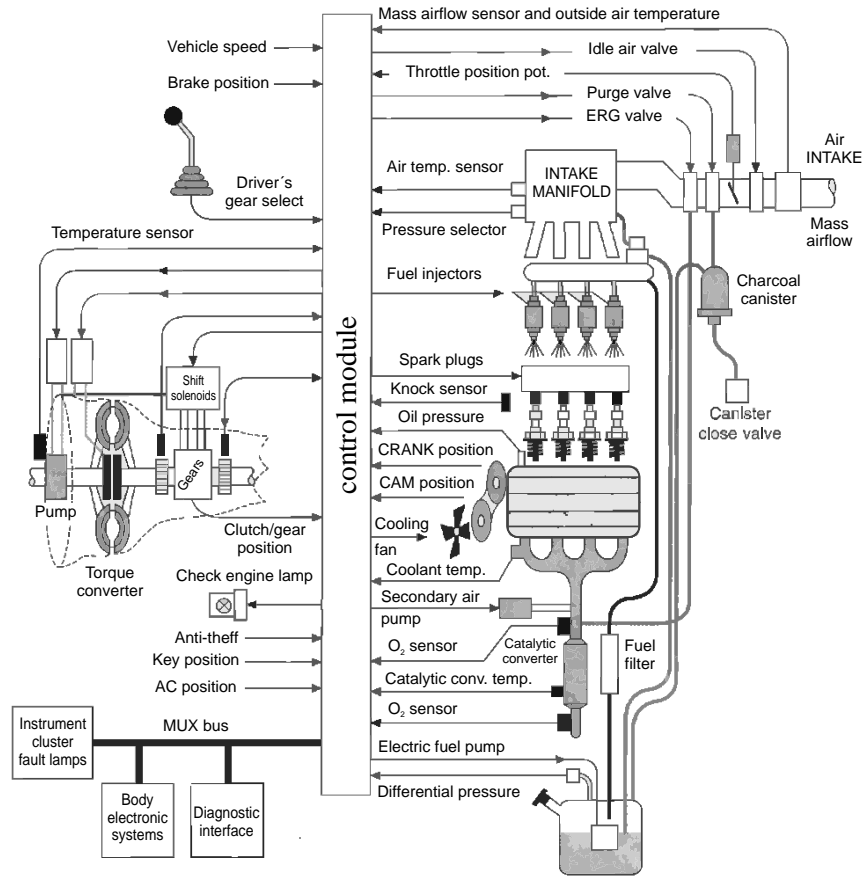


FIGURE 7: Powertrain control unit (Happian-Smith, 2002)

product's *vibration quality* presents the same challenges and constraints of its SQ analysis (Jay, 2007). Examples of vibration quality concerns are (as opposed to vibration exposure) the vibration that may be felt at the steering wheel (steering shudder) or the vibration of mobile phones in silent-mode; rather than hazardous, they carry important information for the receiver.

As far as noise reduction is concerned, some of the first attempts to implement ANC and ASAC for passenger cars can be found in (Oswald, 1984; Elliott et al., 1988; Bao et al., 1991). In principle, if compared to aircraft applications, cars are simpler in the sense that the volume is smaller (lower modal density) and there are fewer regions to control. However, while an aircraft engine keeps roughly the same RPM, in a car, RPM and load conditions are constantly changing, which requires the use of adaptive filters (Elliott, 1994).

For a number of years, publications have predicted the increase in the number of practical ANC implementations, which they claim mainly due to improved and more affordable DSP technology. However, the evolution to practical applications has been slower than expected, mostly due to the complexity of real systems (Park et al., 2002). As mentioned before, most of the successful applications allow simplifications (local control or one-dimensional waves). However, quite some references can be found where different control strategies, sensors and actuators are used to reduce SPL inside passenger cars.

In general, feedback ANC or ASAC systems are used to control broadband disturbances, such as tire/road noise. Costin and Elzinga (1989) suggest the use of a feedback control system with headphones as secondary actuators. Less straightforward (and more reasonable) implementations are described by Elliott (1994); Dehandschutter (1997) and, more recently, by Scheuren (2004) and Olsson (2006). Feedback applications generally use structural sensors and secondary actuators on important structural paths. The issue with acoustic sensors/actuators is the phase lag induced by the distance between them, which makes applications (other than headphones) infeasible (Sas, 2004). Feedforward schemes can also be used to control broadband disturbances, but their performance is limited by the loop delay, i.e., the time delay between the reference and the error sensor; if the delay allows time enough for an adaptive algorithm to converge, it can outperform a feedback controller (Elliott and Sutton, 1996; Dehandschutter, 1997), but that is not often the case.

Probably the most exercised feedforward approach is the use of ANC for engine noise cancelation (Elliott and Nelson, 1993; Bao et al., 1991, 1993; Park et al., 2002, 2004). The vast majority of such demonstrators make use of the filtered x-LMS algorithm and its modified forms. Adaptive feedforward schemes can also be used for external noise control, as in active muffler applications (Boonen, 2003; Fohr

et al., 2002). Although several case studies can be found in the literature, the implementation of these systems requires a powerful DSP, which is still considered costly for mere noise attenuation purposes.

The proper placement of sensors and actuators is also crucial for the controller performance. Some academic study cases can be seen in (De Fonseca et al., 1999; de Oliveira et al., 2006); the latter, in particular, shows that a modal base deterministic technique can give the same optimal placement as suggested by a genetic algorithm optimization. Even if used as a *posteriori* solution, experimental modal data can be used in a similar way to assess the optimal placement, as suggested by (Stöbener and Gaul, 2001; Hurlebaus and Gaul, 2006). However, only integrated design can allow the optimal placement in real applications, as often, there is no space for placing bulky actuators (such as electrodynamic shakers); space that could be predicted if the use of active control had been foreseen as from the concept design phase.

Regarding industrial applications, Sano et al. (2002) and Mackay and Kenchington (2004) present a review of active noise and vibration control applications in the automotive sector. Over the past 20 years, Lotus has developed over 50 technology demonstration vehicles for various OEMs, equipped with active control technologies, to address specific issues in vehicle NVH refinement (Mackay and Kenchington, 2004). They claim these technologies will be taken into mass-production in a near future. Indeed, some applications can be seen in commercial vehicles as highlighted by Sano et al. (2002), e.g., a ANC for booming noise implemented by Nissan in 1997, a Toyota idle ANC from 1997 and two active engine mountings from Nissan and Honda available in 1998 and 2000, respectively. Lotus demonstrators span sports cars, luxury saloons, small hatchbacks, SUVs, commercial vehicles and mid-size family cars but, in both cases, confidentiality means that results cannot be discussed in detail. Another recent example is Toyota, that announced their high-end hybrids will feature ANC system to reduce interior engine noise (Fig. 8), by using microphones and the car audio speakers as sensors and actuators; a system very similar to the Lotus concept proposed and demonstrated two decades ago Elliott and Nelson (1993).

As mentioned before, cost remains an important issue for practical applications, as more powerful DSPs are needed to deal with the higher frequency band and rather complex algorithms. For example, a sound system that adapts the music playing to keep the sound quality accord-

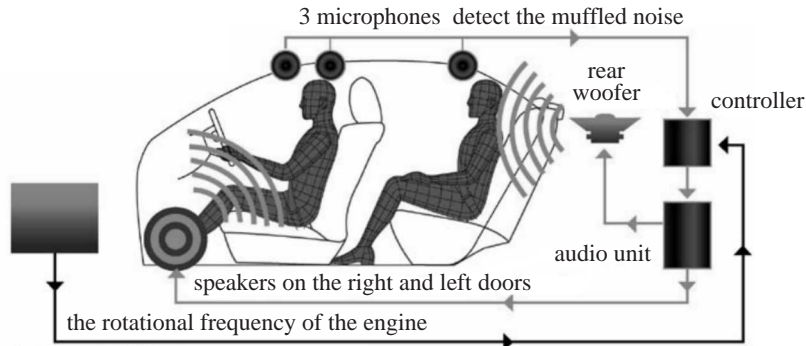


Figure translated by Tech-on!

FIGURE 8: Concept of Toyota's ANC system: source
(<http://techon.nikkeibp.co.jp>)

ing to exterior noise sources (such as the accelerating engine), currently worth around €600. Even more advanced systems, that compensate for people's placement in the vehicle and even to road or rain noise (i.e. broadband random disturbance), can reach €6000, which is 10% of the total cost of the car the sound system is fitted in (www.audi.com). Technically, that is not an ANC system, as it only changes the equalization of the music playing through the speakers, even though, it features a 14-channel DSP board, error microphones and high-end sealed speakers (www.bang-olufsen.com), i.e., technology is at hand, although cost may still be an issue.

The cost involved can have an even worse connotation for strictly ANC systems, as customers tend to think a car should offer enough acoustic comfort by itself, and might not be willing to pay more for an active control system as an option (Sano et al., 2002). Without the masking effect of music, the perceived benefit of ANC can sound disappointing. Unfortunately, that might not be the opinion of the general user only, but rather of the engineers in fields other than noise and vibration and company directors (Sano et al., 2002), who are responsible for decision making. Such over expectation often leads to disappointment when faced with the performance of ANC in real-life situations. Therefore, the market acceptance of active control as a means for noise reduction (and/or sound quality improvement) can only take place if a

clear balance between cost&benefit is met.

Cost can only be accurately assessed if mass-production of the necessary components is taken into account, but to estimate that, minimal performance specifications are needed for sensors, actuators, microprocessors, etc., which depends on the system level performance requirements (benefits). Although ANC performance is often reported in dB, it is difficult to predict how noticeable reductions expressed as such are to the occupants. For example, it is clear that reductions of 10dB or higher will be easily perceived, but again the question remains, if the resulting sound will evoke the desired attributes. That will also depend on the other components of the sound field, as the controlled source can unmask other undesired sounds (Van der Auweraer and Wyckaert, 2004). This is one of the main motivations for the use of SQ metrics to evaluate the performance of such active solutions, as it is discussed in more detail in section 1.3 and Chapter 4 (de Oliveira et al., 2009).

1.2.3 Recent challenges in automotive sound control

The main drivers for product innovation have to be the demands imposed by a competitive market and legislation. While most legislation regarding vehicle noise is focussed on exterior noise (CALM II Network, 2004), market demands for innovation and the recent interest in sound branding affect internal noise.

Another characteristic of the market that influences engineering decision is globalization. Many cars are designed as global products and yet have to attend local markets' expectations. An example is the low frequency acoustic behaviour of accelerating vehicles (Lee, 2008; Shin et al., 2008); due to cultural aspects, while the Japanese market expects a quiet and smooth run-up, the European market allows some booming in such conditions (Abe, 2008). The extensive use of active control in the NVH development of future vehicles would allow a simple software update to adapt the same hardware for distinct market expectations.

Environmental solutions can also affect vehicle NVH. That is the case, e.g., of hybrids and engines with variable displacement technology. On hybrid cars, external and internal noise can be an issue. When running on the electric motor, hybrids can be rather silent, e.g., to catch the attention of pedestrians that are used to the sound of a regular car approaching. As far as interior noise is concerned, active control could also provide the means to set the engine noise, such that the occupants are unaware of driving mode shifts, either by having a

more silent interior when the combustion engine is used or the constant perception of a familiar combustion engine, even when running on the electric motor.

The importance of having the proper engine sound can also be an issue when applying variable displacement technologies, which allows engines to run on a set of its cylinders for fuel economy (e.g., by shutting off a bank of cylinders in a V-engine). The technology is already available in bigger-engine versions of passenger cars from Daimler, GM and Honda. Daimler's solution to preserve the perceived sound of the engine in both conditions uses an active valve to divert the exhaust between two different muffler systems and a variable length intake manifold. In order to preserve the characteristic rumble of its V8 engines, GM uses a special exhaust system with four separate mufflers, two large central ones for V8 mode and two smaller ones for straight-4 operation. Those systems could benefit from lighter active mufflers and intakes that would adapt for the different driving conditions (Boonen, 2003; Fohr et al., 2002).

Another issue with variable displacement is vibration, as the engine and mounting design cannot be optimal for the different driving conditions. Honda is using active engine mounts for that purpose, and with the aid of drive-by-wire gas pedals, claim that the driver is unaware of the switching process (<http://automobiles.honda.com>).

1.3 Sound quality and active control

This section presents a historical overview and the state-of-the-art in active sound quality control (ASQC). It describes the first attempts in bringing human perception criteria into control design/evaluation and the evolution to the most recent implementations of active sound quality control (ASQC).

Historically in automotive product development, an emphasis on noise reduction has been considered critically important to customer perceived quality. Although comfort is an essential attribute, as from 15 to 20 years, it is well understood that a good vehicle sound is not only about being quiet.

A good example is the door slamming sound (Van der Auweraer and Wyckaert, 2004; Plunt and Hellström, 2006; Hufenbach et al., 2008). What seems a rather irrelevant issue is actually assessed by every major manufacturer. The relevance of a good door slam sound is based on

the number of customers that just open and close a car door before purchase, which is much higher than that of those who take it for a test-drive. Customers tend to take the overall refinement of the vehicle for the solidity of the door slam sound.

The interior sound of a vehicle is made up of contributions from many sources. From a SQ engineering perspective, some of these sound sources may be tuned to enhance the vehicle sound quality, invoking some desired emotional responses, while others should be suppressed to reduce annoyance. The sound of a powertrain, for example, can give a sense of powerfulness, effortlessness, refinement, etc., matching desired brand characteristics (Brassow and Clapper, 2005). As a consequence, considering the current level of performance, ride and handling qualities in premium class vehicles, one can clearly notice that NVH has turned into an attribute that expresses a strong brand identity (Penne, 2004).

More specifically, concerning engine SQ, a number of sub-categories could be listed:

- (i) **pure level harmonic problems:** when only noise level is tackled and broadband reduction is needed, e.g., booming.
- (ii) **tonal problems:** similar to the aforementioned pure level problems, but strictly related to a single harmonic, i.e., with a specific sensation of frequency which may be annoying. Typically related to sensations like pitch or tonality as appearing in gear whines, exhausts, etc.
- (iii) **continuity problems:** another type of harmonic level problem, continuity problems are often related to low order levels at certain RPMs, which can affect the perception of power and sportiveness. In opposition to booming, that could be seen as a discontinuity towards higher levels, the focus here is to get the order levels to evolve as smooth as possible with respect to RPM.
- (iv) **multiple-harmonics problems:** when amplitude and phase relation of multiple orders are responsible for the wanted (or unwanted) sound characteristics, such as in roughness, muddiness, rumble, etc.

The novelty in this framework, which is tackled in this thesis, is the use of active control to deal with such SQ issues. The problems in category (i) can be dealt with linear time invariant, broadband controllers.

The same controllers can be used in (ii), although adaptive schemes could be a better alternative, as the disturbance is rather periodic and a coherent reference signal would be readily available. Problems of continuity (iii) require the controller not only to track the order, but also to drive the error to a desired level (rather than zero); which means that the controller has to be capable of matching a desired order profile either by reducing or amplifying the order level at different RPMs. Problems in category (iv) require, in addition to (iii), that the controller tracks amplitude and phase relation of multiple orders. As described in this session, the state-of-the art in SQ control (as the work presented in this thesis) covers (i), (ii) and (iii).

Research done in the last years on smart materials and active control has shown their potential to enhance system dynamic performance which allows lighter and improved products, with promising applications for the automotive industry (Hurlebaus and Gaul, 2006). As a consequence, a recent approach in vehicle NVH is the use of active control for SQ improvement. However, to make the step to the design of active sound quality control (ASQC), the control schemes, along with appropriate simulation procedures, need to become an integral part of the product development process (Van der Auweraer et al., 2007; Vandeurzen and Leuridan, 2008).

The first step towards a SQ control design is the psychoacoustic evaluation of standard ANC and ASAC systems (Mangiante, 2004; Canévet and Mangiante, 2004). An objective way of measuring the improvement in SQ is by evaluating SQ metrics such as loudness, sharpness, roughness, etc. (Zwicker and Fastl, 1999; Glasberg and Moore, 2002), which are used by (Canévet and Mangiante, 2004) to identify the effect of ANC on various stimuli selected from everyday life (exterior aircraft and car noise, interior locomotive, helicopter and car noise). No active control is actually implemented but the recorded sound files are equalized within different frequency bands in order to emulate the control action. In some cases, listeners reported that although the sound had become slightly softer it also felt more unpleasant. More recently (Mangiante and Canevet, 2007), a positive effect on SQ has been observed when low-frequency broadband noise is reduced, which is reflected in the SQ metrics. These results should be interpreted carefully, as a more accurate assessment of the actual effects of active control on SQ requires the implementation of the control systems (virtually or experimentally), as each implementation (feedback, feed-

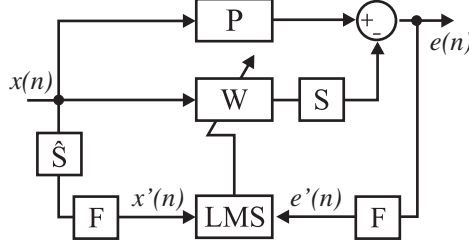


FIGURE 9: Block diagram of the filtered-E LMS algorithm

forward, narrowband, broadband, etc.) will act in a different way. A real-life application will hardly have a global effect on the sound field as an equalization through signal processing, e.g., uncorrelated sources on a feedforward implementation will not be affected, even if on the targeted frequency band.

The first truly SQ controller is the active noise equalizer (ANE), proposed by Kuo et al. (1993), which is capable of reshaping the residual noise left after the convergence of a filtered-x LMS (Fx-LMS) controller. It consists of adding a filter $F(z)$ to the error sensor path and the reference signal (Fig.9), which is designed to be the inverse of the desired residual noise magnitude response. In fact, this reasoning is only valid if the original residual noise spectrum is flat (see Fig.7 in Chap.6). The actual principle behind the ANE is the use of a pseudo-error signal (error filtered by $F(z)$) for the adaptation algorithm, which enables the modification (equalization) of the actual error spectrum, i.e., rather than determining the spectral content of the residual error, $F(z)$ filters the original residual error (Sommerfeldt and Samuels, 2001), reshaping it. In both cases (Kuo et al., 1993; Sommerfeldt and Samuels, 2001) the filter design is based on equal loudness contours (ISO226, 2003), which provides a good insight on the behaviour of such schemes, but is not ideal for its purpose. Equal loudness contours vary according to the disturbance level and, mostly, were designed for single tones rather than multi-tone or broadband noise, so, unless the disturbance is known and stationary, more sophisticated perception models are needed.

Gonzalez et al. (2003) evaluate the ability of ANC to achieve a more pleasant automotive-interior sound. They use jury tests and sound

quality metrics (loudness, roughness, etc.) to evaluate the effect of an ANC system assembled in a room. The setup involved a MIMO Fx-LMS controller with two microphones and two speakers as secondary sources; the primary disturbance is provided by a speaker fed with different signals (harmonic tones, random noise and recorded engine noise). The main conclusions relate the comfort improvement with loudness reduction for the stationary cases, *i.e.*, harmonic disturbance and engine at constant speed. The changes on SQ were not appreciated by the jury for sounds considered sufficiently quiet before control, such as engine idle, which indicates that the mere reduction of noise by means of ANC does not guarantee SQ improvement, similarly to what was concluded by Canévet and Mangiante (2004) with their emulated ANC exercise.

It becomes clear that in order to effectively improve sound quality with active control, the equalization, rather than the reduction, of primary disturbance noise should be pursued. An evolution of the ANE scheme (Kuo et al., 1993), shown in Fig. 10, has been proposed by Kuo and Mallu (2005), who first introduced the term active sound quality control (ASQC). The first feature of this control scheme is the use of a sinewave as a reference signal; like that, the Fx-LMS scheme acts like an adaptive notch-filter, controlling only components on the same frequency as the provided sinewave (Kuo and Morgan, 1996). The equalization feature is obtained by splitting the output of W in two branches where the gains β and $(1 - \beta)$ are inserted. The secondary path is fed with a fraction of the original output (for $0 < \beta < 1$) allowing the error to be tuned; the adaptive algorithm is tricked by being fed with the pseudo-error e' , which is the sum of the actual error and the complementary part of the output.

Based on that scheme, a MIMO version was proposed by Diego et al. (2004) for reshaping multi-tonal stationary noise in a setup similar to the one in Gonzalez et al. (2003), *i.e.* a ANC implementation in an room treated with absorbing material. The effectiveness of this control strategy (and its modified versions) in independently equalizing harmonics from a stationary multi-tonal disturbance is assessed in many references (Kuo et al., 1993, 1995; Diego et al., 2004; Kuo and Mallu, 2005; Rees and Elliott, 2006; Kuo et al., 2007). However, as highlighted by Gonzalez et al. (2003), another important aspect in the use of adaptive ANC schemes is its capability of dealing with non-stationary disturbances, such as engine noise during acceleration. The

improvement of convergence speed in LMS-based adaptive schemes is a recurrent issue (Bao et al., 1993; Paillard et al., 1995; Kuo and Morgan, 1996; Sun and Meng, 2006; Jones et al., 2007). More recently, this subject has been tackled specifically for ASQC (Kuo et al., 2008) where a frequency domain approach is proposed and numerically validated.

In Summary, besides SQ analysis of active control, dedicated SQ controllers have been proposed recently. Each application, however, should pose new challenges, as it is the case of the transient characteristics of accelerating vehicles, that need to be tackled. Experimental validations in more complex systems and/or real life product demonstrators are also lacking. Also, related to the scope of this thesis, general tools/methodologies for the design of such systems need to be proposed in order to allow performance predictions and tradeoff assessments. These subjects are treated in Chapters 6 (de Oliveira et al., 2009).

1.4 Requirements for smart-system development

As a result of the demands for more refined and performing products, such as automobiles, their complexity has increased significantly making the design process a truly multidisciplinary and challenging task.

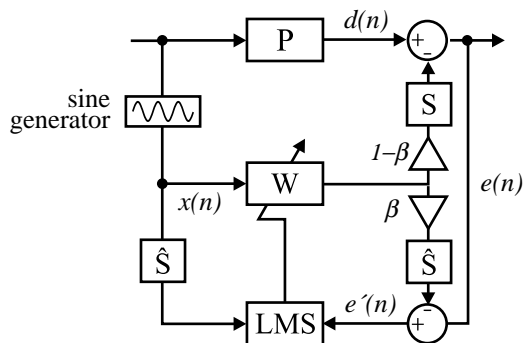


FIGURE 10: Block diagram of the ASQC based on the Fx-LMS algorithm

Several fields (aerodynamics, vehicle dynamics, NVH, electronics, control, etc.) have to come together in a harmonic way with well-balanced tradeoffs in order to achieve the desired design requirements; some objective ones with standardized measures (performance, handling, noise levels, CO₂ emissions, etc.) and some subjective ones (style, hide, comfort, brand image/sound, refinement). Shortening development cycles, reducing design costs and improving product performances require correct design decisions to be made early in the design process. In recent years, major progress has been made on the extensive use of virtual prototyping before the first physical prototypes are available, such as for the powertrain development described in (Nehl et al., 2006). Such approaches are based on performance simulation models which are often part of multi-attribute optimization schemes (Van der Auweraer et al., 2005).

An example of the new challenges in simulation is the design of engine mounts. The definition of mountings' and bushings' stiffness is a well-known trade-off between handling/ride and NVH, since the former requires stiffer and the latter softer elements. It is only recently that NVH groups are allowed to require, in an early design phase, minimal specifications for those elements and suggest, e.g., that space should be foreseen for the eventual installation of active engine mounts (Felice, 2008). The design of such system in an integrated environment could allow the optimal design of such hybrid system, exploring the advantages of the passive system and the flexibility/adaptability of the active system.

The same holds for active noise control. It is well known that, for some applications, active control might be the only solution for reducing low frequency noise, as passive treatment is limited by space/weight (Sas, 2004). However, the tradeoffs amongst passive and active solutions for mid- to high-frequency range, as well as guidelines for the design of hybrid ones, are still an open issue. Another important issue regarding the use of active systems is their adaptation capabilities; in many cases, when the source of disturbance is well known and stationary, passive solutions can be optimized for those conditions. On the other hand, if system and/or disturbance can change and a degree of performance is needed throughout the span or, if tuning is needed either for user preference or market issues (Abe, 2008; Shin et al., 2008), a passive solution will hardly suffice. The latter aspects have to be considered yet in the conceptual design phase, and if active control is

elected as a possible solution, then the aforementioned design tools are essential.

So far, in the automotive industry, active control of noise and vibration has not been considered as a valid design solution as from the early design phase; it is still regarded as a patch solution, to be taken into consideration only when passive treatments have been exhaustively exercised. In this way, the perceived benefits of smart solutions are clearly undermined and the apparent cost overestimated (Maguire, 2008). The reasons for that range from the unavailability of proper design tools through the very design process itself, as a change towards concurrent multi-disciplinary design is also needed (Vandeurzen and Leuridan, 2008).

The advantages of concurrent vs. iterative design have been treated in some recent publications (da Silva et al., 2008; Xianmin et al., 2007; da Silva et al., 2008). In order to bring these concepts to the level of industrial applications, the related design processes have to become part of the complete product development process. This requires that the product functional/performance simulation tools, which are the cornerstone of today's design process, must be capable of supporting the specific aspects related to smart structures, integrated into system level virtual prototypes (Herold et al., 2005; Van der Auweraer et al., 2006; Bein et al., 2007). More specifically, this involves developing modelling capabilities for the intelligent material systems, sensor and actuator components, for the control systems as well as for their integration in systemlevel application designs. The final result will then be a multi-attribute optimization approach integrating noise and vibration performance with reliability, durability and cost aspects. It is clear that no single integrated solution will be able to fulfil all requirements of the various material and control approaches, therefore the focus of the research is on supporting as much as possible the use, combination and extension of existing codes and tools. In this way, a simulation procedure followed by a multi-disciplinary optimization and an experimental validation are presented in Chapters 2 and 3 (de Oliveira et al., 2007b, 2008). The simulation procedure includes the fully coupled vibro-acoustic system and the ASAC system

The last step towards the optimal design of active systems for vehicle applications (or others intended for human operation) is the inclusion of human perception in the loop. As discussed in Section 1.3, the sound of a product has a significant influence on its market po-

sitioning and on the overall perception of its quality. To achieve the desired product sound that will reflect the brand's identity, car manufacturers know that analysing the A-weighting SPL is not sufficient (Sottek et al., 2005). It is also true that with the improvement on the NVH characteristics of modern, more silent cars, occasionally, annoying sounds which have been masked in the formerly louder ones become audible, such as the noise from small electric motors, squeak and rattle. (Sottek et al., 2005) highlights the importance of assessing the perceived SQ during the design phase, which could be done with the extent of present simulation tools and the use of a knowledge base built on previous analyses on similar products (SQ databases such as the one from BMW - Penne, 2004) .

A significant step towards interior noise simulation in vehicles was made by Williams and Steyer (1995) which eventually lead to the development of NVH simulators (Janssens et al., 2003, 2004; Eisele et al., 2005; Williams et al., 2007). These real-time simulation platforms provide SQ-equivalent models which are used in vehicle product development. as it enables the assessment of the NVH characteristics of a virtual (or real) vehicle under various driving conditions. In this framework, the transfer paths can be measured, simulated or hybrid (experimental + numerical structural modifications). Although the use of experimental loads is more common, simulation schemes as the one described in (Nehl et al., 2006), could also provide the necessary information for a fully numerical NVH simulation. The NVH simulator used is the LMS Virtual Car Sound (VCS). Fig.11 shows VCS' concept for real-time sound generation, which can run based on a recorded RPM/speed profile or on real-life inputs (throttle, brake and gear). In this case, the simplified longitudinal performance model provides the RPM and speed for the sound synthesis generation, which is based on the transfer paths and operational loads. The novelty in the work described in Chapters 4 and 5 is the use of VCS as a controllable and repeatable SQ-equivalent primary disturbance source, rather than a NVH auralization tool.

Most of the present state-of-the-use SQ tools in automotive design are merely for analysis. In various applications, recorded and simulated sound files (and/or transfer paths) are edited in order to assess the effect of hypothetical modifications on the perceived interior sound. However, this kind of analysis should be interpreted carefully, mainly when active control is concerned. A more accurate assessment requires the

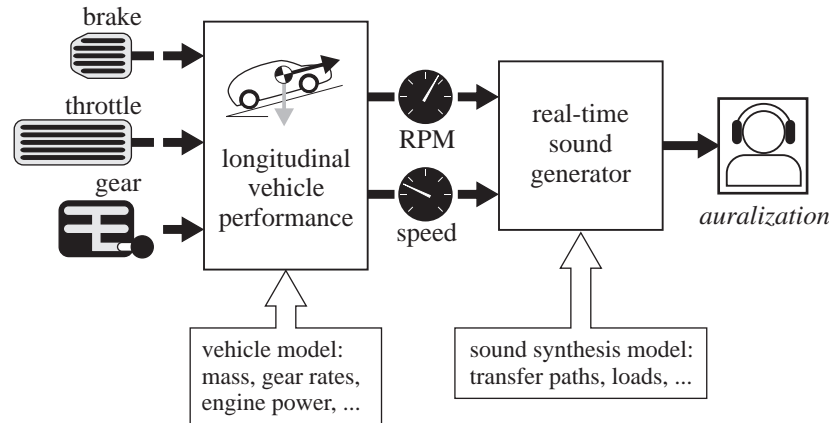


FIGURE 11: LMS Virtual Car Sound interface

implementation of the control systems (virtually or experimentally), as each implementation (feedback, feed-forward, narrowband, broadband, etc.) will act in a different way; a real-life application will hardly have a global effect on the sound field as such editing procedures would suggest, e.g., uncorrelated sources on a feedforward implementation will not be affected, even if in the targeted frequency band. A proper simulation scheme for the SQ assessment of active control is proposed and validated in Chapter 4 (de Oliveira et al., 2009).

The design of ASQC, the ultimate goal of this thesis, has been treated in some recent publications, as discussed in Section 1.3. Besides numerical validations and duct setups, ANC implementations of noise equalizers have been verified in 3D environments (listening rooms with speakers as primary and secondary sources). A more realistic implementation on a vehicle mockup is presented on Chapter 5 (de Oliveira et al., 2008), where the results for feedback and feedforward controllers are contrasted.

Another important aspect in the use of adaptive schemes is its capability of dealing with non-stationary disturbances, such as engine noise during acceleration. The improvement of convergence speed in LMS-based adaptive schemes is a recurrent issue (Bao et al., 1993; Paillard et al., 1995; Kuo and Morgan, 1996; Sun and Meng, 2006; Jones et al., 2007). Chapter 6 (de Oliveira et al., 2009) presents a

novel time domain implementation of an adaptive equalization scheme with improved convergence speed, specifically aiming at engine order equalization for vehicle SQ improvement.

1.5 Contributions

Based on the research goals presented in Section 1.1 and on the state-of-the art, the main contributions of this thesis are:

C1. A modelling procedure for smart structures design:

A general modelling/simulation procedure for ASAC is proposed, which is based on standard FE/FE vibro-acoustic modal models expressed in state-space form. In order to improve accuracy, the system model can be augmented to include sensor/actuator dynamics.

C2. New insights on active control of noise transmission:

The problem of reducing noise transmission from two cavities connected by a flexible firewall has been tackled with the aid of the aforementioned reduced models in a concurrent optimization scheme. The global optimal design results from a non-optimal passive structure, outperforms optimal sequential design.

C3. Sound quality post-processing tool:

The use of the aforementioned simulation scheme, together with more efficient numerical methods to calculate SQ-metrics allow the representation of SQ metrics in 3-dimensional colourmaps, which provides a better understanding of the system modification and/or the control action.

C4. Sound quality as a metric of control performance:

The use of SQ metrics as a measure of control performance is discussed. Standard controllers are evaluated and results are contrasted in this fashion.

C5. NEX-LMS:

A novel adaptive control scheme is proposed to enhance adaptation speed of the available adaptive control algorithms and enable SQ control. Vehicle NVH applications are foreseen, and an experimental validation with SQ-equivalent engine noise is performed.

The thesis contributions (C1~C5) are distributed among the following chapters, according to Fig. 12.

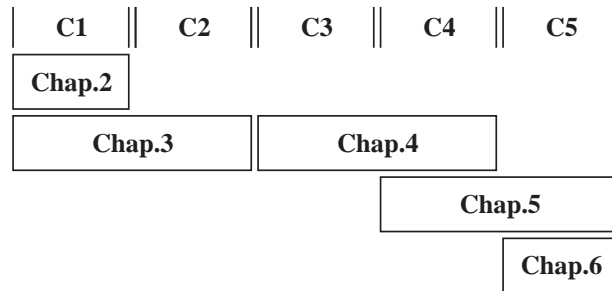


FIGURE 12: Distribution of the thesis main contributions among the reproduced papers

1.6 Thesis structure

The main body of this thesis consists of this introductory chapter, a collection of 5 papers, followed by a general conclusion. A short description follows:

Chapter 1: Places the work presented in this thesis in the context of active control and sound quality, with a special attention, but not only limited to, automotive applications.

Chapter 2: This paper, *In Press in Shock and Vibration*, presents the state-space modelling procedure and preliminary results regarding the use of feedback control on a vehicle mockup study case.

Chapter 3: This paper, published on the *Journal of Sound and Vibration* makes use of the proposed simulation scheme in a concurrent optimization, where structural and control parameters (firewall thickness, sensor/actuator position and feedback gain) are considered. The reduced models are experimentally validated for both passive and optimal active systems. Comparisons between

the standard design procedure and the proposed mechatronic approach reveal the added value of the latter. The counter intuitive results from this optimization gives new insights on the design of ASAC systems.

Chapter 4: This paper, published in *Mechanical Systems and Signal Processing* uses the SQ-metrics and the innovative 3d-colourmaps to evaluate the performance of the optimal feedback controller developed in Chapter 3. As expected, SQ is improved by considerably reducing the perceived loudness in the passenger compartment, although Roughness is not significantly affected. Extrapolation of the experimentally validated results also show that, besides using a single sensor/actuator pair on the firewall, global reduction is achieved in the passenger compartment.

Chapter 5: This paper, presented at the *Acoustics'08* conference, uses the SQ-metrics to evaluate the performance of the aforementioned feedback controller and contrast it with an adaptive feedforward scheme. The results related to the feedforward controller are preliminary and consider only a standard Fx-LMS algorithm. The issue of transient disturbance is raised but not tackled.

Chapter 6: This paper, submitted to *Mechanical Systems and Signal Processing*, presents a novel Active Sound Quality Control scheme, based on a modified version of the Fx-LMS algorithm, with improved convergence speed and equalization features that allow harmonic disturbance equalization. The basic principles are presented with a simple model and the concept is experimentally validated on a vehicle mockup. Results for stationary and transient engine disturbances are discussed.

Chapter 7: Formulates the general conclusion of this thesis, binding together the findings presented in the selected papers and provide recommendations for future work.

Addendum A complete list of references is provided in the Bibliography. The author's CV and list of publication are also provided.

1.7 Conclusions

This introductory chapter presents a review on the state-of-the art on active control, its applications on the mobility industry and, more recently, on sound quality improvement. It also positions the work performed during this doctoral program on the subject and indicates research opportunities related to simulation and optimization of smart systems and active control for sound quality.

Active control of noise (ANC or ASAC) has found successful application in academic research, although a few applications can be found in the market. The main reasons identified are the cost involved and certain market resistance, partially due to customers and partially to the OEMs themselves. However, as vehicles are getting ever more control systems, hence, sensors, actuators and microcontrollers and, with the recent need for sound branding and adaptation of global products to local markets' expectations, the widespread of active solutions for the improvement of perceived vehicle noise might eventually happen.

Based on such expectations, active control for sound quality has recently gained attention, which leads to other issues such as: evaluation of existing techniques facing the new perception criteria, adequate choice of SQ metrics, control design for SQ, convergence speed of adaptive controllers, etc.

Another important aspect related to the use of active control in mass-produced products is its inclusion on the product development cycle which, as discussed in this chapter, requires the development of simulation tools as well as a change in the design procedure itself.

Chapter 2

A state-space modelling approach for active structural acoustic control

Leopoldo P.R. de Oliveira
Paulo S. Varoto
Paul Sas
Wim Desmet

A preliminary version of this paper was presented at the XII DINAME in February 2007 - Ilhabela, Brazil. This final version is accepted for publication on Shock and Vibration.

L.P.R. de Oliveira, P.S. Varoto, P. Sas and Wim Desmet, A state-space modelling approach for active structural acoustic control *Proceedings of the XII International Symposium on Dynamic Problems of Mechanics - DINAME 2007*, Ilhabela-SP, Brazil, 10pp.

L.P.R. de Oliveira, P.S. Varoto, P. Sas and Wim Desmet, A state-space modelling approach for active structural acoustic control *Accepted for publication on the Journal of Shock and Vibration*.

Equation (13) has been edited to fit the thesis borders.

Figures 2 and 13 have been edited to fit the thesis borders.

The state-space formulation presented in this paper is also part of the paper in Chapter 3, *Concurrent mechatronic design approach for active control of cavity noise*.

Abstract

The demands for improvement in sound quality and reduction of noise generated by vehicles are constantly increasing, as well as the penalties for space and weight of the control solutions. A promising approach to cope with this challenge is the use of active structural-acoustic control. Usually, the low frequency noise is transmitted into the vehicle's cabin through structural paths, which raises the necessity of dealing with vibro-acoustic models. This kind of models should allow the inclusion of sensors and actuators models, if accurate performance indexes are to be accessed. The challenge thus resides in deriving reasonable sized models that integrate structural, acoustic, electrical components and the controller algorithm. The advantages of adequate active control simulation strategies relies on the cost and time reduction in the development phase. Therefore, the aim of this paper is to present a methodology for simulating vibro-acoustic systems including this coupled model in a closed loop control simulation framework that also takes into account the interaction between the system and the control sensors/actuators. It is shown that neglecting the sensor/actuator dynamics can lead to inaccurate performance predictions.

1. Introduction

The demands for improvement in sound quality and reduction of noise generated by vehicles are constantly increasing, as well as the penalties for space and weight of the passive control solutions. A promising approach to cope with this challenge is the use of active structural-acoustic control (ASAC). During the design phase, simulation plays an important role in predicting the performance and feasibility of active control solutions. As a result, the demands for more reliable simulation techniques are also ever-increasing. The advantages of adequate simulation strategies rely on the time and cost reduction in the development phase, enabling the engineer to try different schemes, sensors and actuators configuration and control strategies with minimum physical prototyping. Usually, the low frequency noise is transmitted into the vehicle cabin through structural paths, which raises the necessity of dealing with vibro-acoustic models. This kind of models allows the use of acoustic disturbance and secondary sources. It should also allow the inclusion of sensors and actuators models, not only in the sense that their own dynamics may significantly change the original system dynamics, but also that they can pose frequency, phase or amplitude limitations to the control performance. The challenge thus resides in deriving reasonable sized models that integrate acoustic, structural and electrical components together with the controller algorithm.

Therefore, the aim of this paper is to present a methodology for simulating vibro-acoustic systems, including this coupled model in a closed loop control simulation framework that also takes into account the interaction between the system and the control actuators and sensors. This methodology consists of deriving a fully coupled finite element (FE) model of the vibro-acoustic system which is reduced and formulated as a modal state-space model into Matlab/Simulink, where, eventually, models for sensors and actuators are included and the controller implemented.

To demonstrate the proposed modelling procedure, a vehicle mock-up is selected (Fig. 1). It consists of a simplified car cavity with rigid walls, to provide well-defined acoustic boundary conditions, thus avoiding uncertainties during the vibro-acoustic modelling phase. A sound source placed in the engine compartment (EC) works as a primary dis-

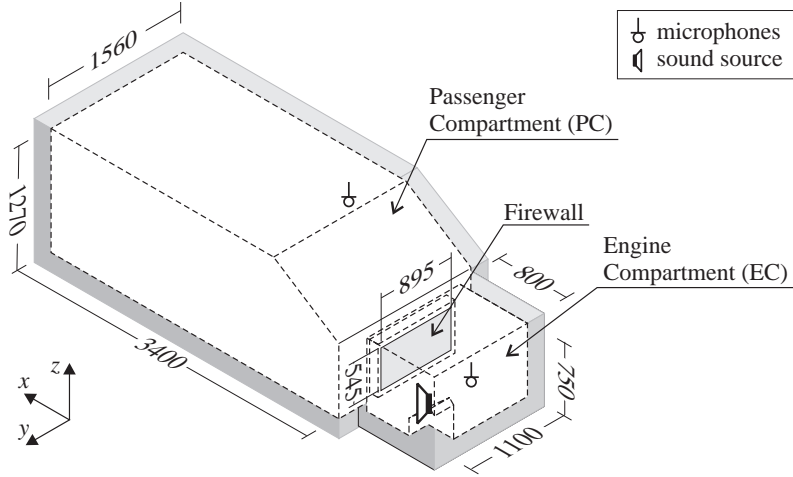


FIGURE 1: Schematic view of the system under study (dimensions in mm)

turbance source. A flexible firewall allows the noise generated in the engine compartment (EC) to be transmitted to the passenger compartment (PC). Collocated velocity feedback is selected as control strategy, due to its relatively simple implementation and guaranteed stability. Decentralized collocated sensor/actuator pairs (SAPs) are placed on the firewall in order to reduce the noise transmitted from the EC to the PC.

The modelling procedure for the fully coupled vibro-acoustic system, the modal state-space formulation and the SAP models are presented in Section 2. The numerical results for the passive and the selected active systems are treated in Section 3. Finally, some conclusions are addressed in Section 4.

2. Modelling Procedure

Bringing research results on intelligent materials to the level of industrial applications requires the design processes of active systems to become part of the complete product development cycle. In other words, it is necessary to extend the use of simulation models, which

are the cornerstone of today's design process, to enable the integration of advanced materials, active systems, actuators, sensors and control algorithms. Moreover, it must be possible to integrate these models into system level virtual prototype models [1]. It is clear that no single integrated solution will be able to fulfil all requirements of the various material and control approaches; therefore the focus of this research is on supporting, as much as possible, the use, combination and extension of existing codes and tools.

Considering a closed compartment, any airborne noise generated outside this cavity can only be perceived by the occupants if transmitted through structural paths. That is the case of the engine noise generated in the EC, which is transmitted to the PC via the firewall. This fluid-structure interaction imposes the necessity of dealing with fully coupled vibro-acoustic models, which are usually computationally expensive. An advantage though, is that fully coupled FE models allow the use of simultaneous acoustic and structural inputs and outputs, which, from the controller perspective, means being able to include either structural or acoustic disturbance, secondary sources and sensors of either kind. Another advantage of using fully-coupled vibro-acoustic models is the accuracy of the estimated control performance, as an uncoupled analysis can overestimate the controller efficiency [2].

Therefore, the first challenges in ASAC simulation resides in deriving reasonable sized vibro-acoustic models which can be integrated in the control simulation environment. This can be accomplished by deriving a fully coupled FE model of the vibro-acoustic system, which is reduced and formulated as a state-space model into Matlab/Simulink where the controller is implemented (Fig. 2).

The models for sensors and actuators can be included directly in the control design environment. If done in this phase, any eventual changes in the SAPs (positions, specifications or even kind) will not demand a recalculation of the full vibro-acoustic system. The inclusion of sensor and actuator models contributes for the model accuracy, not only in the sense that their own dynamics may significantly change the original system response, but also that they can present frequency, phase or amplitude limitations to the control performance.

The full modelling procedure for the present case study is illustrated in Fig. 2. It starts with uncoupled structural and acoustic FE models for the structure and the cavities. An uncoupled modal base is extracted for both models. The vibro-acoustic FE model consists of

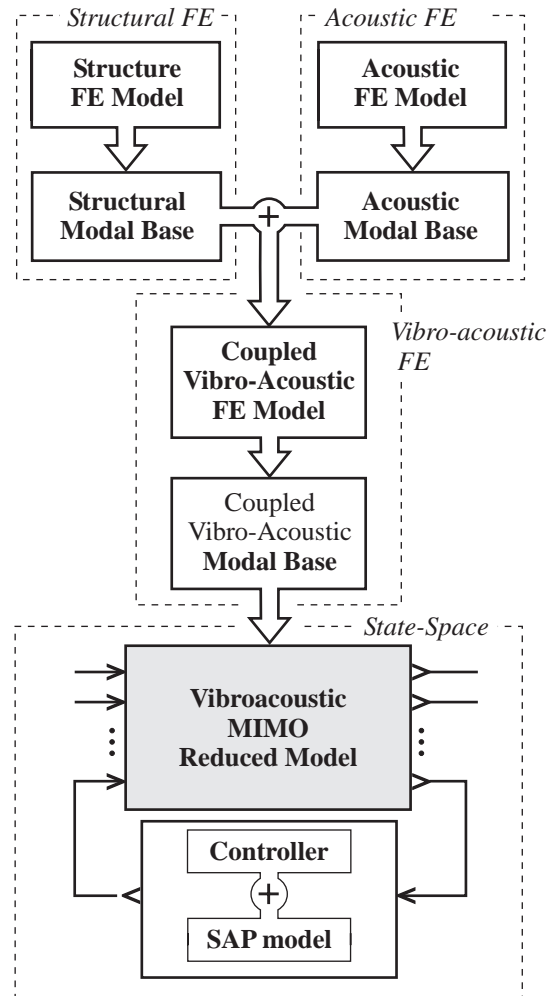


FIGURE 2: Modelling procedure scheme

a modal model with a coupled modal base built with the uncoupled modal bases. The vibro-acoustic modal base is then used to derive a state-space model, which can be used in the control design environment. The different model types and software used for each component are shown in Tab.1. If the sensor and/or actuator electro-mechanical be-

haviour is considered to be negligible, this modal state-space model allows the implementation of control systems with idealized inputs and outputs, namely structural force and volume velocity excitation. Some preliminary results can be achieved with such models, although an accurate access of the controller performance requires a more comprehensive model of the SAP. The next sub-sections describe in detail each one of the required steps.

TABLE 1: Component model type and software

component	model type	software
cavities	FEM	LMS.Sysnoise
firewall	FEM	Patran/Nastran
inertial shaker	state-space	Matlab/Simulink
controller	state-space	Matlab/Simulink

2.1 Vibro-acoustic modelling

One of the coupled vibro-acoustic FE/FE formulation is the Eulerian, in which the structural degrees of freedom (DoFs) are displacement vectors, while the acoustic DoFs are expressed as scalar functions. The latter is usually the acoustic pressure, which yields non-symmetrical mass and stiffness matrices, posing a disadvantage to FE solvers [3,4].

The vibro-acoustic FE modelling of vehicle interiors always requires the setup of FE meshes for both, vehicle structure and interior cavities. Since the acoustic wavelengths are usually longer than the structural ones in the low frequency range, an optimized acoustic mesh can be much coarser than the structural mesh. However, if the meshes are compatible, some intermediate numerical steps can be neglected resulting in a simplified procedure [5]. Therefore a trade-off choice for the size of structural and acoustic FE meshes was taken. In this way, they present coinciding nodes without affecting the accuracy of the predicted results within the frequency range of interest (0 to 200Hz).

The structural mesh is shown in Fig. 3(a) with a total of 231 nodes and 200 4-noded shell elements. The steel firewall, 1.5mm thick, presents 13 modes from 0 to 200Hz. The structural mode shape presenting

the shortest wavelength is the [5;1] well described by this number of elements (Fig. 3b).

The element type chosen for the acoustic mesh is the 8-noded brick (hexahedral), not only by the smaller number of elements needed, but also due to its higher accuracy in post processing pressure derived quantities (velocity and sound intensity) when compared to tetrahedral elements [6]. The maximum frequency of interest (200Hz for this case study) was also taken into account, so that the acoustic model could have the minimum number of elements. The resulting mesh (with 26050 elements and 23196 acoustic DoFs) and the highest mode shape in the frequency band are depicted in Fig. 4. With respect to the elements size, this acoustic model is valid until 514Hz, considering 6 elements per wavelength, which is fairly suitable for this application. As mentioned before, the structural and acoustic models are fully-coupled in this FE/FE modelling approach. The effect of the interfacing fluid on the structure dynamics can be considered as a pressure load on the wet surface, thus turning the structural differential equation into the form of Eq. (1).

$$(\mathbf{K}_s + j\omega\mathbf{D}_s - \omega^2\mathbf{M}_s)\mathbf{u}(\omega) + \mathbf{K}_c\mathbf{p}(\omega) = \mathbf{F}_s(\omega) \quad (1)$$

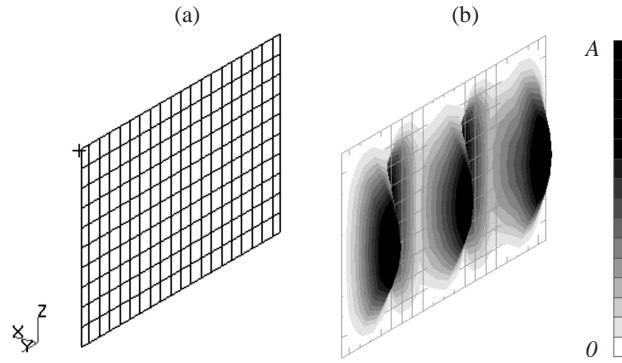


FIGURE 3: Firewall: (a) FE mesh and (b) structural mode at 160Hz [5;1]

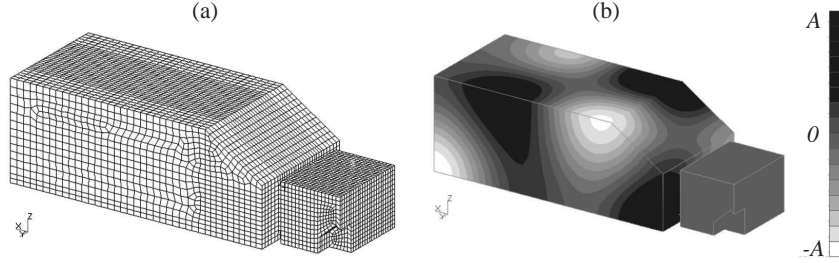


FIGURE 4: Mock-up cavities: (a) FE mesh and (b) uncoupled mode at 192.5Hz

where \mathbf{K}_s , \mathbf{D}_s and \mathbf{M}_s are, respectively, the stiffness, damping and mass matrices of the structural component, \mathbf{K}_c is the coupling matrix, \mathbf{u} is the vector of structural displacement DoFs, \mathbf{p} is the vector of nodal acoustic pressures and \mathbf{F}_s is the structural load vector.

In a similar way, the structural vibration works as an extra acoustic input and therefore must be taken into account as:

$$(\mathbf{K}_a + j\omega\mathbf{D}_a - \omega^2\mathbf{M}_a)\mathbf{p}(\omega) + \omega^2\mathbf{M}_c\mathbf{u}(\omega) = \mathbf{F}_a(\omega) \quad (2)$$

where \mathbf{K}_a , \mathbf{D}_a and \mathbf{M}_a are the acoustic stiffness, damping and mass matrices, \mathbf{M}_c is the coupling matrix and \mathbf{F}_a is the acoustic load vector. For the sake of brevity, any frequency dependent function ‘ $h(\omega)$ ’ is represented just as ‘ h ’ hereafter.

Regarding the special relation, $\mathbf{M}_c = -\rho_0\mathbf{K}_c^T$ [7,8], the combined system of equations in this Eulerian FE/FE formulation yields:

$$\left(\begin{bmatrix} \mathbf{K}_s & \mathbf{K}_c \\ \mathbf{0} & \mathbf{K}_a \end{bmatrix} + j\omega \begin{bmatrix} \mathbf{D}_s & \mathbf{0} \\ \mathbf{0} & \mathbf{D}_a \end{bmatrix} - \omega^2 \begin{bmatrix} \mathbf{M}_s & \mathbf{0} \\ -\rho_0\mathbf{K}_c^T & \mathbf{M}_a \end{bmatrix} \right) \begin{Bmatrix} \mathbf{u} \\ \mathbf{p} \end{Bmatrix} = \begin{Bmatrix} \mathbf{F}_s \\ \mathbf{F}_a \end{Bmatrix} \quad (3)$$

Based on Eq. (3) it is clear that the resulting vibro-acoustic system is coupled, though it is no longer symmetric. As a consequence of this non-symmetric nature, the solution of the associated undamped eigenproblem is computationally more demanding and results in different left and right eigenvectors:

$$\begin{bmatrix} \mathbf{K}_s & \mathbf{K}_c \\ \mathbf{0} & \mathbf{K}_a \end{bmatrix} \{\Phi_R\}_r = \omega_r^2 \begin{bmatrix} \mathbf{M}_s & \mathbf{0} \\ -\rho_0 \mathbf{K}_c^T & \mathbf{M}_a \end{bmatrix} \{\Phi_R\}_r, \quad (4)$$

$r = 1, \dots, n_a + n_s$

$$\{\Phi_L\}_r^T \begin{bmatrix} \mathbf{K}_s & \mathbf{K}_c \\ \mathbf{0} & \mathbf{K}_a \end{bmatrix} = \omega_r^2 \{\Phi_L\}_r^T \begin{bmatrix} \mathbf{M}_s & \mathbf{0} \\ -\rho_0 \mathbf{K}_c^T & \mathbf{M}_a \end{bmatrix}, \quad (5)$$

$r = 1, \dots, n_a + n_s$

where r is the index of the coupled natural frequency ω_r and Φ_L and Φ_R are, respectively, the left and right coupled modes, n_a and n_s are the number of retained acoustic and structural modes, respectively.

Moreover, it has been indicated [8] that, for the Eulerian formulation, the left and right eigenvectors can be related as:

$$\{\Phi_L\}_r = \begin{Bmatrix} \{\Phi_{Ls}\}_r \\ \{\Phi_{La}\}_r \end{Bmatrix} = \begin{Bmatrix} \{\Phi_{Rs}\}_r \omega_r^2 \\ \{\Phi_{Ra}\}_r \end{Bmatrix} \quad r = 1, 2, \dots, n_s + n_a \quad (6)$$

A common practice in solving such vibro-acoustic problems is the use of component mode synthesis (CMS). It consists of expanding the structural DoFs in terms of a set of N_s uncoupled structural modes $\Phi_s \in \mathbb{R}^{n_s \times 1}$ (without any acoustic pressure load along the coupling interface), as well as expanding the acoustic DoFs in terms of a set of N_a uncoupled acoustic modes $\Phi_a \in \mathbb{R}^{n_a \times 1}$ (acoustic boundaries considered rigid at the wetted surface). The structural and acoustic expansions become, respectively,

$$\mathbf{u} = \sum_{r=1}^{N_s} q_{s_r} \{\Phi_s\}_r = \Phi_s \mathbf{q}_s \quad (7)$$

$$\mathbf{p} = \sum_{r=1}^{N_a} q_{a_r} \{\Phi_a\}_r = \Phi_a \mathbf{q}_a \quad (8)$$

where \mathbf{q}_s is the vector of modal amplitudes related to the structural DoFs, \mathbf{q}_a is the vector of modal amplitudes related to the acoustic DoFs and r is the index representing the number of the mode.

This procedure yields non-symmetrical coupled modal stiffness and mass matrices. Therefore, obtaining the modal state-space representation of a reduced model derived from CMS can be a difficult task, since it is necessary to invert the coupled modal mass matrix (which is non-diagonal) and the coupling matrix should be fully available.

An alternative to describe a modal state-space for a fully coupled vibro-acoustic system is to apply a variable substitution to the coupled eigenproblem related to Eq. (3) [9]. This procedure is detailed hereafter.

Substituting the component mode expansions in Eqs. (7) and (8) into Eq. (3) and pre-multiplying the structural and acoustic parts of the resulting matrix equation, respectively, with the transpose of the structural and acoustic modal vectors yields the undamped modal representation:

$$-\omega^2 \begin{bmatrix} \Phi_s^T \mathbf{K}_s \Phi_s & \Phi_s^T \mathbf{K}_c \Phi_a \\ \mathbf{0} & \Phi_a^T \mathbf{K}_a \Phi_a \end{bmatrix} \begin{Bmatrix} \mathbf{q}_s \\ \mathbf{q}_a \end{Bmatrix} - \omega^2 \begin{bmatrix} \Phi_s^T \mathbf{M}_s \Phi_s & \mathbf{0} \\ -\rho_0 \Phi_a^T \mathbf{K}_c^T \Phi_s & \Phi_a^T \mathbf{M}_a \Phi_a \end{bmatrix} \begin{Bmatrix} \mathbf{q}_s \\ \mathbf{q}_a \end{Bmatrix} = \begin{Bmatrix} \Phi_s^T \mathbf{F}_s \\ \Phi_a^T \mathbf{F}_a \end{Bmatrix} \quad (9)$$

Since each uncoupled mode is normalized with respect to the uncoupled mass matrices, the homogeneous system of equations related to Eq. (9) can be written as:

$$\begin{bmatrix} \Omega_s^2 - \omega^2 \mathbf{I} & \Phi_s^T \mathbf{K}_c \Phi_a \\ \omega^2 \Phi_a^T \mathbf{K}_c^T \Phi_s & -\frac{1}{\rho_0} (\Omega_a^2 - \omega^2 \mathbf{I}) \end{bmatrix} \begin{Bmatrix} \mathbf{q}_s \\ \mathbf{q}_a \end{Bmatrix} = \begin{Bmatrix} \mathbf{0} \\ \mathbf{0} \end{Bmatrix} \quad (10)$$

where Ω_s and Ω_a are, respectively, the structural and acoustic diagonal matrices of uncoupled natural frequencies. Equation (10) still results in a non-symmetric eigenproblem and is therefore expensive to solve. The first line of Eq. (10) leads to:

$$\mathbf{q}_s = \omega^2 (\Omega_s^2)^{-1} \mathbf{q}_s - (\Omega_s^2)^{-1} \Phi_s^T \mathbf{K}_c \Phi_a \mathbf{q}_a \quad (11)$$

Applying the substitution $\bar{\mathbf{q}}_s = \omega^2 \mathbf{q}_s$ in Eq. (11) yields:

$$\begin{Bmatrix} \mathbf{q}_s \\ \mathbf{q}_a \end{Bmatrix} = \begin{bmatrix} (\Omega_s^2)^{-1} & -(\Omega_s^2)^{-1} \Phi_s^T \mathbf{K}_c \Phi_a \\ \mathbf{0} & \mathbf{I} \end{bmatrix} \begin{Bmatrix} \bar{\mathbf{q}}_s \\ \mathbf{q}_a \end{Bmatrix} \quad (12)$$

Using Eq. (12) it is possible to rewrite Eq. (10) as a symmetric system of equations in $\{\bar{\mathbf{q}}_s \quad \mathbf{q}_a\}^T$:

$$\begin{bmatrix} \mathbf{T}_s & \mathbf{T}_c^T \\ \mathbf{T}_c & \mathbf{T}_a \end{bmatrix} \begin{Bmatrix} \bar{\mathbf{q}}_s \\ \mathbf{q}_a \end{Bmatrix} = \begin{Bmatrix} \mathbf{0} \\ \mathbf{0} \end{Bmatrix}, \quad (13)$$

$$\mathbf{T}_s = \mathbf{I} - \omega^2(\boldsymbol{\Omega}_s^2)^{-1},$$

$$\mathbf{T}_c = \omega^2(\boldsymbol{\Omega}_s^2)^{-1}\boldsymbol{\Phi}_a^T\mathbf{K}_c^T\boldsymbol{\Phi}_s,$$

$$\mathbf{T}_a = -\frac{1}{\rho_0}(\boldsymbol{\Omega}_a^2 - \omega^2\mathbf{I}) - \omega^2\boldsymbol{\Phi}_a^T\mathbf{K}_c^T\boldsymbol{\Phi}_s(\boldsymbol{\Omega}_s^2)^{-1}\boldsymbol{\Phi}_s^T\mathbf{K}_c\boldsymbol{\Phi}_a.$$

The coupled modal vector $\bar{\boldsymbol{\Phi}}$, resulting from the eigenproblem associated with Eq. (13) can be interpreted as the left eigenvector $\boldsymbol{\Phi}_L$ of the eigenproblem in Eq. (6) on. The right eigenvector $\boldsymbol{\Phi}_R$ can be retrieved using Eq. (6).

Since the uncoupled bases $\boldsymbol{\Phi}_a$ and $\boldsymbol{\Phi}_s$ result from symmetric eigenproblems, solving Eq. (13) may seem less demanding when compared to the solution of Eqs. (5) and (6). However, the reduction on the computational effort is rather small, as to accurately represent the coupled modes, it is necessary to retain a higher number of uncoupled modes. Nevertheless, the advantage of this method is the possibility of using dedicated software for each component uncoupled modal analysis.

2.2 Reduced State-Space formulation

Starting from the first order generalized state-space representation:

$$\dot{\mathbf{x}} = \mathbf{A}\mathbf{x} + \mathbf{B}\mathbf{F} = \begin{bmatrix} \mathbf{0} & \mathbf{I} \\ -\mathbf{M}^{-1}\mathbf{K} & -\mathbf{M}^{-1}\mathbf{C} \end{bmatrix} \mathbf{x} + \begin{bmatrix} \mathbf{0} \\ \mathbf{b} \end{bmatrix} \mathbf{F} \quad (14)$$

$$\mathbf{y} = \mathbf{C}\mathbf{x} = [\mathbf{c} \quad \mathbf{0}] \mathbf{x} \quad (15)$$

where \mathbf{M} , \mathbf{C} and \mathbf{K} are respectively the full mass, damping and stiffness matrices, \mathbf{x} is the vector of states, \mathbf{F} is the load vector, \mathbf{y} is the output vector and \mathbf{b} and \mathbf{c} are rectangular matrices with ones on the desired DoFs positions and zeros everywhere else.

In this formulation, structural and acoustic DoFs are projected using the modal bases $\boldsymbol{\Phi}_L$ and $\boldsymbol{\Phi}_R$ and the modal coordinate \mathbf{q} using the following expansion:

$$\begin{Bmatrix} \mathbf{u} \\ \mathbf{p} \end{Bmatrix} = \sum_{r=1}^{N_s+N_a} q_r \boldsymbol{\Phi}_{Rr} = \boldsymbol{\Phi}_R \mathbf{q} \quad (16)$$

Moreover, the left and right eigenvectors are normalized such that:

$$\Phi_L^T \begin{bmatrix} \mathbf{K}_s & \mathbf{K}_c \\ \mathbf{0} & \mathbf{K}_a \end{bmatrix} \Phi_R = \Omega^2 \quad (17)$$

$$\Phi_L^T \begin{bmatrix} \mathbf{D}_s & \mathbf{0} \\ \mathbf{0} & \mathbf{D}_a \end{bmatrix} \Phi_R = \Gamma \quad (18)$$

$$\Phi_L^T \begin{bmatrix} \mathbf{M}_s & \mathbf{0} \\ -\rho_0 \mathbf{K}_c^T & \mathbf{K}_a \end{bmatrix} \Phi_R = \mathbf{I} \quad (19)$$

where \mathbf{I} , Ω^2 and Γ are, respectively, the identity, the squared coupled natural frequencies and the modal damping matrices.

Applying the modal expansion described by Eq. (16) into Eq. (3) and pre-multiplying it by Φ_L^T , yields:

$$\begin{aligned} & \Phi_L^T \begin{bmatrix} \mathbf{K}_s & \mathbf{K}_c \\ \mathbf{0} & \mathbf{K}_a \end{bmatrix} \Phi_R \mathbf{q} + \Phi_L^T \begin{bmatrix} \mathbf{D}_s & \mathbf{0} \\ \mathbf{0} & \mathbf{D}_a \end{bmatrix} \Phi_R \dot{\mathbf{q}} \\ & + \Phi_L^T \begin{bmatrix} \mathbf{M}_s & \mathbf{0} \\ -\rho_0 \mathbf{K}_c^T & \mathbf{M}_a \end{bmatrix} \Phi_R \ddot{\mathbf{q}} = \Phi_L^T \begin{Bmatrix} \mathbf{F}_s \\ \mathbf{F}_a \end{Bmatrix} \end{aligned} \quad (20)$$

Recalling Eqs. (14) and (15), the relations described in Eqs. (17), (18) and (19) allow Eq. (20) to be rewritten in a modal state-space form:

$$\begin{Bmatrix} \dot{\mathbf{q}} \\ \mathbf{q} \end{Bmatrix} = \begin{bmatrix} \mathbf{0} & \mathbf{I} \\ -\Omega^2 & -\Gamma \end{bmatrix} \begin{Bmatrix} \mathbf{q} \\ \dot{\mathbf{q}} \end{Bmatrix} + \begin{bmatrix} \mathbf{0} \\ \Phi_L^T \mathbf{b} \end{bmatrix} \begin{Bmatrix} \mathbf{F}_s \\ \mathbf{F}_a \end{Bmatrix} \quad (21)$$

$$\begin{Bmatrix} \mathbf{u}_o \\ \mathbf{p}_o \end{Bmatrix} = \begin{bmatrix} \mathbf{c} \Phi_R & \mathbf{0} \end{bmatrix} \begin{Bmatrix} \mathbf{q} \\ \dot{\mathbf{q}} \end{Bmatrix} \quad (22)$$

In this way, a fully coupled vibro-acoustic system can be written in a reduced modal state-space formulation with order $(2N \times 2N)$. Since the coupled vibro-acoustic model is derived from uncoupled structural and acoustic modal bases, it is necessary to retain a higher number of modes in order to accurately represent the dynamic behaviour in the desired frequency range. Therefore, both uncoupled modal bases were evaluated up to 400 Hz, which is adequate to represent the vibro-acoustic system in the frequency range of interest (0 to 200Hz). Applying the aforementioned procedure, the original 24192 DoFs (23196 unconstrained acoustic and 1026 unconstrained structural) have been reduced to a SS model with 214 states related to the 107 coupled modes

in the 0 to 400Hz frequency range. The inputs can comprise forces applied to the firewall and volume velocity sources in either the cavities. The outputs are structural displacement and acoustic pressure.

2.3 SAP model

In active control, sensors, actuators and structure are put together in such a way that the level of interaction between those elements turns any separately approach of the subsystems impossible [10]. Therefore, a unifying approach that takes into account the fully coupled system is needed. Among the present solutions are those based on the inclusion of sensor, actuators and control laws models into CAE software such as FE, multibody systems (MBS), etc [11]. Another possible solution, when two time domain simulations are involved, is the co-simulation, usually applied to MBS models and a controller in Simulink [12]. Finally, the methodology adopted in this work involves the inclusion of a reduced model of the vibro-acoustic systems into the control system design environment (Matlab/Simulink), where the interaction between structure and sensor/actuator is eventually taken into account.

A set of collocated SAPs is placed on the firewall to realize the collocated velocity feedback in order to reduce the noise transmitted from the EC to the PC (Fig. 5a). Collocated accelerometers and inertial shakers are used as structural SAPs. Appropriate accelerometers are selected, for the frequency range of interest, such that the voltage signal generated by these devices can be considered proportional to the measured quantity. However, for the inertial shakers, a more detailed model for the electro-mechanical coupling within the actuator and its interaction with the structure is considered.

The causes and effects of the interaction between electrodynamic exciters and the structure under test (SUT) has been an issue for the experimentalists since the very beginning of modal analysis as in [13,14] and still is a subject of research [15-18]. Figure 6 shows the electro-mechanical model of an inertial shaker. Equations (23) and (24) describe the dynamics of the coupled electro-mechanical system with the amplifier set in voltage mode of operation. As it can be seen, the coupling occurs in Eq. (23) as the right-hand side expresses the magnetic force (acting on the moving mass m_i) proportionally to the current I flowing on the circuit; and in Eq. (24) in which the electric potential $k_f(\dot{u}_i - \dot{u}_s) = E_{bemf}$ is the voltage generate by the movement of coil in the magnetic field, thus written in terms of the relative velocity

between the SUT driving point and the shaker moving mass. More detailed information about the shaker dynamics as well as the amplifier modes of operation can be found in [16,17].

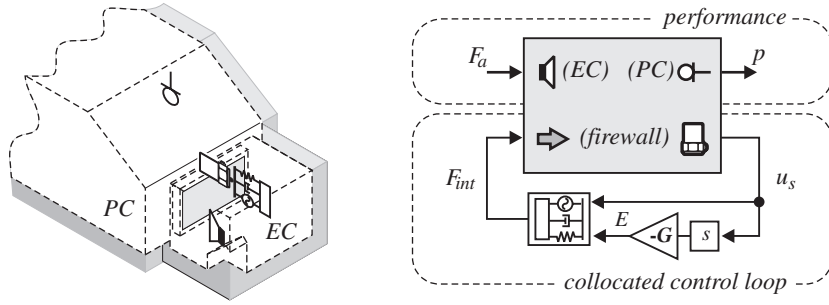


FIGURE 5: Control scheme (a) positions of sensors and actuators and (b) block diagram

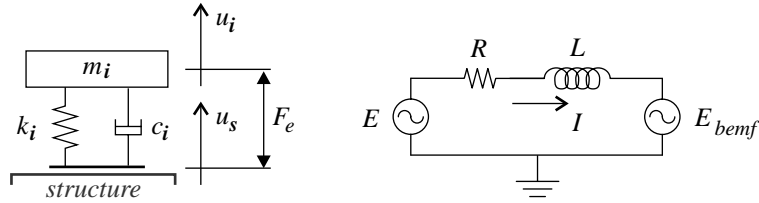


FIGURE 6: Electro-mechanical model of an inertial shaker: (a) mechanical and (b) electrical model

$$m_i \ddot{u}_i + c_i (\dot{u}_i - \dot{u}_s) + k_i (u_i - u_s) = k_f I \quad (23)$$

$$RI + L\dot{I} + k_f (u_i - u_s) = E \quad (24)$$

As mentioned before, the objective of the proposed modelling procedure is to include the actuator (considering its interaction with the SUT) in the controller design environment. At this point, the SUT is represented by a reduced modal model, from which the displacement of the driving point is available. Since the shaker is rigidly connected to

the structure, the movement of the base will be the same as the SUT driving point. In this way the inertial shaker can be represented by the moving mass and the active interface (passive suspension plus electromagnetic force). As proposed by [19] for a hybrid isolation mount, the shaker active interface can also be modelled as a lumped impedance element that contains the passive and active parameters (Fig. 7). Thus, it is possible to include one or more inertial shakers, given the driving point displacements and the driving voltage E . It is important to state that the feedback gain(s) for the structural SAP(s) should be optimized with respect to the pressure at the driver's ear, rather than the firewall vibration. This ASAC strategy is applicable when the acoustic source is transmitted into a cavity through a limited number of structural paths [20]. As shown in Fig. 5(b), in the adopted ASAC strategy, the structural sensors and actuators are involved in the control loop whereas the performance is evaluated at the acoustic sensor.

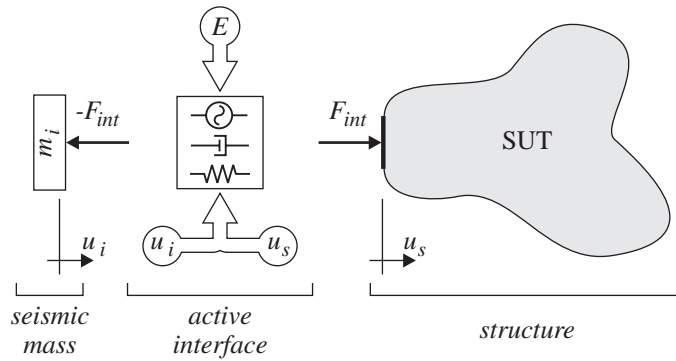


FIGURE 7: Inertial shaker active interface model

3. Results

The next subsections show the simulation results obtained using the proposed methodology. Subsection 3.1 deals with the passive system simulation and the interaction between the firewall and the exciter, while 3.2 shows how the modelling procedure can be applied to ASAC simulations where one or more SAPs are used in velocity feedback

controllers.

3.1 Passive results

A 2-input/2-output state-space model has been built (Fig. 5b). The structural and acoustical inputs are respectively, the force (F_{int}) and the volume velocity (F_a); the outputs are the collocated displacement (u_s) on the firewall driving point and pressure (p) at the driver's head position.

Figure 8 illustrates the forced responses calculated with the state-space model for both kinds of inputs: volume-velocity ($1 \times 10^{-6} \text{m}^3/\text{s}$) from the acoustic source in the EC and normal force (1N) at an arbitrary position on the firewall. The graphics show the pressure at the driver's head position and the displacement from the driving point on the firewall. From these graphs, it can be seen that the model is indeed

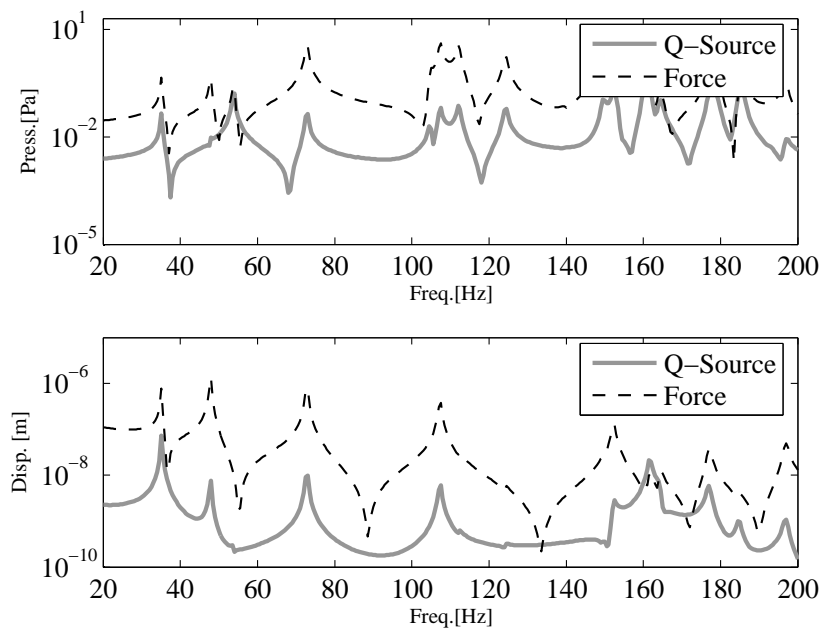


FIGURE 8: State-space forced responses: (a) acoustic output and (b) structural output

coupled.

The forced responses on Fig. 8 came merely from the system transfer functions, i.e., the input force is assumed ideal. However, if the model of the exciter is included in the simulation, it is possible to observe phenomena inherent to the use of such electrodynamic devices, *e.g.* force drop-off. Figure 9 shows, in the upper part, the structural FRF and in the lower part, a comparison of the idealized force input and the actual load provided by an inertial shaker. It can be seen that in the low frequency range and in the vicinities of structural resonances, the force level drops, as a result of shaker/structure interaction [13,16].

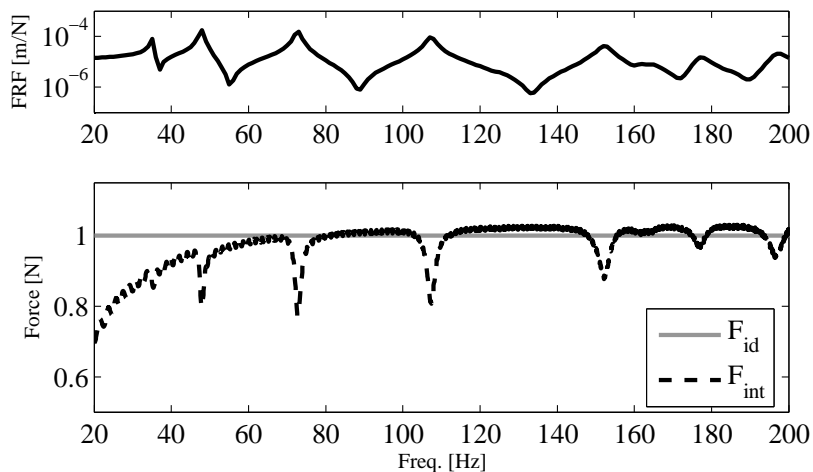


FIGURE 9: System driving point FRF and input forces

The mass loading and drops in the excitation force can lead to errors in the experimental FRFs [17,18] but mainly, as far as the active control system is concerned, can result in overestimated authority and performance.

3.2 ASAC Simulation

The choice of using only structural sensors and actuators in this ASAC approach is based on the robustness of the control system. Since feedback is going to be used, an important aspect to the efficiency and

stability of the control system is the transfer function between the sensor and actuator. The phase angle between these two signals should be bounded by $\pm 90^\circ$, otherwise the system can become unstable. Usually, the use of acoustic sensors and/or actuators presents a fast phase loss, which would impose severe limitations to the controller frequency range [20]. However, since the SAP is collocated it can be proved that the control system acts in fact like a passive system and stability is always guaranteed, independent of the feedback gain [10, 21].

Also, the structural transfer functions are much less sensitive to typical changes in this kind of systems, such as open window or the placement of more people inside the vehicle. On the other hand, the control system just senses (directly) the structural DoFs. As a result, it is expected that only the predominantly structural resonances will be affected by the controller, while the predominantly acoustic ones may not be.

The description of the vibro-acoustic system as a state-space modal model allows closed-loop simulations in time and frequency domain. The collocated velocity feedback control loop can be implemented in Matlab/Simulink (Fig. 10a).

The basic principle of this controller is to feed the actuator with an amplified voltage proportional to the velocity from its collocated sensor. Therefore, the inertial shaker block is connected to the structural input/output ports of the state-space model in a velocity feedback configuration. Figure 10(b) shows in more detail the inertial shaker block diagram. The structure driving point and the shaker moving mass displacements (and velocities) are used, together with the input voltage, to compute the interface force (F_{int}) acting on the system.

Equation 25 is the differential equation governing the block diagram in Fig. 10(b). It is based on Eqs. (23) and (24) where the coil inductance is neglected as suggested by [22,23]. Since the system is in a velocity feedback configuration, the input voltage E will be proportional to the driving point velocity (Fig. 10a).

$$m_i \ddot{u}_i + \left(d_i + \frac{k_f^2}{R} \right) (\dot{u}_i - \dot{u}_s) + k_i (u_i - u_s) = \frac{k_f}{R} E \quad (25)$$

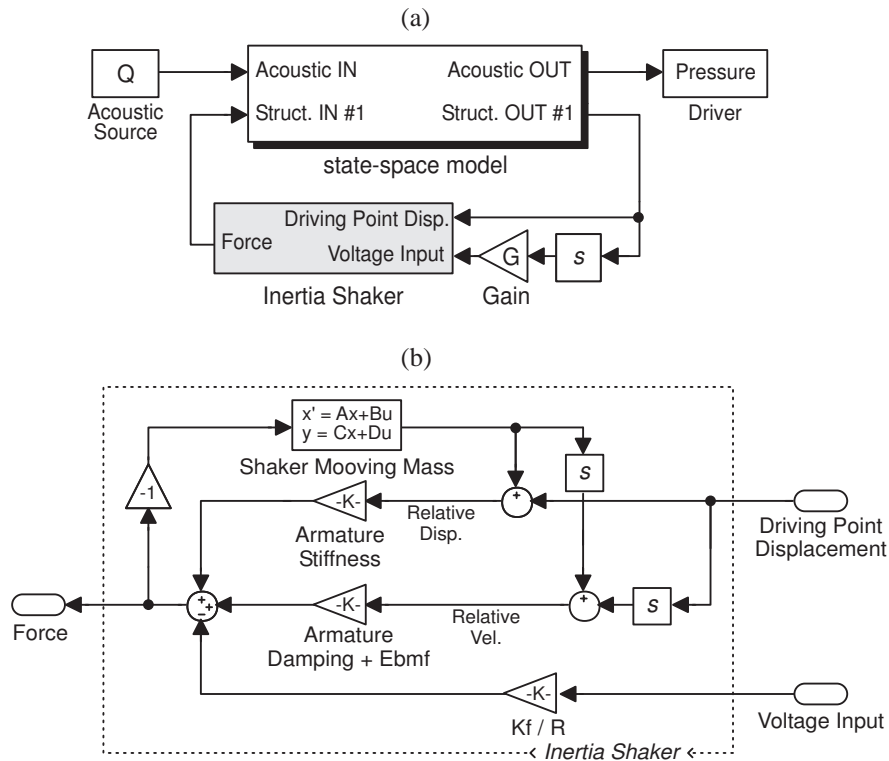


FIGURE 10: Block diagrams: (a) ASAC simulation (b) detailed shaker block

Figure 11 shows the pressure at the driver's head position for a chirp acoustic disturbance and different conditions: passive system, active system with idealized velocity feedback and active system with shaker model (as in Fig. 10). As expected, it is possible to notice that the idealized force approach overestimate the control performance, mainly in the low frequency range and close to resonances. As a result, for the same feedback gain ($G = 450\text{V}/(\text{m/s})$), the estimated reduction on the sound pressure level (SPL) for the idealized force approach is 4dB while, when the shaker model is included, it is 2.8dB.

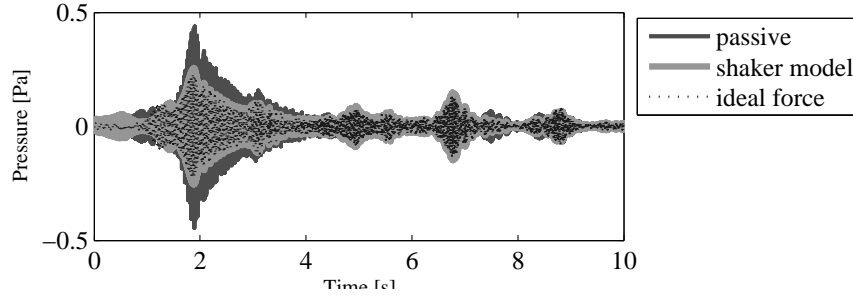


FIGURE 11: Pressure at the drive's head position for different conditions ($G=450$ V/(m/s))

Figure 12 shows the overall noise reduction as a function of the feedback gain for both, idealized force and shaker model approaches. As it can be seen, in either case there is an optimum gain with respect to the SPL at the drive's head position. The performance evaluated with idealized forces is almost ever overestimated when compared to the one calculated with the shaker model. The latter is just not true for low values of G , where the inclusion of the shaker model results in slightly lower SPL. This effect can be noticed even for $G = 0$, *i.e.* the passive system, as the shaker represents an additional mass-spring-damper system attached to the firewall.

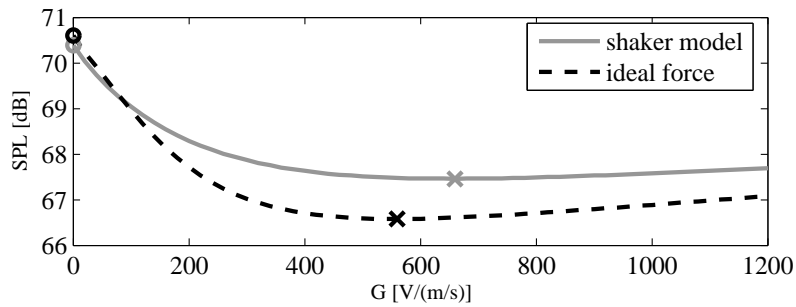


FIGURE 12: Sound pressure level at driver's head position: (o) passive and (x) optimal active

It is important to notice that the positioning of the SAP plays an important role in the maximum achievable noise reduction. One could also consider the firewall thickness as a variable in this design process, resulting in a multi-disciplinary optimization task. The use of state-space models, as the one described in this paper, for the evaluation and optimization of such active control systems can be seen in more details in [24, 25].

Furthermore, the 2.8dB SPL reduction achieved with one arbitrarily placed SAP can be improved if more SAPs are used. To demonstrate a simulation scheme with multiple SAPs, a configuration with 2 collocated SAPs in a decentralized velocity-feedback control loop is applied to the firewall (Fig 13). Again, as an optimization of the SAPs location is out of the scope of this work, their placement is made upon previous experience. As demonstrated by [26], an arbitrary placement can lead to satisfactory results if the feedback gains are optimized. The state-space model has been augmented with the extra structural input/output point (Fig. 13a), resulting in the 2 SAPs positions depicted in Fig. 13(b).

Figure 14 shows how the control system performance varies with respect to the feedback gains G_1 and G_2 . The performance is considered as the SPL reduction in dB at the driver's ear. It is possible to access the optimal gains for both SAPs based on the solution surface on Fig. 14. As a result, the overall system performance is 5.1dB, with feedback gains G_1 and G_2 respectively -350 and $-160\text{V}/(\text{m/s})$.

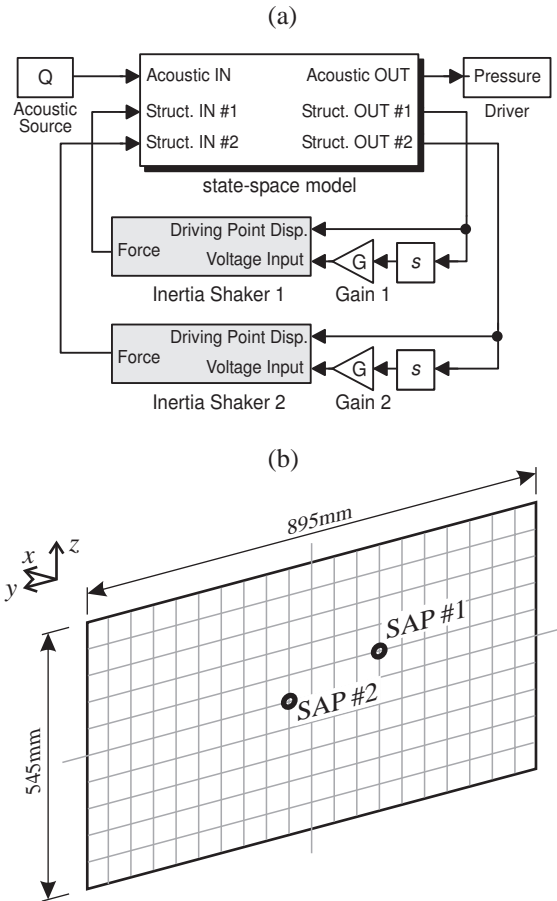


FIGURE 13: 2 SAPs ASAC: (a) block diagram and (b) SAP positions on the firewall

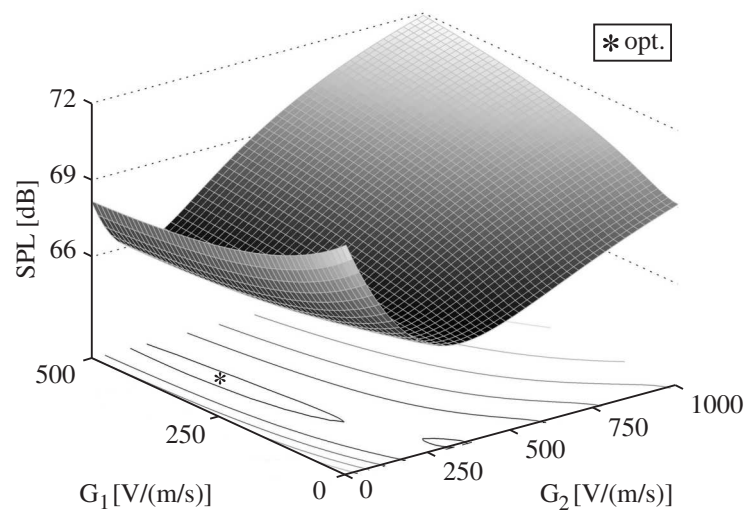


FIGURE 14: Solution surface for 2 SAPs: Performance X feedback gains

4. Summary and Conclusions

A modelling procedure for ASAC simulation, considering a fully coupled vibro-acoustic system has been presented. Structural FE models are used to calculate a vibro-acoustic coupled modal base, which is eventually exported and formulated as a state-space modal model. Finally, the models for the inertial shakers are incorporated and the control system can be implemented.

The displacement/pressure Eulerian modal base allows the representation of the vibro-acoustic FE model in a state-space formulation featuring coupled structural and acoustical inputs and outputs. The inertial shaker was modelled as a lumped mass connected by an active interface to the structure. The results obtained through this time-domain procedure, as the force drop-off phenomenon, are similar to those found in the literature for electrodynamic shakers. Hence, the modelling procedure succeeded in representing such a coupled electro-vibro-acoustic system. The overestimate error from the idealized force controller reached up to 1.2dB in 2.8dB overall reduction, highlighting the importance of including the SAP dynamics.

The ASAC simulation allows the inclusion of any kind of controller that uses structural or acoustical sensors and actuators. As an example, decentralized velocity feedback with 1 and 2 SAPs were presented. A Total reduction of 5.1dB was achieved with 2 SAPs. It is probable that the SAP placement is not optimum, therefore an increase in the achievable reduction can still be reached, even if the current configuration (2 collocated SAPs) is kept. This solution could be accessed by an optimization routine that takes into account not only the feedback gain, but also the SAP placement. The amount of reduction could also be increased if more SAPs are placed simultaneously on the firewall. However, the design space grows exponentially with respect to the number of variables, which significantly increases the computational effort for the optimization procedure. The use of reduced models, as shown in this paper, is crucial for the feasibility of such optimizations.

Besides all the advantages of a collocated velocity-feedback controller, and the fact that structural SAPs would be robust against changes on the acoustic system, it presented a rather weak effect on damping the predominantly acoustic modes. However, as far as the primary source has a random nature, e.g. aerodynamic or tire noise, the feedback approach is probably the most convenient solution. If the

objective is to prevent the transmission of engine noise to the passenger compartment, and considering that a good reference signal is available (engine speed), a feedforward approach may lead to better results. In any case, the modelling approach proposed here fulfils the simulation requirements, providing a more accurate model of the plant which can include sensors and actuators dynamics.

Acknowledgements

The research of Leopoldo P.R. de Oliveira is financed by a scholarship in the framework of a selective bilateral agreement between the K.U.Leuven and the University of So Paulo. Part of this research was done in the framework of the European FP6 Integrated Project: Intelligent Materials for Active Noise Reduction - InMAR.

References

- [1] H. Van der Auweraer, K. Janssens, L.P.R. Oliveira, M.M. Silva, W. Desmet, Virtual Prototyping for Sound Quality Design of Automobiles, *S V Sound and Vibration* 41(4), (2007), 26-30.
- [2] J.I. Mohammed, S.J. Elliott, Active control of fully coupled structural-acoustic system, *Proceeding of Inter-Noise 2005*, Rio de Janeiro - Brazil, 2005, 10p.
- [3] P. Sas, C. Bao, F. Augusztinovicz, W. Desmet, Active control of sound transmission through a double panel partition, *Journal of Sound and Vibration* 180(4) 1995, 609-625.
- [4] W. Desmet, B. Pluymers, P. Sas, Vibro-acoustic analysis procedures for the evaluation of the sound insulation characteristics of agricultural machinery cabins, *Journal of Sound and Vibration* 266(3) 2003, 407-441.
- [5] J.P. Coyette, Y. Dubois-Plerin, An efficient coupling procedure for handling large size interior structural-acoustic problems, *Proceedings of ISMA-19*, Leuven BELGIUM, 1994, pp.729-738.
- [6] N. El-Masri, M. Tournour, C. McCulloch, Meshing procedure for vibro-acoustic models, *Proceedings of ISMA 2002*, Leuven BELGIUM, 2002, pp.2151-2157.

- [7] W. Desmet, D. Vandepite, Finite Element Method in acoustics, *ISAAC 15 - Seminar on Advanced Techniques in Applied and Numerical Acoustics*, Leuven BELGIUM, 2004, 48p.
- [8] J. Luo, H.C. Gea, Modal Sensitivity analysis of coupled acoustic-structural systems, *Journal of Vibration and Acoustics*, v.119, 1997, 545-550.
- [9] *Synnoise rev. 5.5 User's Manual*, LMS International, Leuven, Belgium, 2000.
- [10] A. Preumont, *Vibration Control of Active Structures: An Introduction*, Kluwer Academic Publishers, 2002, Ed.2.
- [11] P. Fisette, O. Brls, J. Swevers, Multiphysics modelling of mechatronic multibody systems, *Proceedings of the International Conference on Noise and Vibration Engineering - ISMA 2006*, Leuven BELGIUM, 2006, pp.41-68.
- [12] M.M. da Silva, W. Desmet, H. Van Brussel, Design of mechatronic systems with configuration-dependent dynamics: simulation and optimization, *IEEE/ASME Trans. on Mechatronics*, 2008, 13(6), 9pp.
- [13] G.R. Tomlinson, Force Distortion in Resonance Testing of Structures with Electrodynamical Vibration Exciters, *Journal of Sound and Vibration*, 63(3) 1979 pp.337-350.
- [14] K. Unholtz, *Vibration testing machines - Shock and Vibration Handbook*, McGraw-Hill Book Co., New York, 1961, v.2, pp.25.1-25.74, Ed.1.
- [15] G.F. Lang, Understanding the Physics of Electrodynamical Shaker Performance, *Sound and Vibration* - October 2001, pp.1-9.
- [16] K.G. McConnell, *Vibration Testing: Theory and Practice*, John Wiley & Sons, 1995, NY - USA, Ed.1.
- [17] P.S. Varoto, L.P.R. Oliveira, On the Force Drop-off Phenomenon in Shaker Testing in Experimental Modal Analysis, *Shock and Vibration* 9 (4-5 SPEC.), (2002), pp. 165-175.

-
- [18] P.S. Varoto, L.P.R. Oliveira, Interaction between a vibration exciter and the structure under test, *S V Sound and Vibration* 36 (10), (2002), pp. 20-26.
- [19] S. Herold, H. Atzrodt, D. Mayer, M. Thomaier, Integration of different approaches to simulate active structures for automotive applications, *Proceedings of Forum Acusticum 2005*, Budapest HUNGARY, 2005, pp.909-914.
- [20] P.A. Nelson, S.J. Elliott, *Active Control of Sound*, Academic Press, 1 992, Ed.1.
- [21] K. Henriouille, P. Sas, Experimental validation of a collocated PVDF volume velocity sensor/actuator pair, *Journal of Sound and Vibration* 265(3) 2003 pp.489-506.
- [22] D.K. Rao, Electrodynamic Interaction Between a Resonating Structure and an Exciter, *Proceedings of the 5th International Modal Analysis Conference - V IMAC*, 1987, v.2, pp.1142-1150.
- [23] N.M.M. Maia, J.M.M. Silva, *Theoretical and Experimental Modal Analysis*, Research Studies Press Ltd., 1997, England, Ed.1.
- [24] L.P.R. de Oliveira, M.M. da Silva, P. Sas, H. Van Brussel, W. Desmet, Concurrent mechatronic design approach for active control of cavity noise, *Journal of Sound and Vibration* 314 (2008) 507-525.
- [25] L.P.R. de Oliveira, K. Janssens, P. Gajdatsy, H. Van der Auweraer, P.S. Varoto, P. Sas, W. Desmet, Active sound quality control of engine induced cavity noise, *Mechanical Systems and Signal Processing* 23 (2009) 476- 488.
- [26] L.P.R. Oliveira, B. Stallaert, W. Desmet, J. Swevers, P. Sas, Optimisation Strategies for Decentralized ASAC, *Proceedings of Forum Acusticum 2005*, Budapest HUNGARY, 2005, , pp.875-880

Chapter 3

Concurrent mechatronic design approach for active control of cavity noise

Leopoldo P.R. de Oliveira

Maíra M. da Silva

Paul Sas

Hendrik Van Brussel

Wim Desmet

Paper published on the Journal of Sound and Vibration:

L.P.R. de Oliveira, M.M. da Silva, P. Sas, H. Van Brussel, W. Desmet, Concurrent mechatronic design approach for active control of cavity noise, *J. Sound. and Vib.* 314 (2008) 507-525.

This work is the result of a fruitful collaboration between Leopoldo P.R. de Oliveira and Maíra M. da Silva.

The contribution of Leopoldo P.R. de Oliveira is mainly related to:

- the derivation of the fully coupled vibro-acoustic model, including the interpretation of Eq. 4.14, which furnishes the modal base for the reduced model;
- the inclusion of the actuator dynamics into the optimization problem;
- the experimental validation of the passive and active vibro-acoustic system.

The contribution of Maíra M. da Silva is mainly related to:

- the model reduction approach yielding a state-space representation of the coupled vibro-acoustic model and
- the optimization approach considering control and structural parameters concurrently yielding the main results of this work.

Equations (9) and (14) have been edited to fit the thesis borders.

Abstract

Active control is a potential solution to many noise and vibration problems for improving the low-frequency performance. Cavity noise reduction as encountered for instance in aircraft cabins and vehicle interiors, is a typical example. However, the conventional design of these active solutions may lead to suboptimal products, since the interaction between the vibro-acoustic plant dynamics and control dynamics is usually not considered. A proper way to design such active systems would be considering control and plant parameters concurrently. To cope with this approach, a methodology to derive a fully coupled mechatronic model that deals with both the vibro-acoustic plant dynamics as well as the control parameters is proposed. The inclusion of sensor and actuator models is investigated, since it contributes to the model accuracy as it can present frequency, phase or amplitude limitations to the control performance. The proposed methodology provides a reduced state-space model derived from a fully coupled vibro-acoustic finite element model. Experimental data on a vibro-acoustic vehicle cabin mock-up are used to validate the model reduction procedure. Regarding noise reduction, optimization results are presented considering both vibro-acoustic plant features, such as thicknesses, and control parameters, such as sensor and actuator placement and control gains. A collocated sensor/actuator pair is considered in a velocity feedback control strategy. The benefits of a concurrent mechatronic design when dealing with active structural-acoustic control solutions are addressed, illustrated and experimentally validated.

1. Introduction

The demands for improvement in sound quality and reduction of noise generated by vehicles are steadily increasing, as well as the penalties for space and weight of passive solutions. Active solutions have the potential to enhance the dynamic performance beyond the passive performance which may allow a lighter and improved product [1].

Demonstrations about the viability of active noise control (ANC) and active structural-acoustic control (ASAC) in cavity noise applications, including automotive interior noise reduction, have been described by several authors [1-6]. A relatively new development in ASAC is the use of decentralized controllers, *i.e.*, systems with sensors and actuators connected as independent pairs in feedback loops, rather than through a centralized control unit. This technique has received considerable attention [7-11], mainly because of its advantages over the centralized strategy in terms of the practical realization (simpler connections and savings on cabling) and the system transducer fault tolerance [11]. The importance of the proper placement of sensors and actuators has also been highlighted in [9, 11-13].

Nowadays, virtual prototyping techniques are being developed in order to support the design process and to improve product performance, while reducing design costs and shortening development cycles [14]. In order to bring active solutions to the level of industrial applications, the designer needs numerical tools that allow the inclusion of sensors/actuators and control strategy in the virtual product design and optimization. In this way, the design of active solutions for noise reduction should be performed along the lines of a mechatronic design approach. For the purpose of this study, mechatronic design is defined as the approach that deals with the integrated design of a mechanical system and its embedded control system [15]. This approach has been illustrated by performing a concurrent optimization for a 3-axis machine tool considering control and structural aspects, resulting in an improved system performance [16]. For active noise control, the concurrent mechatronic approach has been rarely employed. Recently, a simultaneous structural and control optimization of a flexible linkage mechanism for noise attenuation has been described [17]. In that case, the aim is to reduce the structural-acoustic radiation of a flexible mech-

anism considering in the objective function the weight of the structure, the vibration energy and the control system energy. It is claimed that the integrated approach improved significantly the acoustic radiation (performance) and the controller inputs (effort) for that case study.

In this paper, a concurrent mechatronic approach to active control design for interior cavity noise reduction, as encountered for instance in automotive interior applications, is proposed using simulation and optimization. The benefits of this methodology are demonstrated on a vibro-acoustic cabin mock-up (Figs. 1 and 2). It consists of a simplified car cavity with concrete walls to provide well-defined acoustic boundary conditions, thus reducing uncertainties during the vibro-acoustic modelling phase. The system is divided into two closed cavities: the passenger compartment (PC) and the engine compartment (EC). A rectangular clamped steel panel resembles the firewall, allowing the disturbance noise generated by the acoustic source in the EC to be transmitted to the PC. The PC main dimensions are 3400 x 1560 x 1270mm; the EC is 800 x 1100 x 750mm and the firewall is 895 x 545 x 1.5mm (Fig. 2). A structural sensor/actuator pair (SAP) placed on the firewall realizes the control signals for noise reduction in the PC. One of the challenges resides in deriving reasonably sized models that integrate the structural, acoustic and electrical components along with the control algorithm. Moreover, the presence of distinct

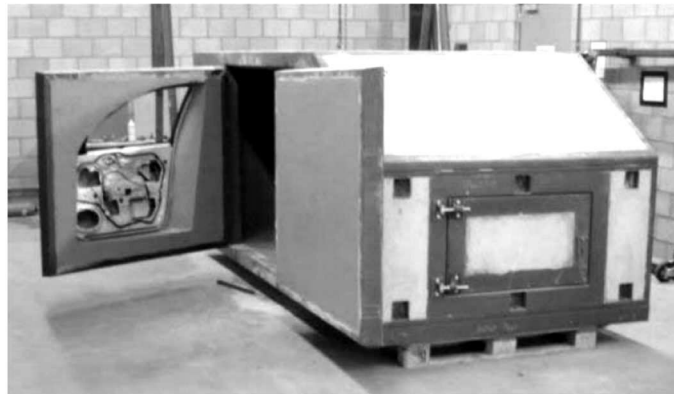


FIGURE 1: Photo of the experimental set-up: the vibro-acoustic cabin mock-up

paths (fluid-structure-fluid) imposes the necessity of dealing with fully coupled vibro-acoustic models. In order to fulfil this requirement, a fully coupled finite element (FE) model of the vibro-acoustic system is reduced and exported as a state-space model into Matlab/Simulink. The inclusion of sensor and actuator models, which can be realized in this environment, contributes to the model accuracy, since their own dynamics may change the original system response significantly.

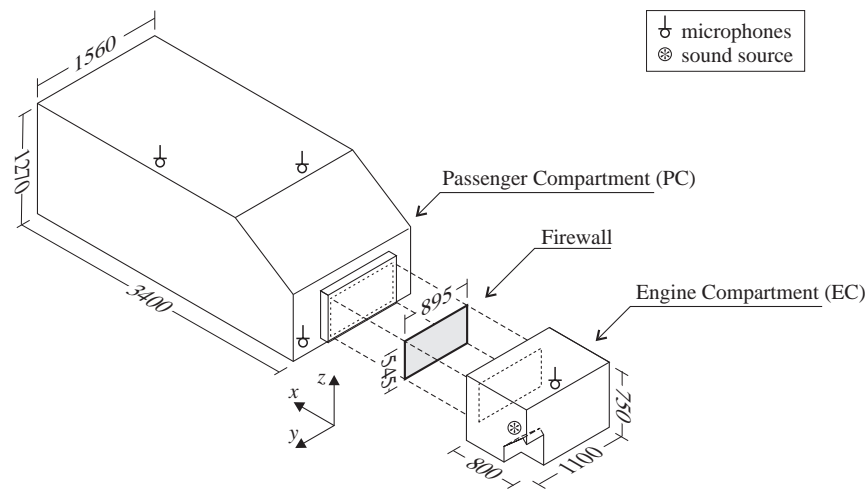


FIGURE 2: Schematic view of the system under study (dimensions in mm)

The modelling approach for the fully coupled vibro-acoustic system and its experimental validation are presented in Section 2. The integrated design of the active system is treated in Section 3. Finally, some conclusions are addressed in Section 4.

2. Fully Coupled Vibro-Acoustic Modelling Approach

Vibro-acoustic systems can be modelled using Computer Aided Engineering (CAE) tools such as finite element (FE) and/or boundary ele-

ment (BE) methods. In order to improve the prediction of the structural behaviour in the presence of fluid loads, simulation procedures have been proposed [18-20], where the influence of the fluid (modelled with BE) is added to the original structural FE models. The present case study, however, requires not only the fluid load on the structure, but also the interaction between the structural vibrations and the pressure field. In other words, the vibro-acoustic model should be fully coupled. To cope with this, a coupled vibro-acoustic FE/FE modelling approach is adopted [21]. As a result, any combination of structural and acoustic inputs/outputs can be used for the control design, *e.g.*, an acoustic source in the EC, structural sensors and actuators on the fireball and a microphone in the PC.

Another advantage of using a fully coupled vibro-acoustic approach is the accuracy of the estimated closed-loop performance, as an uncoupled analysis can overestimate the controller efficiency [22]. It is also required that the modelling approach fits into an optimization loop, as the design of an active control system usually requires the setting of some controller parameters (*e.g.* sensor and actuator positions and control gains).

One of the coupled FE/FE formulations is the Eulerian, in which the structural degrees of freedom (DoFs) are displacement vectors, while the acoustic DoFs are expressed as scalar functions. The latter is usually the acoustic pressure, but can also be the fluid velocity potential [23-27]. If pressure is adopted, the system of equations yields non-symmetrical mass and stiffness matrices, posing a disadvantage to FE solvers. The choice of velocity potential as acoustic DoF also presents a drawback, as the vibro-acoustic coupling terms populate the damping matrix, yielding a symmetric but complex model, which is computationally more expensive than the non-symmetric one [28]. Moreover, the modal base resulting from the non-symmetric eigenproblem can easily be handled by the modelling procedure, as will be described in more detail in the next section. Therefore, a displacement/pressure Eulerian formulation is adopted hereafter.

2.1. From vibro-acoustic FE to state-space formulation

Usually, control design and simulation is performed in a dedicated time-domain environment, raising the necessity of deriving a compatible representation of the system under study. An appropriate approach would be a modal representation of the FE model in a state-space

(SS) formulation. This representation is a mathematical model of a physical system as a set of input, output and state variables related by first-order differential equations, providing a convenient and compact way to model and analyze systems with multiple inputs and outputs. A number of control design tools are available for systems described in this form such as Linear-Quadratic-Gaussian (LQG) design, linear-quadratic state-feedback regulator design (LQR) and H_∞ controller synthesis. The purpose of this paper is to deliver tools to allow the designer to perform a concurrent mechatronic design; therefore the SS representation suits better this objective.

A first step in the FE modelling of vibro-acoustic systems is the definition of appropriate meshes for the acoustic and structural components. Coincident structural and acoustic meshes are adopted over the coupling boundary resulting in a simplified procedure [29]. The frequency range of interest is limited to 0-200Hz to reduce the computational effort during the modelling procedure. It may not be representative for all interior acoustic problems, but is sufficient to demonstrate the proposed technique and to provide general insights. Moreover, this choice is not a limiting factor, since this technique is valid as far as FE models can be used.

The size of the structural elements is chosen such that the highest-order mode (at 160 Hz: see Fig. 3b and Table 1), is represented by at least 6 linear elements. The structural mesh (Fig. 3a) has 200 4-noded shell elements, yielding 1026 DoFs since the borders of the firewall are clamped. The chosen 4-node shell element was an isoparametric quadrilateral element with the evaluation of the forces at the centroid of the element (QUAD4). This element may exhibit locking effects for trapezoidal shapes [30]. Due to the characteristic of the geometry, a rectangular mesh was employed avoiding this phenomenon. Experimental validation, showed hereafter, confirms the model accuracy. However, locking phenomenon should be addressed properly when more complicated geometries and meshes are involved. The 1.5mm-thick firewall presents 12 modes between 0 and 200Hz (Table 1). The element type chosen for the acoustic mesh is the 8-noded brick element. The resulting mesh, with 26050 elements, and the mode shape at 192.5Hz are depicted in Fig. 4. The total number of acoustic DoFs is 23196. With respect to the element size, this acoustic model exhibits a minimum of 6 linear elements per wavelength up to 500Hz. Table 1 shows the resonance frequencies for the coupled vibro-acoustic model and the un-

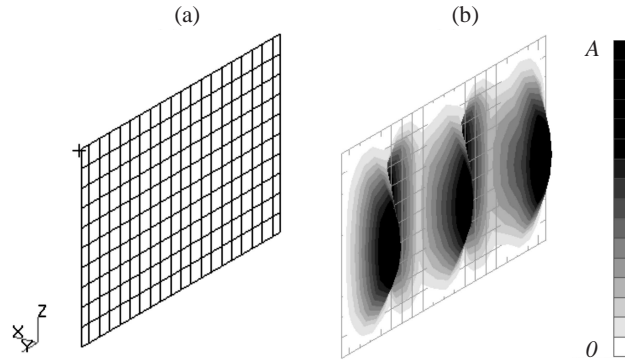


FIGURE 3: Firewall: (a) FE mesh and (b) uncoupled mode at 160Hz [5,1]

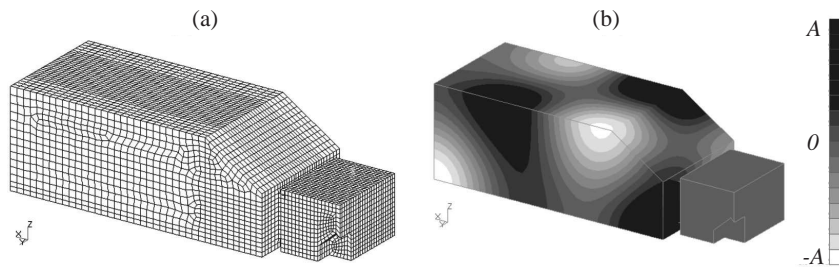


FIGURE 4: Acoustic cavities: (a) FE mesh and (b) uncoupled mode at 192.5Hz

coupled structural and acoustic components. It shows also the mode shapes in terms of the number of half wavelengths in the x, y and z directions for the uncoupled modes. In a coupled FE/FE approach, the effect of the fluid on the structure dynamics can be considered as a pressure load on the wetted surface. For a system with n_s structural DoFs and n_a acoustic DoFs, the structural differential equation takes the form of Eq. (1).

TABLE 1: Resonance frequencies for coupled and uncoupled systems

vibro-acoustic modes		uncoupled structural modes		uncoupled acoustic modes	
modes #	freq. [Hz]	freq. [Hz]	half-wavelength [y,z]	freq. [Hz]	wavelength [x,y,z]
1	0			0	EC - [0,0,0] ^a
2	0			0	PC - [0,0,0] ^b
3	35.3	34.2	[1,1]		
4	49.1	48.3	[2,1]		
5	52.5			52.1	PC - [1,0,0]
6	75.6	75.6	[3,1]		
7	85.9	86.0	[1,2]		
8	99.4	99.4	[2,2]		
9	101.8			101.6	PC - [2,0,0]
10	110.5			110.6	PC - [0,1,0]
11	112.5	112.6	[4,1]		
12	122.4	122.5	[3,2]		
13	122.9			122.8	PC - [1,1,0]
14	137.2			137.2	PC - [0,0,1]
15	145.9			145.9	PC - [3,0,0]
16	151.3			151.3	PC - [2,1,0]
17	155.7	155.7	[4,2]		
18	157.1			157.2	PC - [1,0,1]
19	159.0			158.7	EC - [0,1,0]
20	160.0	159.9	[5,1] ^c		
21	164.5	164.5	[1,3]		
22	176.0			176.0	PC - [0,1,1]
23	177.8	177.8	[2,3]		
24	182.9			182.8	PC - [2,0,1]
25	184.1			184.1	PC - [1,1,1]
26	192.5			192.5	PC - [2,1,1] ^d
27	198.9	199.0	[3,3]		
28	199.4			199.7	PC - [4,0,0]

^aEC = Engine Compartment^bPC = Passenger Compartment^cmode depicted in Fig. 3^dmode depicted in Fig. 4

$$(\mathbf{K}_s + j\omega\mathbf{D}_s - \omega^2\mathbf{M}_s)\mathbf{u}(\omega) + \mathbf{K}_c\mathbf{p}(\omega) = \mathbf{F}_s(\omega) \quad (1)$$

where \mathbf{K}_s , \mathbf{D}_s and $\mathbf{M}_s \in \mathbb{R}^{n_s \times n_s}$ are, respectively, the stiffness, damping and mass matrices of the structural component, $\mathbf{K}_c \in \mathbb{R}^{n_s \times n_a}$ is the coupling matrix, $\mathbf{u} \in \mathbb{R}^{n_s \times 1}$ is the vector of structural displacement DoFs, $\mathbf{p} \in \mathbb{R}^{n_a \times 1}$ is the vector of nodal acoustic pressures and $\mathbf{F}_s \in \mathbb{R}^{n_s \times 1}$ is the structural load vector.

In a similar way, the structural vibrations provide an acoustic velocity input and therefore must be taken into account in the acoustic model as:

$$(\mathbf{K}_a + j\omega\mathbf{D}_a - \omega^2\mathbf{M}_a)\mathbf{p}(\omega) + \omega^2\mathbf{M}_c\mathbf{u}(\omega) = \mathbf{F}_a(\omega) \quad (2)$$

where \mathbf{K}_a , \mathbf{D}_a and $\mathbf{M}_a \in \mathbb{R}^{n_a \times n_a}$ are the acoustic stiffness, damping and mass matrices, $\mathbf{M}_c \in \mathbb{R}^{n_a \times n_s}$ is the coupling matrix and $\mathbf{F}_a \in \mathbb{R}^{n_a \times 1}$ is the acoustic load vector. For the sake of brevity, any frequency dependent function ‘ $h(\omega)$ ’ is represented just as ‘ h ’ hereafter.

Using the relation $\mathbf{M}_c = -\rho_0\mathbf{K}_c^T$ [31-34], where ρ_0 is the fluid density, the combined system of equations, known as the Eulerian FE/FE model, yields:

$$\left(\begin{bmatrix} \mathbf{K}_s & \mathbf{K}_c \\ \mathbf{0} & \mathbf{K}_a \end{bmatrix} + j\omega \begin{bmatrix} \mathbf{D}_s & \mathbf{0} \\ \mathbf{0} & \mathbf{D}_a \end{bmatrix} - \omega^2 \begin{bmatrix} \mathbf{M}_s & \mathbf{0} \\ -\rho_0\mathbf{K}_c^T & \mathbf{M}_a \end{bmatrix} \right) \begin{Bmatrix} \mathbf{u} \\ \mathbf{p} \end{Bmatrix} = \begin{Bmatrix} \mathbf{F}_s \\ \mathbf{F}_a \end{Bmatrix} \quad (3)$$

Based on Eq. (3) it is clear that the resulting vibro-acoustic system is coupled, though it is no longer symmetric. As a consequence of such non-symmetric nature, the solution of the associated undamped eigenproblem is computationally more demanding and results in different left and right eigenvectors:

$$\begin{bmatrix} \mathbf{K}_s & \mathbf{K}_c \\ \mathbf{0} & \mathbf{K}_a \end{bmatrix} \{\Phi_R\}_r = \omega_r^2 \begin{bmatrix} \mathbf{M}_s & \mathbf{0} \\ -\rho_0\mathbf{K}_c^T & \mathbf{M}_a \end{bmatrix} \{\Phi_R\}_r, \quad (4)$$

$r = 1, \dots, n_a + n_s$

$$\{\Phi_L\}_r^T \begin{bmatrix} \mathbf{K}_s & \mathbf{K}_c \\ \mathbf{0} & \mathbf{K}_a \end{bmatrix} = \omega_r^2 \{\Phi_L\}_r^T \begin{bmatrix} \mathbf{M}_s & \mathbf{0} \\ -\rho_0\mathbf{K}_c^T & \mathbf{M}_a \end{bmatrix}, \quad (5)$$

$r = 1, \dots, n_a + n_s$

where r is the index of the coupled natural frequency ω_r and Φ_L and $\Phi_R \in \mathbb{R}^{(n_s+n_a) \times 1}$ are, respectively, the left and right coupled modes.

Moreover, it has been indicated [35] that, for the Eulerian formulation, the left and right eigenvectors, can be related as:

$$\{\Phi_L\}_r = \begin{Bmatrix} \{\Phi_{Ls}\}_r \\ \{\Phi_{La}\}_r \end{Bmatrix} = \begin{Bmatrix} \{\Phi_{Rs}\}_r \omega_r^2 \\ \{\Phi_{Ra}\}_r \end{Bmatrix} \quad r = 1, 2, \dots, n_s + n_a \quad (6)$$

where the indexes a and s represent, respectively, the acoustic and structural DoFs.

A common practice in solving such vibro-acoustic problems is the use of component mode synthesis (CMS). It consists of expanding the structural DoFs in terms of a set of N_s uncoupled structural modes $\Phi_s \in \mathbb{R}^{n_s \times 1}$ (without any acoustic pressure load along the coupling interface), as well as expanding the acoustic DoFs in terms of a set of N_a uncoupled acoustic modes $\Phi_a \in \mathbb{R}^{n_a \times 1}$ (acoustic boundaries considered rigid at the wetted surface). The structural and acoustic expansions become, respectively,

$$\mathbf{u} = \sum_{r=1}^{N_s} q_{s_r} \{\Phi_s\}_r = \Phi_s \mathbf{q}_s \quad (7)$$

$$\mathbf{p} = \sum_{r=1}^{N_a} q_{a_r} \{\Phi_a\}_r = \Phi_a \mathbf{q}_a \quad (8)$$

where $\mathbf{q}_s \in \mathbb{R}^{N_s \times 1}$ is the vector of modal amplitudes related to the structural DoFs, $\mathbf{q}_a \in \mathbb{R}^{N_a \times 1}$ is the vector of modal amplitudes related to the acoustic DoFs, $\Phi_s \in \mathbb{R}^{n_s \times N_s}$ is the structural modal matrix, $\Phi_a \in \mathbb{R}^{n_a \times N_a}$ is the acoustic modal matrix and r is the index representing the number of the mode.

This procedure yields non-symmetrical coupled modal stiffness and mass matrices [34]. Therefore, obtaining the modal SS representation of a reduced model derived from CMS can be a difficult task, since it is necessary to invert the coupled modal mass matrix (which is non-diagonal) and the coupling matrix should be fully available. An alternative to describe a modal SS for a fully coupled vibro-acoustic system is to apply a variable substitution to the coupled eigenproblem related to Eq. (3) [36]. This procedure is detailed hereafter.

Substituting the component mode expansions in Eqs. (7) and (8) into Eq. (3) and pre-multiplying the structural and acoustic parts of the resulting matrix equation, respectively, with the transpose of the structural and acoustic modal vectors yields the undamped modal representation:

$$-\omega^2 \begin{bmatrix} \Phi_s^T \mathbf{K}_s \Phi_s & \Phi_s^T \mathbf{K}_c \Phi_a \\ \mathbf{0} & \Phi_a^T \mathbf{K}_a \Phi_a \end{bmatrix} \begin{Bmatrix} \mathbf{q}_s \\ \mathbf{q}_a \end{Bmatrix} - \begin{bmatrix} \Phi_s^T \mathbf{M}_s \Phi_s & \mathbf{0} \\ -\rho_0 \Phi_a^T \mathbf{K}_c^T \Phi_s & \Phi_a^T \mathbf{M}_a \Phi_a \end{bmatrix} \begin{Bmatrix} \mathbf{q}_s \\ \mathbf{q}_a \end{Bmatrix} = \begin{Bmatrix} \Phi_s^T \mathbf{F}_s \\ \Phi_a^T \mathbf{F}_a \end{Bmatrix} \quad (9)$$

The homogeneous system of equations related to Eq.(9) can be written as:

$$\begin{bmatrix} \Phi_s^T (\mathbf{K}_s - \omega^2 \mathbf{M}_s) \Phi_s & \Phi_s^T \mathbf{K}_c \Phi_a \\ \omega^2 \Phi_a^T \mathbf{K}_c^T \Phi_s & -\frac{1}{\rho_0} \Phi_a^T (\mathbf{K}_a - \omega^2 \mathbf{M}_a) \Phi_a \end{bmatrix} \begin{Bmatrix} \mathbf{q}_s \\ \mathbf{q}_a \end{Bmatrix} = \begin{Bmatrix} \mathbf{0} \\ \mathbf{0} \end{Bmatrix} \quad (10)$$

Since each uncoupled mode is normalized with respect to the uncoupled mass matrices, Eq. (10) yields:

$$\begin{bmatrix} \Omega_s^2 - \omega^2 \mathbf{I} & \Phi_s^T \mathbf{K}_c \Phi_a \\ \omega^2 \Phi_a^T \mathbf{K}_c^T \Phi_s & -\frac{1}{\rho_0} (\Omega_a^2 - \omega^2 \mathbf{I}) \end{bmatrix} \begin{Bmatrix} \mathbf{q}_s \\ \mathbf{q}_a \end{Bmatrix} = \begin{Bmatrix} \mathbf{0} \\ \mathbf{0} \end{Bmatrix} \quad (11)$$

where $\Omega_s \in \mathbb{R}^{N_s \times N_s}$ and $\Omega_a \in \mathbb{R}^{N_a \times N_a}$ are, respectively, the structural and acoustic diagonal matrices of uncoupled natural frequencies.

Equation (11) still results in a non-symmetric eigenproblem and is therefore expensive to solve. The first line of Eq. (11) leads to:

$$\mathbf{q}_s = \omega^2 (\Omega_s^2)^{-1} \mathbf{q}_s - (\Omega_s^2)^{-1} \Phi_s^T \mathbf{K}_c \Phi_a \mathbf{q}_a \quad (12)$$

Applying the substitution $\bar{\mathbf{q}}_s = \omega^2 \mathbf{q}_s$ in Eq. (12) yields:

$$\begin{Bmatrix} \mathbf{q}_s \\ \mathbf{q}_a \end{Bmatrix} = \begin{bmatrix} (\Omega_s^2)^{-1} & -(\Omega_s^2)^{-1} \Phi_s^T \mathbf{K}_c \Phi_a \\ \mathbf{0} & \mathbf{I} \end{bmatrix} \begin{Bmatrix} \bar{\mathbf{q}}_s \\ \mathbf{q}_a \end{Bmatrix} \quad (13)$$

Using Eq. (13) it is possible to rewrite Eq. (11) as a symmetric system of equations in $\{\bar{\mathbf{q}}_s \quad \mathbf{q}_a\}^T$:

$$\begin{bmatrix} \mathbf{T}_s & \mathbf{T}_c^T \\ \mathbf{T}_c & \mathbf{T}_a \end{bmatrix} \begin{Bmatrix} \bar{\mathbf{q}}_s \\ \mathbf{q}_a \end{Bmatrix} = \begin{Bmatrix} \mathbf{0} \\ \mathbf{0} \end{Bmatrix}, \quad (14)$$

$$\mathbf{T}_s = \mathbf{I} - \omega^2(\boldsymbol{\Omega}_s^2)^{-1},$$

$$\mathbf{T}_c = \omega^2(\boldsymbol{\Omega}_s^2)^{-1}\boldsymbol{\Phi}_a^T\mathbf{K}_c^T\boldsymbol{\Phi}_s,$$

$$\mathbf{T}_a = -\frac{1}{\rho_0}(\boldsymbol{\Omega}_a^2 - \omega^2\mathbf{I}) - \omega^2\boldsymbol{\Phi}_a^T\mathbf{K}_c^T\boldsymbol{\Phi}_s(\boldsymbol{\Omega}_s^2)^{-1}\boldsymbol{\Phi}_s^T\mathbf{K}_c\boldsymbol{\Phi}_a.$$

The coupled modal vector $\bar{\boldsymbol{\Phi}} \in \mathbb{R}^{(n_s+n_a) \times (N_s+N_a)}$, resulting from the eigenproblem associated with Eq. (14) on $\{\bar{\mathbf{q}}_s \quad \mathbf{q}_a\}^T$, can be interpreted as the left eigenvector $\boldsymbol{\Phi}_L$ of the eigenproblem in Eq. (6) on $\{\mathbf{q}_s \quad \mathbf{q}_a\}^T$. The right eigenvector $\boldsymbol{\Phi}_R$ can be retrieved using Eq. (6).

Since the uncoupled bases $\boldsymbol{\Phi}_a$ and $\boldsymbol{\Phi}_s$ result from symmetric eigenproblems, solving Eq. (14) may seem less demanding when compared to the solution of Eqs. (5) and (6). However, the reduction on the computational effort is rather small, as to accurately represent the coupled modes, it is necessary to retain a higher number of uncoupled modes. Nevertheless, the advantage of this method is the possibility of using dedicated software for each component uncoupled modal analysis.

Eventually, the structural and acoustic DoFs $\{\mathbf{u} \quad \mathbf{p}\}^T$ can be projected using the modal base ($\boldsymbol{\Phi}_L$ and $\boldsymbol{\Phi}_R$) and the modal coordinate \mathbf{q} using the following expansion:

$$\begin{Bmatrix} \mathbf{u} \\ \mathbf{p} \end{Bmatrix} = \sum_{r=1}^{N_s+N_a} q_r \{\boldsymbol{\Phi}_R\}_r = \boldsymbol{\Phi}_R \mathbf{q} \quad (15)$$

Moreover, the left and right eigenvectors are normalized such that:

$$\boldsymbol{\Phi}_L^T \begin{bmatrix} \mathbf{M}_s & \mathbf{0} \\ -\rho_0\mathbf{K}_c^T & \mathbf{M}_a \end{bmatrix} \boldsymbol{\Phi}_R = \mathbf{I} \quad (16)$$

$$\boldsymbol{\Phi}_L^T \begin{bmatrix} \mathbf{K}_s & \mathbf{K}_c \\ \mathbf{0} & \mathbf{K}_a \end{bmatrix} \boldsymbol{\Phi}_R = \boldsymbol{\Omega}^2 \quad (17)$$

$$\boldsymbol{\Phi}_L^T \begin{bmatrix} \mathbf{D}_s & \mathbf{0} \\ \mathbf{0} & \mathbf{D}_a \end{bmatrix} \boldsymbol{\Phi}_R = \boldsymbol{\Gamma} \quad (18)$$

where \mathbf{I} , $\boldsymbol{\Omega}^2$ and $\boldsymbol{\Gamma} \in \mathbb{R}^{(N_s+N_a) \times (N_s+N_a)}$ are, respectively, the identity, the squared coupled natural frequencies and the modal damping matrices.

Applying the modal expansion described by Eq. (15) into Eq. (3) and pre-multiplying it by $\boldsymbol{\Phi}_L^T$, Eq. (3) can be re-written as

$$\begin{aligned} & \boldsymbol{\Phi}_L^T \begin{bmatrix} \mathbf{K}_s & \mathbf{K}_c \\ \mathbf{0} & \mathbf{K}_a \end{bmatrix} \boldsymbol{\Phi}_R \mathbf{q} + \boldsymbol{\Phi}_L^T \begin{bmatrix} \mathbf{D}_s & \mathbf{0} \\ \mathbf{0} & \mathbf{D}_a \end{bmatrix} \boldsymbol{\Phi}_R \dot{\mathbf{q}} \\ & + \boldsymbol{\Phi}_L^T \begin{bmatrix} \mathbf{M}_s & \mathbf{0} \\ -\rho_0 \mathbf{K}_c^T & \mathbf{M}_a \end{bmatrix} \boldsymbol{\Phi}_R \ddot{\mathbf{q}} = \boldsymbol{\Phi}_L^T \begin{Bmatrix} \mathbf{F}_s \\ \mathbf{F}_a \end{Bmatrix} \end{aligned} \quad (19)$$

Using the relations described by Eqs. (16), (17) and (18), Eq. (19) can be described in a modal state-space form:

$$\begin{Bmatrix} \dot{\mathbf{q}} \\ \ddot{\mathbf{q}} \end{Bmatrix} = \begin{bmatrix} \mathbf{0} & \mathbf{I} \\ -\boldsymbol{\Omega}^2 & -\boldsymbol{\Gamma} \end{bmatrix} \begin{Bmatrix} \mathbf{q} \\ \dot{\mathbf{q}} \end{Bmatrix} + \begin{bmatrix} \mathbf{0} \\ \boldsymbol{\Phi}_L^T \mathbf{B} \end{bmatrix} \begin{Bmatrix} \mathbf{F}_{si} \\ \mathbf{F}_{ai} \end{Bmatrix} \quad (20)$$

$$\begin{Bmatrix} \mathbf{u}_o \\ \mathbf{p}_o \end{Bmatrix} = \begin{bmatrix} \mathbf{C} \boldsymbol{\Phi}_R & \mathbf{0} \end{bmatrix} \begin{Bmatrix} \mathbf{q} \\ \dot{\mathbf{q}} \end{Bmatrix} \quad (21)$$

where $\mathbf{B} \in \mathbb{R}^{(n_a+n_s) \times N_i}$ is a matrix with ones on the N_i desired input DoFs and zeros everywhere else, $\mathbf{F}_{si} \in \mathbb{R}^{N_{si} \times 1}$ is the structural input load vector, $\mathbf{F}_{ai} \in \mathbb{R}^{N_{ai} \times 1}$ is the acoustic input load vector (with $N_{si} + N_{ai} = N_i$), $\mathbf{u}_o \in \mathbb{R}^{N_{so} \times 1}$ is the structural output vector, $\mathbf{p}_o \in \mathbb{R}^{N_{ao} \times 1}$ is the acoustic output vector (with $N_{so} + N_{ao} = N_o$), and $\mathbf{C} \in \mathbb{R}^{N_o \times (n_a+n_s)}$ is a matrix with ones on the N_o desired output DoFs and zeros everywhere else. In this formulation, the role of \mathbf{B} and \mathbf{C} is to select, respectively, columns from $\boldsymbol{\Phi}_L^T$ and rows from $\boldsymbol{\Phi}_R$ according to the desired inputs and outputs DoFs.

Applying the aforementioned procedure, the original 24192 DoFs (23196 unconstrained acoustic and 1026 unconstrained structural) have been reduced to a SS model with $2 \times (N_s + N_a)$ DoFs, related to the kept modal amplitudes \mathbf{q} and their derivatives $\dot{\mathbf{q}}$, with force and volume velocity as inputs and displacement and pressure as outputs. The number of kept acoustic modal amplitudes is the same for all configurations, since the cavity compartments are not modified during the optimization procedure. Thus, $N_a = 78$, *i.e.* the number of uncoupled acoustic modes with a natural frequency up to 400 Hz, which is adequate to represent the acoustic system in the frequency range of interest (0-200Hz). In order to represent the structure (firewall) in the frequency range of interest, N_s may vary according to the number of

modes occurring from 0 to 400Hz. Table 2 shows N_s for several firewall thicknesses. Considering the nominal 1.5mm firewall, the total number of states is 214 ($2 \times (78 + 29)$). Fewer states would lead to inaccuracies within the frequency of interest.

TABLE 2: Kept structural modal amplitudes (N_s) for different firewall thickness

firewall thickness [mm]	0.5	1.0	1.5	2.0	2.5	3.0	3.5	4.0	4.5
N_s	94	47	29	20	15	13	10	7	7

The validity of the reduced model is illustrated by comparing FRFs from the original model with the reduced model (Fig. 5). The system inputs are volume velocity applied in the EC (acoustic input) and force applied on the firewall (structural input); and the outputs are pressure measured at the PC (acoustic output) and displacement measured at the firewall (structural output). The good correlation between the reduced SS and the direct FE models validates the model reduction procedure.

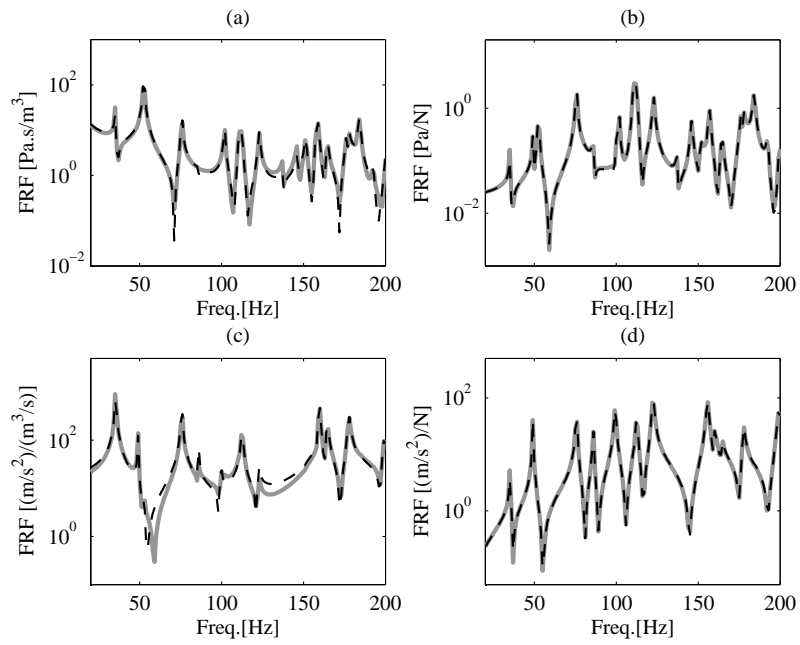


FIGURE 5: Comparison between (- -) FE and (-) SS FRFs: (a) Acoustic/Acoustic, (b) Acoustic/Structural, (c) Structural/Acoustic and (d) Structural/Structural

2.2. Experimental Validation

The FRFs derived from the SS model are compared with the FRFs measured on the cabin mock-up. The considered FRFs include structural and acoustic inputs and outputs. As depicted in Fig. 6(a), the structural excitation is performed with a LDS shaker (model V201/3), the force transducer is a PCB 208C04 and the accelerometers are PCB 352C67. Figure 6(b) shows the LMS acoustic source (model E-LMFVVS) placed at the EC. The microphones used are B&K 4188. The vibro-acoustic system has been excited with white noise. The FRFs are measured with an Hv estimator, while input and output signals are filtered with Hanning windows.

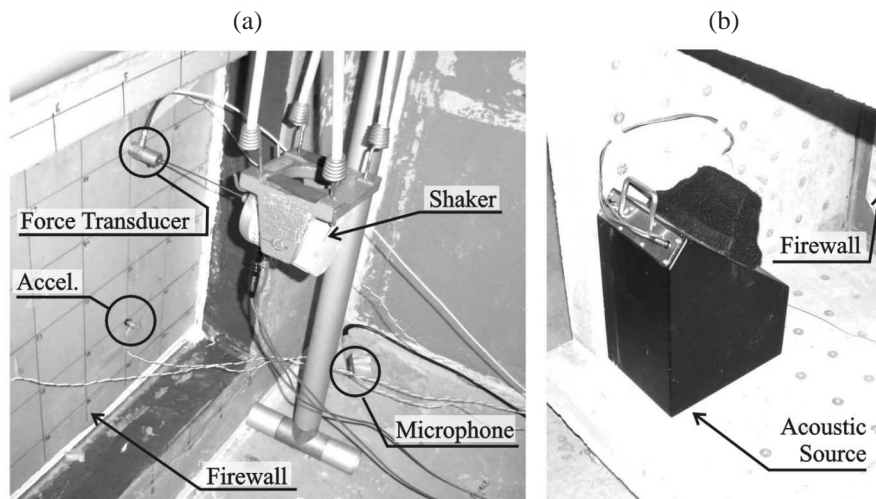


FIGURE 6: Experimental setup: (a) view from the passenger compartment with shaker and sensors and (b) view from the engine compartment with sound source

Figure 7 shows a comparison between the experimental and the simulated (derived from the SS model) FRFs. The material properties adopted for this model (nominal case) are: speed of sound in the air $c_o = 344.7\text{m/s}$, air density $\rho_0 = 1.185\text{kg/m}^3$, firewall density (steel) $\rho_s = 7800\text{kg/m}^3$ and elasticity modulus $E = 2.33 \cdot 10^{11}\text{Pa}$. A single modal damping ratio of 0.35% is applied in the state-space model.

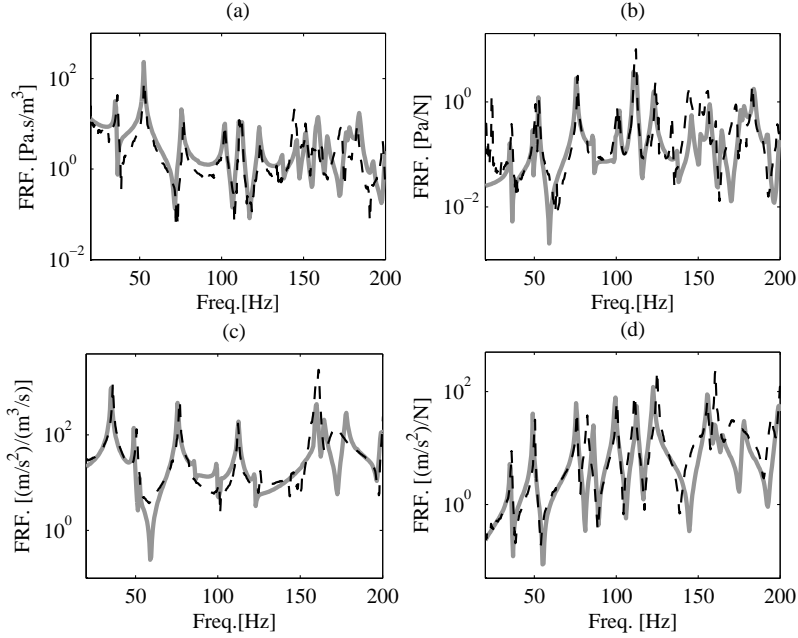


FIGURE 7: Comparison between (-) SS and (- -) experimental FRFs: (a) Acoustic/Acoustic, (b) Acoustic/Structural, (c) Structural/Acoustic and (d) Structural/Structural

As it can be seen, the resulting FRFs present a good agreement up to 150Hz. Discrepancies above this frequency arise among others from the lack of accuracy in determining the exact place of the disturbance source, sensor/actuator pairs and microphones and from assuming the disturbance source as an ideal point source. Such mismatches are expected and reflect a limitation in the FE modelling rather than in the use of the reduced models in closed loop form, which are the focal point of this work.

2.3. Inclusion of sensor and actuators pairs (SAP) models

For ASAC simulations, the models must integrate not only structural and acoustic components, but also sensors, actuators and the controller algorithm. The importance of including detailed information about the

controller and the secondary paths is critical for an accurate assessment of the actual performance, since sensor and actuator dynamics can present frequency, phase and amplitude limitations. In order to cope with this strategy, the reduced model of the system, derived from the aforementioned methodology and described in a state-space representation, is included into the control system design environment (Matlab/Simulink), where the interaction between structure and sensor/actuator can be taken into account.

In this case study, sensors and actuators are, respectively, accelerometers and inertial-shakers. Appropriate accelerometers are selected, for the frequency range of interest, such that the voltage signal generated by these devices can be considered proportional to the measured quantity. However, for the inertial-shakers, a more detailed model for the electro-mechanical coupling within the actuator and its interaction with the structure must be taken into account. The interaction between an electrodynamic shaker and the structure under test has been an issue since the very beginning of modal test methods (see *e.g.* Ref. [37,38]) and is still a subject of research [39-41].

Figure 8 shows the electromechanical model of an inertial-shaker. The mechanical model (Fig. 8a) comprises the moving mass $m_i = 0.03\text{kg}$, the suspension stiffness $k_i = 29.6\text{N/m}$ and damping $c_i = 0.1\text{N/(m/s)}$; the moving mass displacement u_i , the structure connecting point displacement u_s and the electro-magnetic force F_e . The electro-magnetic force is proportional to the current I in the circuit, $F_e = k_f I$, where $k_f = 4\text{N/A}$ is the force-current constant.

The electrical model (Fig. 8b) includes the current I , the voltage input E , the circuit resistance $R = 4\Omega$, the inductance $L = 5\mu\text{H}$ and

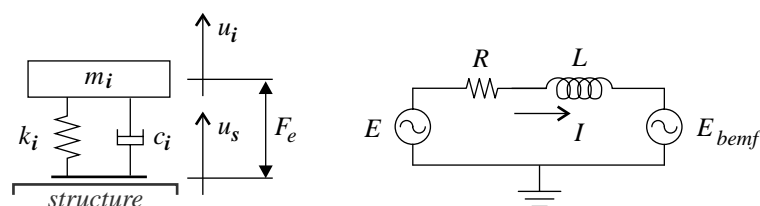


FIGURE 8: Electromechanical model of an inertial shaker: (a) Mechanical and (b) Electrical model

the voltage generated by the moving coil E_{bemf} . The latter can be written in terms of the voltage constant $k_v = 4V/(m/s)$ and the relative velocity between the structure connecting point and the moving mass, $E_{bemf} = k_v(\dot{u}_s - \dot{u}_i)$. Equations (22) and (23) describe the dynamics of this coupled electro-mechanical system operating in voltage mode (ideal power amplifier).

$$RI + L\dot{I} + E_{bemf} = E \quad (22)$$

$$m_i\ddot{u}_i + c_i(\dot{u}_s - \dot{u}_i) + k_i(u_s - u_i) = F_e \quad (23)$$

As proposed in [42], the inertial-shaker/structure interaction can be modelled as a moving mass and an active interface, that includes the mechanical suspension and the electro-magnetic force (Fig. 9). Given the shaker model, the input voltage and the connecting point displacement, it is possible to estimate the force acting on the structure at the interface point (F_{int}). Substituting the current value I in Eq. (22) into Eq. (23) and neglecting the inductance L , since it is usually small [43], yields:

$$F_{int} = \frac{k_f}{R}E - \left[\frac{k_f}{R}k_v + c_i \right] (\dot{u}_s - \dot{u}_i) - k_i(u_s - u_i) \quad (24)$$

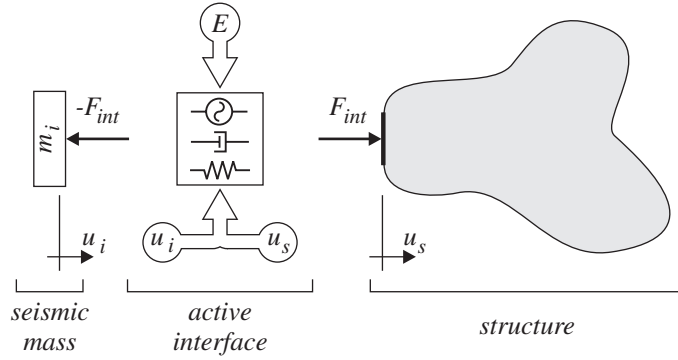


FIGURE 9: Inertia-shaker active interface model

Figure 10(a) shows the structural FRF defined by u_s/F_{int} of the vibro-acoustic model and (b) a comparison between the idealized force input defined by $F_{id} = k_f E/R$, constant over frequency, the simulated

load provided by an inertial-shaker, F_{int} , and the actual measured force, F_{exp} . It can be seen that, in the low frequency range and in the vicinity of structural resonances, the force level drops, as a result of the shaker/structure interaction. The inclusion of the actuator model in the simulation, allows the assessment of a phenomenon inherent to the use of such electrodynamic devices, *i.e.*, the force drop-off around resonances frequencies. The drops in the excitation force can lead to errors in the experimental FRFs [40,41] but mainly, when the active control system is concerned, can result in overestimated authority and performance of the active solution [44].

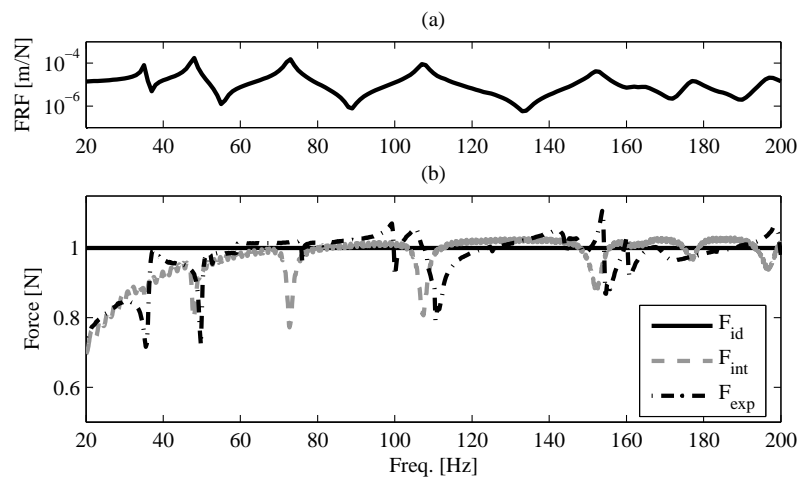


FIGURE 10: (a) System driving point FRF and (b) input forces

The shaker model can be externally connected to any DoF of the firewall, with the advantage of the SS model of the passive plant remaining unchanged (Fig. 11b). This is a useful structure for optimization as the SAP positions, *i.e.* the SS inputs, can be variables of the optimization procedure.

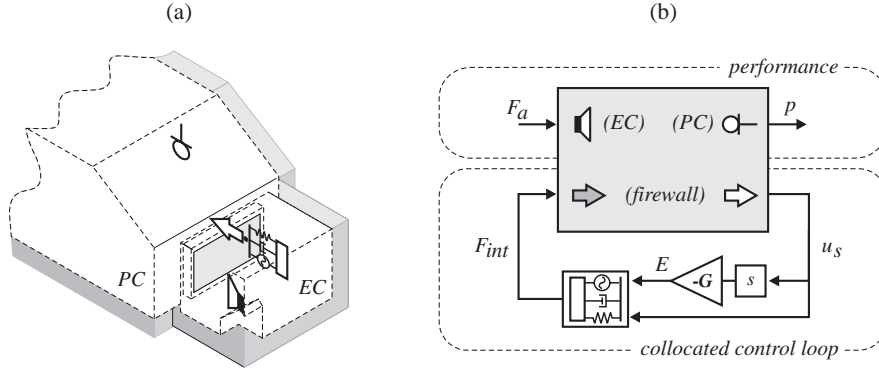


FIGURE 11: Control scheme for the closed loop vibro-acoustic system
 (a) positions of sensors and actuators and (b) block diagram

3. Concurrent Mechatronic Design of Active Systems

The main objective of the considered active control system is to minimize the noise transmitted from the EC to the PC. Among the parameters addressed during the design of an active system is the controller design; more specifically, the definition of a control strategy, the selection and configuration of sensors and actuators, the parameters setting, etc. In a concurrent mechatronic approach, plant dynamic parameters could also be taken into account, aiming at an improved active system design.

Due to its relatively simple implementation, a time-invariant collocated velocity feedback is selected. In this application, the feedback gain on the structural SAP is optimized with respect to the pressure at the driver's ear, rather than the firewall vibration. This ASAC strategy is applicable when the acoustic source is transmitted into a cavity through a limited number of structural paths [1,45]. Figure 11(a) shows a scheme of sensor and actuator positions and Fig. 11(b) shows a scheme of the adopted ASAC with the structural sensors and actuators involved in the control loop and the acoustic sensors and actuators related to the performance evaluation.

As a disturbance signal, an acoustic source in the EC that resembles engine noise is used (F_a in Fig. 11b). At constant speed, the

characteristic frequency content of engine noise is a combination of the fundamental frequency (rotating speed), its harmonics and the background noise. During a run-up, these frequencies are swept, exciting a broad spectrum. After analyzing a series of time signals from real engine run-ups, the average amplitude of the disturbance signal was defined as depicted in Fig. 12.

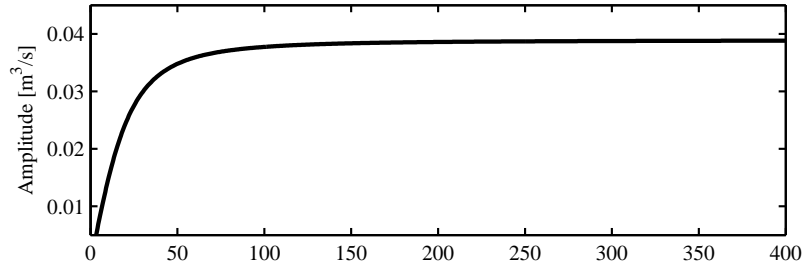


FIGURE 12: Disturbance spectrum - acoustic input

Since the control strategy is selected, the control design consists of determining the position of the SAP and the velocity feedback gain. The structural design parameter is the thickness of the firewall, as it directly affects the vibro-acoustic behaviour of the system.

The metrics adopted to evaluate the design are the system performance, the control effort and the structural firewall mass. The performance of the system is defined as the sound pressure level (*SPL*), in dB, at the driver's ear position (Eq. 25) and the control effort is defined as the applied control effort (*COE*), in V, (Eq. 26).

$$SPL = 20 \log \left(\frac{p_{rms}}{2 \cdot 10^{-5}} \right) \quad (25)$$

$$COE = G \dot{u}_{rms} \quad (26)$$

where p , in Pa, is the acoustic pressure, G , in V/(m/s), is the velocity feedback gain and \dot{u} , in m/s, is the structural velocity.

In a conventional design procedure, the structure is first optimized based on the passive performance and then, afterwards, an active control system is designed. Figure 13 shows the passive performance for different firewall thicknesses (from 0.5mm to 4.5mm with 0.1mm step).

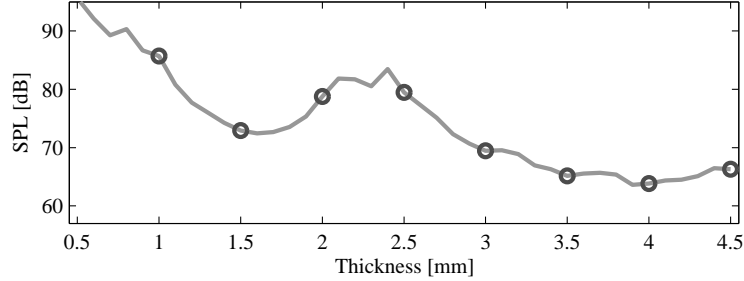


FIGURE 13: Passive performance for several firewall thicknesses

Different performances occur due to the coupling between the structural and acoustic resonances. A good coupling between these resonances allows the noise at the EC to be transmitted through the firewall to the PC more efficiently, decreasing the performance, as occurs for instance for firewalls around 2.0mm. On the other hand, the noise at EC will not be efficiently transmitted when the resonances and modes are not strongly coupled, increasing the performance, *e.g.* for the 1.5mm firewall (Table 1). The markers on Fig. 13 represent the typical plate thicknesses readily available on the market, and therefore will be considered as the only feasible choices hereafter.

The presented optimization problem adopting a concurrent mechatronic design approach assumes that the controller is performed by a single collocated SAP. Therefore, the variables are the firewall thickness, the velocity feedback gain and the position of the SAP. This optimization problem deals with continuous variables, *i.e.* the feedback gain, and discrete variables, *i.e.* the firewall thickness (discrete values readily available on the market) and the SAP position (node locations on the firewall FE model). In addition, this problem is non-convex and nonlinear. Since the model is of reduced size, an extensive search is performed for all possible configurations, comprising: all free nodes of the firewall as possible positions for the SAP (171 positions as indicated in Fig. 14), different thicknesses of the firewall (1.0, 1.5, 2.0 and 2.5mm) and several feedback gains (from 0 to $10kN/(m/s)$).

Multi-objective optimization problems, usually, have conflicting objective functions. Therefore, the derivation of a single cost function as a weighted summation of those objectives [46] is not a trivial task since it may cause a huge impact on the optimal design.

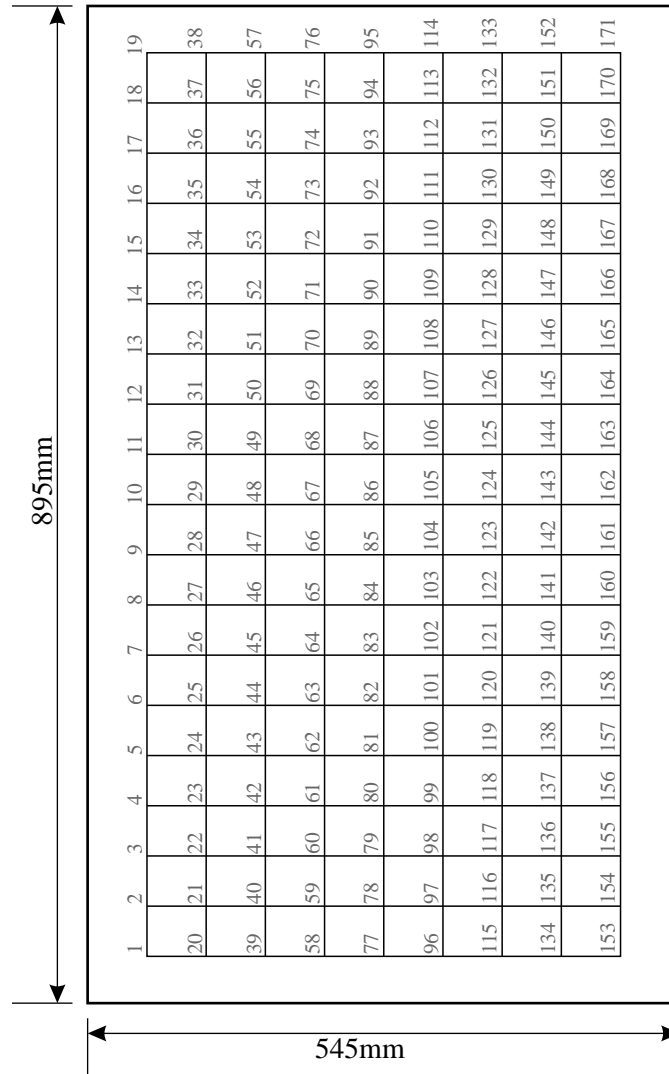


FIGURE 14: Possible SAP positions on the firewall: the nodes on the firewall FE model

A more comprehensive strategy is to find the tradeoffs among sev-

eral objectives. The Pareto plot represents the best obtainable compromises between all the conflicting objective functions [47]. This plot shows the feasible and infeasible design regions in the objective space. Figure 15 shows the feasible region in the design space limited by the design constraints and its mapping to the objective space. The lower border between the feasible and infeasible regions in the objective space is the Pareto front. It contains the possible optimal combinations of the objectives. Objectives out of the border may lead to infeasible or suboptimal designs, *i.e.*, for a solution belonging to this border it is not possible to improve one objective function without worsening another one [47]. Eventually, the solution derived by any single cost function is captured by the Pareto front. In this way, the designer can choose one single solution belonging to the Pareto front that suits better other design criteria.

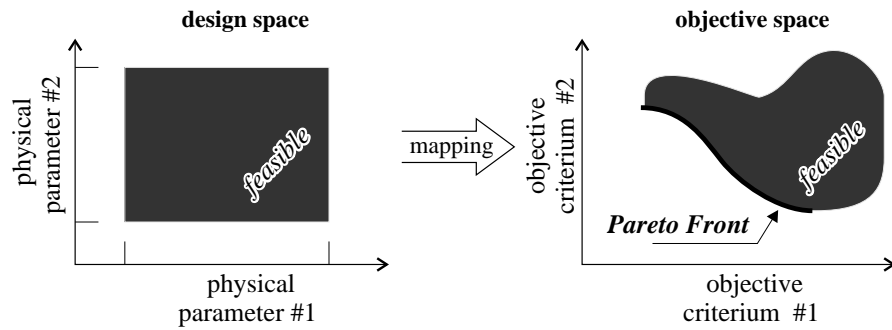


FIGURE 15: Mapping from the design to the objective space

Figure 16 shows, for different firewall thicknesses, the Pareto plot considering performance and control effort. All feasible configurations, derived from an extensive search for various SAP locations and feedback gains, are shown in this Pareto plot. The first conclusion that can be drawn is that the lightest option (1.0mm) presents unsatisfactory passive and active performances. Therefore, considering performance and effort as design criteria, three configurations may be suitable: 1.5, 2.0, and 2.5mm firewall. Among them, the lighter configuration, 1.5mm, presents the best passive performance (72.4dB as already indicated in Fig. 13).

According to a conventional design sequence, a natural choice would

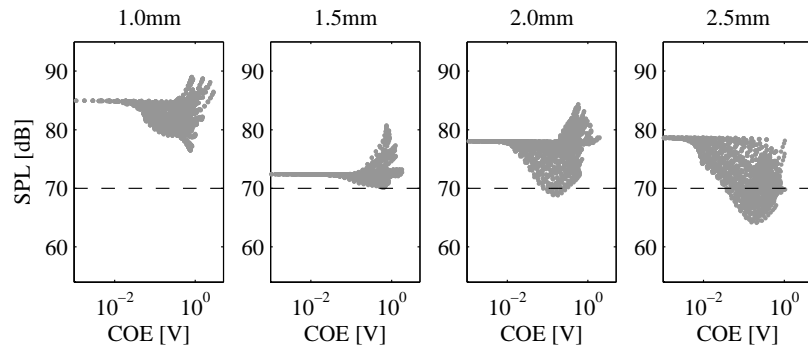


FIGURE 16: Performance and control effort for different firewall thicknesses - Pareto plot

be to select the thinner firewall (1.5mm), resulting in the lightest design and the best passive configuration. However, when the closed-loop performance is analyzed, the performance improvement of the lightest configuration is rather limited compared to the other configurations. For instance, requiring that the performance of the active system should be below 70.0dB, the lightest configuration barely achieves such target (Fig. 16). Considering this target, the thicker configurations would achieve higher noise reduction; despite their lower passive performance. For a 70.0dB target the lightest design is the 2.0mm firewall. Moreover, it is possible to reach the same performance with less control effort by selecting the 2.5mm firewall.

In summary, a conventional design sequence would lead to 1.5mm firewall with the best possible closed-loop performance of 70.2dB, while the concurrent mechatronic approach would lead to 2.0mm firewall with closed-loop performance up to 68.8dB or even 2.5mm achieving up to 64.1dB. The concurrent mechatronic approach delivers better results than the conventional design sequence, since the system passive performance is not considered independently from the control dynamics.

Additionally, Fig. 16 shows that some SAP positions with high velocity feedback gain value, *i.e.* high effort values, can deteriorate the system performance compared with the passive performance. This phenomenon occurs because high velocity feedback gains may clamp this position, modifying the dynamic behaviour of the firewall, shift-

ing natural frequencies and modes. Thus, the coupling between the acoustic and structural resonances can be amplified, deteriorating the system performance.

The system performance, according to the collocated SAP position, depends strongly on the firewall thickness. Figure 17 shows the best achievable performance for each SAP position on the firewall (z and y -directions) for different thicknesses. As mentioned before, this behaviour can be explained by the fact that different thicknesses lead to differences in the structural resonance frequencies and, consequently, variations on the vibro-acoustic coupling. In this way, different vibro-acoustic modes may have a stronger contribution on the transmissibility process, resulting in distinct topologies for the optimum surfaces. As it can be observed in Figs. 16 and 17, the same performance can be achieved by different configurations. These results justify the mechatronic design approach and illustrate the limits in the conventional design methodology for active vibro-acoustic applications.

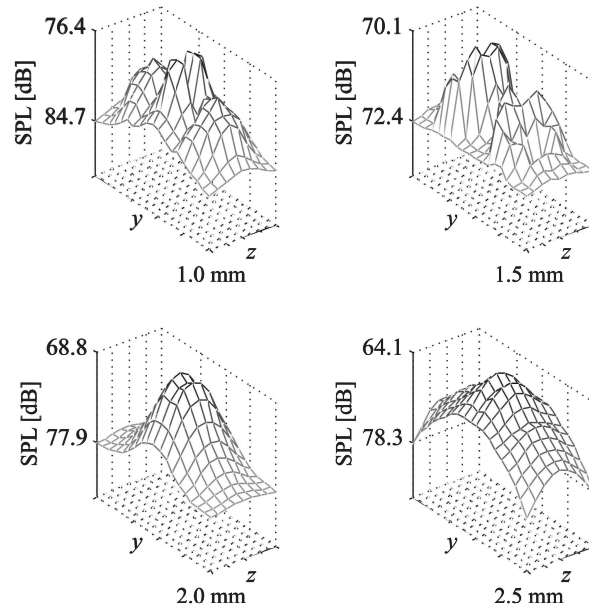


FIGURE 17: Sound pressure level at each SAP position (with optimal gain) for different firewall thicknesses

Figure 17 results from *a priori* derivation of reduced models for each

TABLE 3: Experimental and simulated SPL at the driver's ear for passive, sub-optimal and optimal solutions

Solution	Experiments		Simulation	
	SPL [dB]	Reduction [dB]	SPL [dB]	Reduction [dB]
Passive	76.7	-	78.0	-
Sub-optimal	75.8	0.9	76.6	1.4
Optimal	67.9	8.8	68.8	9.2

firewall thickness. Each firewall thickness requires a reduced model. The required calculation time for deriving a reduced model depends a.o. on the modal density (see Table 2). Using a Pentium IV, with a processor of 1.4GHz, the CPU time varied from 580s for deriving the reduced model for the 2.5mm firewall to 750s for deriving the reduced model for the 1.0mm firewall. The model reduction procedure is performed just once for each firewall thickness, since all possible SAP positions are kept during the model reduction procedure. Once the reduced model is derived, the Pareto plot can be built finding the best gain for each possible SAP position. Using the same processor, this derivation took about 1500s for each reduced model.

The numerical results have been verified experimentally by comparing the passive and active sound spectra at the driver's ear position for the 2.0mm firewall. Figure 18 shows the sub-optimal case, where the SAP is placed closer to the border (node 130 in Fig. 14) and the feedback gain is set to 466V/(m/s). Figure 19 shows the global optimal solution, with SAP at node 87 and feedback gain 466V/(m/s). Table 3 summarizes the SPL and the noise reduction for the passive, sub-optimal and optimal solutions depicted in Figs 18 and 19. The good agreement between experiment and simulation corroborates the results presented and emphasizes the benefits of the proposed concurrent mechatronic approach.

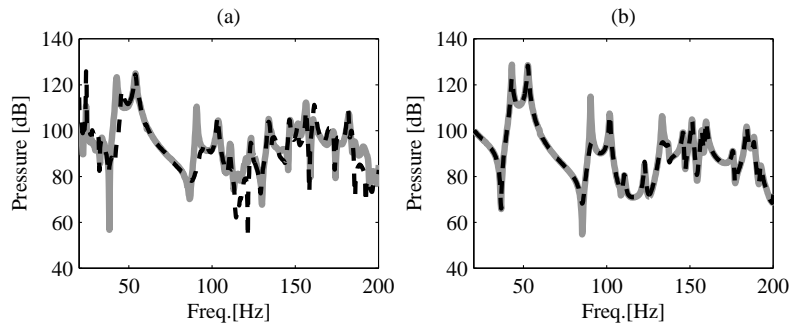


FIGURE 18: Sound spectra at driver's ear position for (-) passive system and (- -) suboptimal active system : (a) Experimental and (b) Simulation

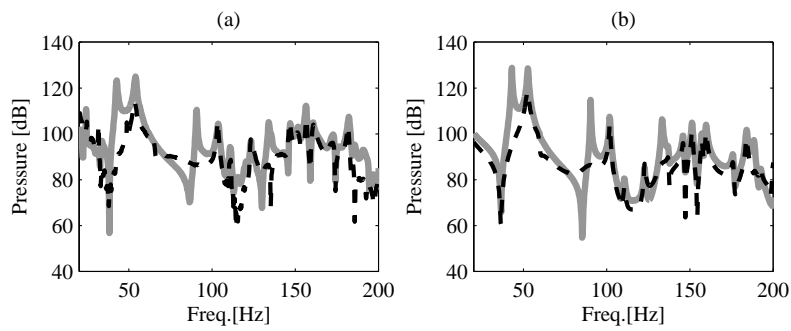


FIGURE 19: Sound spectra at driver's ear position for (-) passive system and (- -) optimal active system : (a) Experimental and (b) Simulation

4. Conclusions and Future Work

A concurrent mechatronic approach for ASAC, considering a fully coupled vibro-acoustic system with SAP models, has been presented. This general approach allows the inclusion of any kind of controller that uses structural or acoustic sensors and actuators. The modelling procedure was validated by correlating the direct FE and the reduced SS models. Eventually, the vibro-acoustic model reduction procedure was experimentally validated for a system that resembles a passenger vehicle interior.

The benefits of this approach have been exploited in some investigations considering structural and control parameters as the firewall thickness, the velocity feedback gain and the position of the SAP. The first conclusion that can be outlined is that optimal passive performance systems may have inferior closed-loop performance. Consequently, an optimal design can only be achieved when considering structure and control concurrently.

Considering that an ASAC modelling procedure is a multi-disciplinary assignment, distinct objectives arise from these disciplines. Capturing the design tradeoffs, using for instance the Pareto front, can assist the designer to gain better insights into the problem.

Comparisons between experimental and simulation results for the passive, sub-optimal and optimal solutions showed good agreement confirming the benefits of the proposed concurrent mechatronic approach for ASAC design.

Given the potential of piezoelectric materials for active control purposes, a next step in this study will be the inclusion of distributed sensors and actuators in the methodology. As optimization variables, not only the placements and the control gains, but also the shape of the piezo-patches may then be considered.

Acknowledgements

The research of Leopoldo P. R. de Oliveira is supported in the framework of a bilateral agreement between KU Leuven and University of São Paulo. The support for the research of Maíra M. da Silva is provided by CAPES, Brazilian Foundation Coordination for the Improvement of Higher Education Personnel. The research presented in this paper was performed as part of the FP6-Integrated Project InMAR, "Intelligent

Materials for Active Noise Reduction". We are also grateful to LMS International for the technical support and encouragement.

Bibliography

- [1] S.J. Elliott, Active control of structure-borne noise, *Journal of Sound and Vibration* 177 (1994) 651-673.
- [2] S.J. Elliott, I.M. Stothers, P.A. Nelson, A.M. McDonald, D.C. Quinn and T. Saunders, The active control of engine noise inside cars, *InterNoise 88*, Avignon, France, September 1988, pp. 987-990.
- [3] W. Dehandschutter, P. Sas, Active control of structure-borne road noise using vibration actuators, *Journal of Vibration and Acoustics* 120(2) (1998) 517-523.
- [4] C. Park, C. Fuller, M. Kidner, Evaluation and demonstration of advanced active noise control in a passenger automobile, *Proceedings of ACTIVE 2002*, Southampton, UK, July 15-17 2002, pp. 275-284.
- [5] C.G. Park, C. Fuller, J.P. Carneal, V. Collin, J.T. Long, R.E., Powell, J.L. Schmidt, On-road demonstration of noise control in a passenger automobile - Part 2, *Proceedings of ACTIVE 04*, Williamsburg, Virginia, September 20-22 2004, pp. 1-12.
- [6] A. Gonzaleza, M. Ferrera, M. de Diegoa, G. Pineroa, J.J. Garcia-Bonito, Sound quality of low-frequency and car engine noises after active noise control, *Journal of Sound and Vibration* 265 (2003) 663679.
- [7] K. Henriouille, P. Sas, Experimental validation of a collocated PVDF volume velocity sensor/actuator pair, *Journal of Sound and Vibration* 265 (2003) 489506.
- [8] S.J. Elliott, P. Gardonio, T.C. Sors, M.J. Brennan, Active vibroacoustic control with multiple local feedback loops, *Journal of the Acoustical Society of America* 111 (2002) 908-915.
- [9] L.P.R. Oliveira, B. Stallaert, W. Desmet, J. Swevers, P. Sas, Optimisation strategies for decentralized ASAC, *Proceedings of Forum Acusticum 2005*, Budapest, 2005, pp. 875-880.

- [10] A. Preumont, *Vibration Control of Active Structures: An Introduction*, 2nd edition, Kluwer Academic Publishers, 2002.
- [11] O.N. Baumann, W.P. Engels, S.J. Elliott, A Comparison of centralised and decentralised control for the reduction of kinetic energy and radiated sound power, *Proceedings of ACTIVE 04*, Williamsburg, Virginia, September 20-22 2004, pp. 1-11.
- [12] P. de Fonseca, P. Sas, H. Van Brussel, A comparative study of methods for optimizing sensor and actuator locations in active control applications, *Journal of Sound and Vibration* 221 (1999) 651-679.
- [13] W. Liu, Z. Hou, M.A. Demetriou, A computational scheme for the optimal sensor/actuator placement of flexible structures using spatial H2 measures, *Mechanical Systems and Signal Processing* 20 (2006) 881-895.
- [14] H. Van der Auweraer, K. Janssens, L. de Oliveira, M. da Silva, W. Desmet, Virtual prototyping for sound quality design of automobiles, *Sound and Vibration* April (2007) 26-30.
- [15] J. Van Amerongen, P. Breedveld, Modelling of physical systems for the design and control of mechatronic systems, *Annual Reviews in Control* 27 (2003) 87117.
- [16] H. Van Brussel, P. Sas, I. Németh, P. De Fonseca, P. Van den Braembussche, Towards a mechatronic compiler, *IEEE/ASME Transactions on Mechatronics*, Vol. 6, No. 1, March 2001, pp. 90-105.
- [17] Z. Xianmin, L. Jianwei, S. Yunwen, Simultaneous optimal structure and control design of flexible linkage mechanism for noise attenuation, *Journal of Sound and Vibration* 299 (2007) 1124-1133.
- [18] J.A. Giordano, G.H. Koopmann, G.H., State-space boundary element-finite element coupling for fluid-structure interaction analysis, *J. Acoust. Soc. Am.* 98 (1995) 363-372.
- [19] K.A. Cunefare, S. De Rosa, S., An improved state-space method for coupled fluid-structure interaction analysis, *J. Acoust. Soc. Am.* 105 (1999) 206-210.

-
- [20] S. Li, A state-space coupling method for fluid-structure interaction analysis of plates, *J. Acoust. Soc. Am.* 118 (2005) 800-805.
- [21] L.P.R. Oliveira, A. Deraemaeker, J. Mohring, H. Van der Auweraer, P. Sas, W. Desmet, A CAE modeling approach for the analysis of vibroacoustic systems with distributed ASAC control, *Proceedings of ISMA2006*, Leuven - Belgium, September 2006, pp. 321-336.
- [22] J.I. Mohammed, S.J. Elliott, Active control of fully coupled structural-acoustic systems, *Proceeding of Inter-Noise 2005*, Rio de Janeiro - Brazil, 2005, pp. 1-10.
- [23] W. Desmet, B. Pluymers, P. Sas, Vibro-acoustic analysis procedures for the evaluation of the sound insulation characteristics of agricultural machinery cabins, *Journal of Sound and Vibration* 266 (2003) 407441.
- [24] P. Sas, C. Bao, F. Augustinovicz, W. Desmet, Active control of sound transmission through a double panel partition, *Journal of Sound and Vibration* (1995) 180(4) 609-625.
- [25] G. Pan and D.A. Bies, The effect of fluid structure coupling on the sound waves in an enclosure: theoretical part, *J. Acoust. Soc. Am.* 2(1987) 691-706.
- [26] G.C. Everstine, A symmetric potential formulation for fluid-structure interactions, *Journal of Sound and Vibration* 79 (1981) 157-160.
- [27] L.G. Olson, K.J. Bathe, Analysis of fluid-structure interactions: a direct symmetric coupled formulation based on the fluid velocity potential, *Computers & Structures* 21 (1985) 21-32.
- [28] W. Desmet, D. Vandepitte, Finite element method in acoustics, *Seminar on Advanced Techniques in Applied and Numerical Acoustics - ISAAC17*, Leuven - Belgium, September 2006, pp. 1-48.
- [29] J.P. Coyette, Y. Dubois-Plerin, An efficient coupling procedure for handling large size interior structural-acoustic problems, *Proceedings of ISMA-19*, Leuven - Belgium, September 1994, pp. 729-738.
- [30] MSC. Nastran Reference Manual, MSC Software, USA, 2004.

- [31] G.C. Everstine, Structural acoustic analogies for scalar field problems, *International Journal of Numerical Methods in Engineering*, 17(3)(1981), 471-476.
- [32] G.C. Everstine, Finite element formulations of structural acoustics problems, *Computers & Structures* 65 (1997) 307-321.
- [33] S. De Rosa, G. Pezzullo, L. Lecce, F. Marulo, Structural acoustic calculations in the low frequency range, *AIAA Journal of Aircraft*, 31(6)(1994), 1387-1394.
- [34] W. Desmet, A wave based prediction technique for coupled vibro-acoustic analysis, PhD Thesis, Katholieke Universiteit Leuven, Mechanical Engineering Department - PMA, 1998.
- [35] J. Luo, H.C. Gea, Modal sensitivity analysis of coupled acoustic-structural systems, *Journal of Vibration and Acoustics* 119 (1997) 545-550.
- [36] Sysnoise rev. 5.5 User's Manual, LMS International, Leuven, Belgium, 2000.
- [37] K. Unholtz, *Vibration testing machines - Shock and Vibration Handbook*, McGraw-Hill Book Co., New York, v.2, pp. 25.1 - 25.74, ed.1, 1961.
- [38] G.R. Tomlinson, Force Distortion in Resonance Testing of Structures with Electrodynamical Vibration Exciters, *Journal of Sound and Vibration* 63 (1979) 337-350.
- [39] K.G. McConnell, *Vibration Testing: Theory and Practice*, John Wiley and Sons, NY, EUA, 1995.
- [40] T. Olbrechts, P. Sas, D. Vandepitte, FRF measurement errors caused by the use of inertia mass shakers, *Proceedings of the 15 International Modal Analysis Conference, IMAC* , 1997, pp. 188-194.
- [41] L.P.R. Oliveira, P.S. Varoto, On the Force Drop-off Phenomenon in Shaker Testing in Experimental Modal Analysis, *Journal of Shock and Vibration* 9 (2002) 165-175.

- [42] S. Herold, H. Atzrodt, D. Mayer, M. Thomaier, Integration of different approaches to simulate active structures for automotive applications, *Proceedings of Forum Acusticum 2005*, Budapest - Hungary, 2005, pp. 909-914.
- [43] N.M.M. Maia, J.M.M. Silva, *Theoretical and Experimental Modal Analysis*, John Wiley and Sons Inc., 1997.
- [44] L.P.R. Oliveira, P.S. Varoto, P. Sas, W. Desmet, A state-space approach for ASAC simulation, *Proceedings of the XII International Symposium on Dynamic Problems of Mechanics (DINAME 2007)*, 2007, pp. 1-10.
- [45] P.A. Nelson, S.J. Elliot, *Active Control of Sound*, Academic Press, 1992.
- [46] S. De Rosa, A. Sollo, F. Franco, K. A. Cunefare, Structural-Acoustic Optimisation of a Partial Fuselage with a Standard Finite Element Code, *7th AIAA/CEAS Aeroacoustics Conference and Exhibit*, Maastricht, Netherlands, May 28-30, 2001; Collection of Technical Papers. Vol. 1 (A01-30800 07-71) AIAA-2001-2114.
- [47] M. Gobbi, F. Levi, G. Mastinu, Multi-objective stochastic optimisation of the suspension system of road vehicles, *Journal of Sound and Vibration* 298 (2006) 1055-1072.

Chapter 4

Active sound quality control of engine induced cavity noise

Leopoldo P.R. de Oliveira

Karl Janssens

Peter Gajdatsy

Herman Van der Auweraer

Paulo S. Varoto

Paul Sas

Wim Desmet

Paper published on Mechanical Systems and Signal Processing:

Leopoldo P.R. de Oliveira, Karl Janssens, Peter Gajdatsy, Herman Van der Auweraer, Paulo S. Varoto, Paul Sas, Wim Desmet, Active sound quality control of engine induced cavity noise, *Mechanical Systems and Signal Processing* 23 (2009) 476-488.

Equations (2) has been edited to fit the thesis borders.

Abstract

Active control solutions appear to be a feasible approach to cope with the steadily increasing requirements for noise reduction in the transportation industry. Active controllers tend to be designed with a target on the sound pressure level reduction. However, the perceived control efficiency for the occupants can be more accurately assessed if psychoacoustic metrics can be taken into account. Therefore, this paper aims to evaluate, numerically and experimentally, the effect of a feedback controller on the sound quality of a vehicle mockup excited with engine noise. The proposed simulation scheme is described and experimentally validated. The engine excitation is provided by a sound quality equivalent engine simulator, running on a real-time platform that delivers harmonic excitation in function of the driving condition. The controller performance is evaluated in terms of specific loudness and roughness. It is shown that the use of a quite simple control strategy, such as a velocity feedback, can result in satisfactory loudness reduction with slightly spread roughness, improving the overall perception of the engine sound.

1. Introduction

The successful development of new products relies on the capability of assessing the performance of conceptual design alternatives in an early design phase. In recent years, major progress was made hereto, based on the extensive use of virtual prototyping, particularly in the automotive industry. The state-of-the-art in CAE modelling techniques which can be used for the analysis of time-harmonic acoustic problems is presented in [1]. An overview is given, with automotive interior noise applications, on recently investigated extensions and enhancements to enlarge the application range of different techniques. The efficiency of present CAE techniques allows the use of optimization, *e.g.*, in improving the NVH characteristics of a full-scale engine [2] or a vehicle body [3]. The novelty on this framework is to account for the human perception when defining product performance criteria as in [4,5].

Additionally, active control has shown the potential to enhance system dynamic performance which allows lighter and improved products. Research done in the last years on smart materials and control concepts has led to practical applications with promising results for the automotive industry [6]. However, to make the step to the design of *active sound quality control* (ASQC), the control schemes, along with appropriate simulation procedures, need to become an integral part of the product development process [7]. In other words, this requires: (i) the product performance metrics to be based on human perception attributes and (ii) the simulation models to support the specific aspects related to smart structures (active systems, actuators, sensors and control logic).

In order to demonstrate the proposed simulation procedure and evaluate the effect of active control on the perceived sound quality (SQ), a vibro-acoustic cabin mock-up is selected (Fig. 1). It consists of a simplified car cavity with rigid acoustic boundary condition. The passenger compartment (PC) and the engine compartment (EC) are connected through a flexible firewall which allows noise generated in the EC to be transmitted to the PC. A sound source placed in the EC works as a primary disturbance source. The primary source is driven by a real-time engine simulator, capable of delivering a harmonic excitation based on the engine orders' amplitude and phase [8]. The controller is

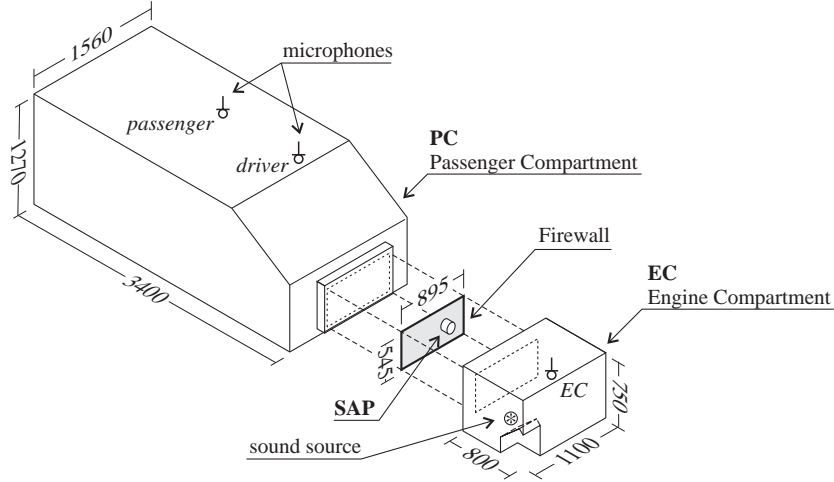


FIGURE 1: Schematic view of the vehicle mock-up (dimensions in mm)

based on a collocated structural sensor/actuator pair (SAP) connected to the firewall in a time-invariant velocity feedback loop.

The simulation procedure and experimental validation of the active structural acoustic control (ASAC) system are presented in Section 2. The SQ metrics and algorithms used in this paper are reviewed in Section 3. The results, concerning Roughness, Specific Loudness and Zwicker Loudness are treated in Section 4. Finally, some general conclusions are addressed in Section 5.

2. ASAC simulation scheme and experimental validation

The active control scheme adopted is an ASAC scheme involving a collocated velocity feedback controller with structural sensors and actuators. This choice is made given the advantages of such a scheme with respect to implementation, stability and reliability to system modification (or uncertainties) [9-11]. It is important however to mention that different control strategies can be adopted under the same simulation framework, which, in the end, reveals the functionality of such an approach to the assessment of conceptual design performance [7,12,13].

2.1 From vibro-acoustic FE to state-space model

In order to bring active solutions to the level of industrial applications, the designer needs tools that allow the inclusion of sensors/actuators and control strategy in the product development phase. Eventually, one should be able to quantify the improvement in some performance design criteria (in this case SQ metrics) after adopting a certain control strategy.

One of the challenges resides in deriving reasonably sized models that integrate the structural and acoustic components along with the control algorithm. In order to fulfil this requirement, a fully coupled finite element (FE) model of the vibro-acoustic system is written as a modal state-space (SS) model. As a result of using the coupled vibro-acoustic modal base, any combination of structural and acoustic inputs/outputs can be used for the control design, *e.g.*, an acoustic source in the EC, structural sensors and actuators on the firewall and microphones on the PC.

One of the possible coupled FE/FE formulations is the Eulerian, in which the structural degrees of freedom (DoFs) are displacement vectors, while the acoustic DoFs are expressed as scalar functions. The latter is usually the acoustic pressure [14-16]. If pressure is adopted, the system of equations yields non-symmetrical mass and stiffness matrices. The modal base resulting from such non-symmetric eigenproblem presents distinct left and right eigenvectors, denoted here respectively by Φ_L and $\Phi_R \in \mathbb{R}^{n \times 1}$ with n being the total number of structural and acoustic DoFs.

The adopted FE tool provides Φ_R [17]. However, it has been indicated [18] that, particularly for the displacement/pressure Eulerian formulation, the left and right eigenvectors can be related as:

$$\{\Phi_L\}_r = \left\{ \begin{array}{l} \{\Phi_{Ls}\}_r \\ \{\Phi_{La}\}_r \end{array} \right\} = \left\{ \begin{array}{l} \{\Phi_{Rs}\}_r \omega_r^2 \\ \{\Phi_{Ra}\}_r \end{array} \right\} \quad r = 1, 2, \dots, N \quad (1)$$

where r is the index of the coupled natural frequency ω_r , a indicates the acoustic components, s the structural, and $N < n$ is the number of kept modes in the coupled modal base. Therefore, using the right eigenvector and Eq. (1), it is possible to retrieve the left eigenvectors to build the complete modal model.

$$\begin{aligned} \Phi_L^T \begin{bmatrix} \mathbf{K}_s & \mathbf{K}_c \\ \mathbf{0} & \mathbf{K}_a \end{bmatrix} \Phi_R \mathbf{q} + \Phi_L^T \begin{bmatrix} \mathbf{D}_s & \mathbf{0} \\ \mathbf{0} & \mathbf{D}_a \end{bmatrix} \Phi_R \dot{\mathbf{q}} \\ + \Phi_L^T \begin{bmatrix} \mathbf{M}_s & \mathbf{0} \\ -\rho_0 \mathbf{K}_c^T & \mathbf{M}_a \end{bmatrix} \Phi_R \ddot{\mathbf{q}} = \Phi_L^T \begin{Bmatrix} \mathbf{F}_s \\ \mathbf{F}_a \end{Bmatrix} \end{aligned} \quad (2)$$

where ρ_0 is the air density, \mathbf{K} , \mathbf{D} and \mathbf{M} are the stiffness, damping and mass matrices, respectively; \mathbf{K}_c is the vibro-acoustic coupling matrix; \mathbf{F} is the load vector and \mathbf{q} is the vector of modal amplitudes, related to the structural DoFs \mathbf{u} and the acoustic DoFs \mathbf{p} as in Eq.(3)

$$\begin{Bmatrix} \mathbf{u} \\ \mathbf{p} \end{Bmatrix} = \sum_{r=1}^N q_r \{\Phi_R\}_r = \Phi_R \mathbf{q} \quad (3)$$

Moreover, the left and right eigenvectors are normalized such that:

$$\Phi_L^T \begin{bmatrix} \mathbf{M}_s & \mathbf{0} \\ -\rho_0 \mathbf{K}_c^T & \mathbf{M}_a \end{bmatrix} \Phi_R = \mathbf{I} \quad (4)$$

$$\Phi_L^T \begin{bmatrix} \mathbf{K}_s & \mathbf{K}_c \\ \mathbf{0} & \mathbf{K}_a \end{bmatrix} \Phi_R = \mathbf{\Omega}^2 \quad (5)$$

$$\Phi_L^T \begin{bmatrix} \mathbf{D}_s & \mathbf{0} \\ \mathbf{0} & \mathbf{D}_a \end{bmatrix} \Phi_R = \mathbf{\Gamma} \quad (6)$$

where \mathbf{I} , $\mathbf{\Omega}^2$ and $\mathbf{\Gamma} \in \mathbb{R}^{N \times N}$ are the identity, the squared coupled natural frequencies and the modal damping matrices, respectively.

Using the relations described by Eqs. (4), (5) and (6), Eq. (2) can be rewritten in a modal state-space form:

$$\begin{Bmatrix} \dot{\mathbf{q}} \\ \ddot{\mathbf{q}} \end{Bmatrix} = \begin{bmatrix} \mathbf{0} & \mathbf{I} \\ -\mathbf{\Omega}^2 & -\mathbf{\Gamma} \end{bmatrix} \begin{Bmatrix} \mathbf{q} \\ \dot{\mathbf{q}} \end{Bmatrix} + \begin{bmatrix} \mathbf{0} \\ \Phi_L^T \mathbf{B} \end{bmatrix} \begin{Bmatrix} \mathbf{F}_{si} \\ \mathbf{F}_{ai} \end{Bmatrix} \quad (7)$$

$$\begin{Bmatrix} \mathbf{u}_o \\ \mathbf{p}_o \end{Bmatrix} = \begin{bmatrix} \mathbf{C} \Phi_R & \mathbf{0} \end{bmatrix} \begin{Bmatrix} \mathbf{q} \\ \dot{\mathbf{q}} \end{Bmatrix} \quad (8)$$

where $\mathbf{B} \in \mathbb{R}^{n \times N_i}$ is a matrix with ones on the N_i desired input DoFs and zeros everywhere else, $\mathbf{F}_{si} \in \mathbb{R}^{N_{si} \times 1}$ is the structural input load vector, $\mathbf{F}_{ai} \in \mathbb{R}^{N_{ai} \times 1}$ is the acoustic input load vector (with $N_{si} + N_{ai} = N_i$), $\mathbf{u}_o \in \mathbb{R}^{N_{so} \times 1}$ is the structural output vector, $\mathbf{p}_o \in \mathbb{R}^{N_{ao} \times 1}$ is the acoustic output vector (with $N_{so} + N_{ao} = N_o$) and $\mathbf{C} \in \mathbb{R}^{N_o \times n}$ is a matrix with ones on the N_o desired output DoFs and zeros everywhere else. In this formulation, the role of \mathbf{B} is to select columns from Φ_L^T

according to the desired input DoFs; the role of \mathbf{C} is to select rows from Φ_R according to the desired output DoFs. For a more detailed description of the state-space model, the reader is referred to [19].

The original FE model consists of the firewall and cavities meshes (Fig. 2) with coincident nodes over the wet surface. The structural mesh contains 200 4-noded quadrilateral plate elements (Fig. 2a). The acoustic mesh with 26050 8-noded brick elements is depicted in Fig. 2(b). The acoustic elements size is such that this model exhibits a minimum of 6 linear elements per wavelength up to 500Hz.

Applying the aforementioned procedure, the original 24192 DoFs (23196 unconstrained acoustic and 1026 unconstrained structural) have been reduced to a SS model with $2 \times N$ DoFs, related to the kept modal amplitudes \mathbf{q} and their derivatives $\dot{\mathbf{q}}$, with force and volume velocity as inputs and displacement and pressure as outputs. The modal base was built with modes ranging from 0 to 400Hz, resulting in $N = 107$.

The numerical validity of the reduced model is illustrated by comparing FRFs from the original FE model with the reduced SS model (Fig. 3). The system inputs are volume velocity applied in the EC (acoustic input) and force applied on the firewall (structural input); and the outputs are pressure measured in the PC (acoustic output) and displacement measured on the firewall (structural output). The good correlation between the SS and the FE model validates the model reduction procedure.

More detailed information on this modelling procedures can be found in [19].

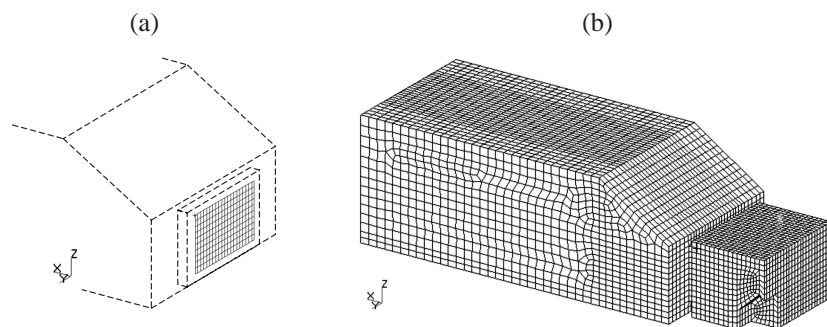


FIGURE 2: FE meshes: (a) firewall and (b) acoustic cavities

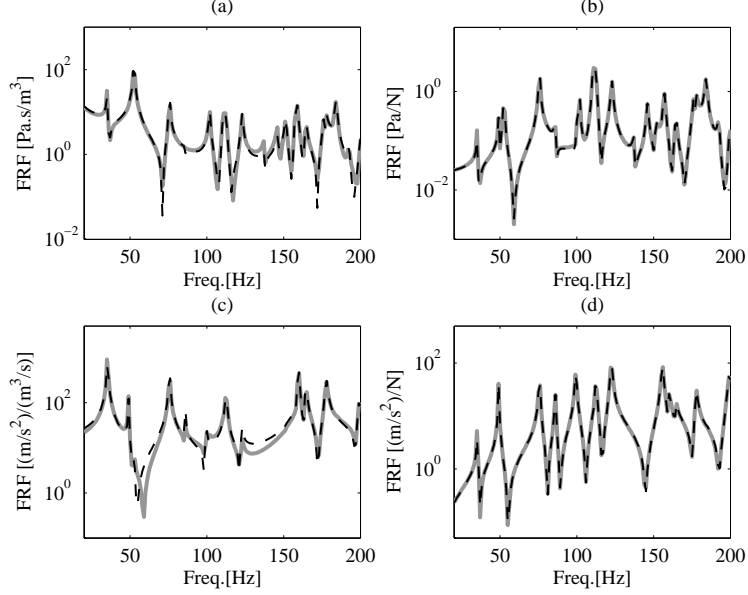


FIGURE 3: Comparison between (- -) FE and (-) SS FRFs: (a) Acoustic/Acoustic, (b) Acoustic/Structural, (c) Structural/Acoustic and (d) Structural/Structural

2.2 Control strategy: collocated velocity feedback

Due to its relatively simple implementation, and promising noise level reduction for the present case study [19], a time invariant collocated velocity feedback controller is selected. A consequence of choosing the feedback strategy is the use of structural sensors and actuators, since the use of acoustic sensors and actuators may present a large phase loss, imposing severe limitations to the feedback controller frequency range [20].

Since feedback is used, an important aspect to the efficiency and stability of the control system is the transfer function between sensor and actuator. This transfer function should present alternating poles and zeros, *i.e.*, the phase angle between these two signals should be bounded by $\pm 90^\circ$, otherwise the system can become unstable. If the SAP is collocated, this property is observed (Fig. 3d), resulting in a

stable control loop independent of the feedback gain [10].

The use of structural sensors and actuators also provides robustness against perturbations on the system, rather common in this kind of application, since an extra passenger or an open window could be more easily sensed by an acoustic sensor. Despite being structurally sensed and actuated, the parameters of the active control can be tuned with respect to acoustic quantities. In this ASAC application, the feedback gain on the structural SAP is set to minimize the pressure level at the driver's ear, rather than the firewall vibration. Figure 4(a) shows a scheme of the adopted ASAC setup, with a structural SAP performing the control loop, the source in the EC and the microphones in the PC.

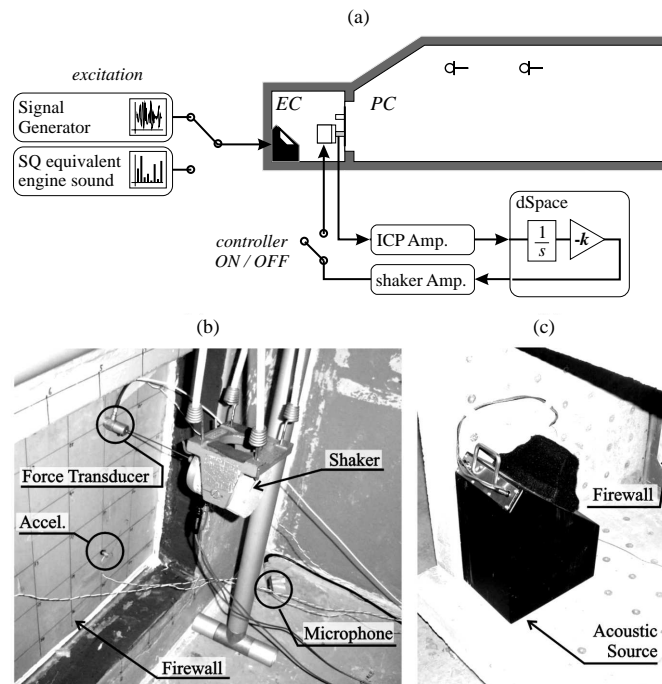


FIGURE 4: Experimental setup: (a) Schematic view, (b) shaker and sensors attached to the firewall and (c) sound source in the engine compartment

2.3 Passive and active system experimental validation

In order to have an engine-like excitation, which allows meaningful SQ measurements, a real-time engine simulator was used [8]. Sound quality equivalent engine models are used in product development, as it enables one to experience and assess the NVH of a virtual (or real) vehicle under various driving conditions [8,21]. The novelty here is the use of such device as a source of excitation (Fig. 4a). In this case, the engine sound, which is a function of the driving condition (engine speed, gear, throttle and brake positions, etc.) is fed to the acoustic source in the EC. Results obtained as such, benefit from this sound quality equivalence and, therefore, allow the correlation with real engine sounds.

For the experimental validation of the SS model, the FRFs derived from it are compared with the FRFs measured on the cabin mock-up. The measured FRFs include structural and acoustic inputs and outputs. As depicted in Fig. 4(b), the structural excitation is performed with a LDS shaker (model V201/3), the force transducer is a PCB 208C04 and the accelerometers are PCB 352C67. Figure 4(c) shows the acoustic source (LMS E-LMFVVS) placed at the EC. The microphones used are B&K 4188. For the system validation, either the shaker or the acoustic source were fed with white noise. The FRFs are measured with an Hv estimator, while input and output signals are filtered with Hanning windows. Figure 5 shows a comparison between the experimental and the simulated (derived from the SS model) FRFs.

As it can be seen, the resulting FRFs present a good agreement up to 200Hz. Few discrepancies arise, *a.o.*, from the lack of accuracy in determining the exact place of the disturbance source, sensor/actuator pair, microphones and from assuming the disturbance source as an ideal point source. Such mismatches are expected and reflect a limitation in the FE modelling rather than in the use of the reduced models in open and closed loop form, which are the focal point of this work.

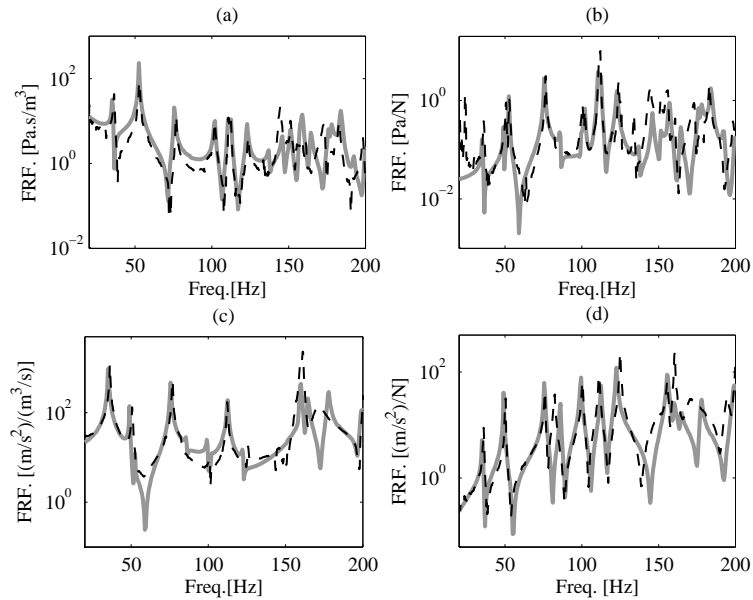


FIGURE 5: Comparison between (-) SS and (- -) experimental FRFs: (a) Acoustic/Acoustic, (b) Acoustic/Structural, (c) Structural/Acoustic and (d) Structural/Structural

The passive system response under white noise excitation, and the effect of the controller over the pressure at three locations (two in the PC and one in the EC) can be observed in Fig. 6. Plots on the left-hand side show experimental results, whereas those on the right-hand side are the corresponding simulation results. The values on the plots represent the overall sound pressure level (SPL) reduction in each case, revealing a quite good agreement between simulated and measured results. By contrasting passive and active responses, either for the driver's ear microphone (top plots) or for the passenger's ear microphone (middle plots), it can be observed that the simulation results predicted efficiently the control behaviour over the frequency range. Even the microphone on the EC (bottom plots), that was not a target for the control strategy, show good agreement when simulation and experiment are concerned.

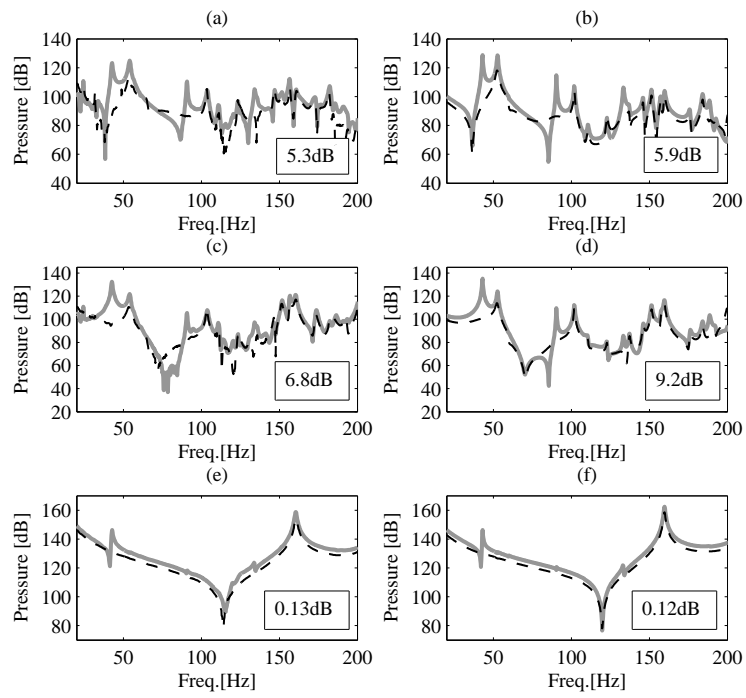


FIGURE 6: Sound spectra for (-) passive and (- -) active system at: Drive's ear position (a) experimental and (b) simulation; Passenger's ear position (c) experimental and (d) simulation; Engine compartment (e) experimental and (f) simulation

3. Sound quality assessment

Sound quality is the science that studies the human appreciation to a determined auditive stimulus. More than the mathematical interpretation of pressure signals, SQ and psychoacoustics try to correlate acoustic stimuli with hearing sensation [22,23]. It is also important to define which is the most appropriate set of metrics for each application. Loudness and Roughness have been indicated, *a.o.*, as the most important for engine noise [24,25].

3.1 Specific Loudness and Zwicker Loudness

In spite of showing some correlation with actual human perception, and therefore being widely used, dB(A) measurements simply superimpose the effects of different frequency components on complex sound. In this sense, it neglects an important mechanism within the ear transduction of pressure fluctuations into signals to the brain, namely frequency masking [23].

Masking is related to the way hair-cells are positioned in the cochlea, so that a tonal (or narrow band) stimulus excites a specific region in the cochlea with effects on its neighbourhood, turning them insensitive to another (lower level) excitation, which rises the concept of critical bands of excitation, measured in Barks. This phenomenon is responsible, for instance, for the way speech intelligibility is affected by background noise. The capability of recognizing a specific sound (test sound) in the presence of another one (masker sound) is very much related to their relations in level and spectral content. Indeed, masking can be interpreted as the variation on the hearing threshold curve to a test sound in the presence of a masker, *i.e.*, if the test sound spectrum lies below the masked threshold it will be inaudible. In that case, while being inaudible, it would still be computed by a SPL-meter, which raised the need for alternative ways of estimating the human perception to the sound level such as the ISO standardized Specific Loudness [26].

From the available techniques, only the method developed by Zwicker and Fastl [23] is valid to broadband excitation, with or without tonal components in free and diffuse fields [27]. As depicted in (Fig. 7), the first step in the numerical procedure consists of filtering the signal with critical band filters, followed by a masking check. In this stage, if the proceeding band level falls under the masking curve of

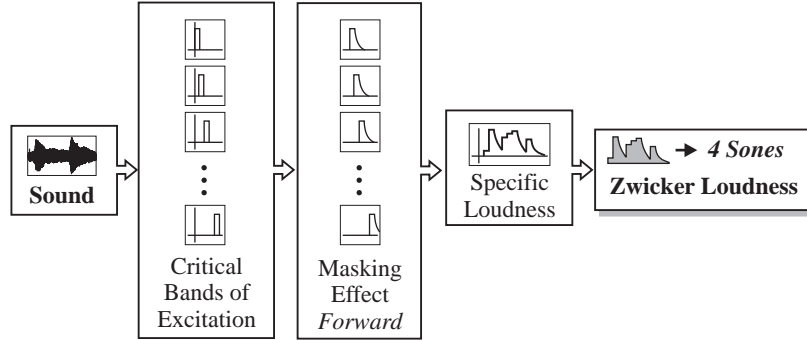


FIGURE 7: Zwicker Loudness calculation flow chart

the preceding one, this value is neglected; otherwise the value is kept. Following this procedure, the Specific Loudness graph is obtained with units Sones/Bark. The value for Zwicker Loudness is defined as the integral of the Specific Loudness over Bark, with values expressed in Sones. The advantage of the Sones scale is its linear correlation with the human perception of volume, *i.e.*, an acoustic stimulus of 4Bark sounds twice as low as an 8Bark stimulus.

3.2 Roughness and Modulation Index

The stimuli used in this paper are engine noise. Thanks to the harmonic nature of such sounds, instead of the classical roughness calculation procedure [28], a more efficient algorithm, recently developed by Janssens *et al.* [29], can be used. The classical algorithm starts with the pressure time-history; alternatively, the order-based roughness algorithm uses the engine orders (frequency, amplitude and phase). The main advantages of such methodology are: (i) fast calculation, (ii) frequency-domain based calculations, typically available in steady-state FE simulations and (iii) an analytical approach for the envelope calculations, which helps understanding certain modulation problems in relation to amplitude and phase of specific order components.

The flow chart of the order-based roughness algorithm is presented in Fig. 8. The algorithm is composed of the following steps:

(I) Critical Bands and Filtering: Specific excitation spectra are calculated within adjacent 1-Bark-wide critical bands with equally spaced centres $z_i = i$ Barks, with $i = 1, 2, 3, 4, \dots, 24$. The contribution of the different orders $k = 1, 2, \dots, n$ to a certain critical band i is as follows:

- If the Bark value z_k is higher than the upper limit of the band, *i.e.*, $z_k > z_i + 0.5$, its contribution is $L_k + S_1[z_k - (z_i + 0.5)]$, where $S_1 = -27\text{dB/Bark}$ and $L_k = 20 \log_{10}(A_k/(2 \times 10^{-5}))$.
- If $z_k < z_i - 0.5$, its contribution is $L_k + S_2[(z_i - 0.5) - z_k]$, where $S_2 = (0.2L_k - 230/f_k - 24)\text{dB/Bark}$.
- If z_k falls into the interval $(z_i - 0.5) \leq z_k \leq (z_i + 0.5)$, its unchanged level L_k fully contributes to the specific excitation spectrum of band i .

This critical band filtering in the frequency domain is the same as in the classical approach, but is limited here to a reduced set of order frequencies.

(II) Envelopes Analytical Calculation: The main difference to the classical approach lies in this step, where a sound envelope is calculated for each critical band. This is done in a fully analytical way from the amplitude, phase and frequency of the different orders exciting the band.

Consider, for example, a stationary engine sound at 6000rpm with four significant orders 4, 4.5, 5 and 5.5, and suppose that the excitation spectrum for the critical band with $z_i = 5$ Bark is as shown in Fig. 9(a) and (b). According to [29,30], the sound envelope $Env(t)$ for this frequency band can then be calculated as:

$$Env(t) = \sqrt{DC^2 + AC_1^2 + AC_2^2 + AC_3^2} \quad (9)$$

where DC is the envelope DC -component (Eq. 10) and AC_i are the several AC -components according to the combinations of orders (Eqs. 11-13).

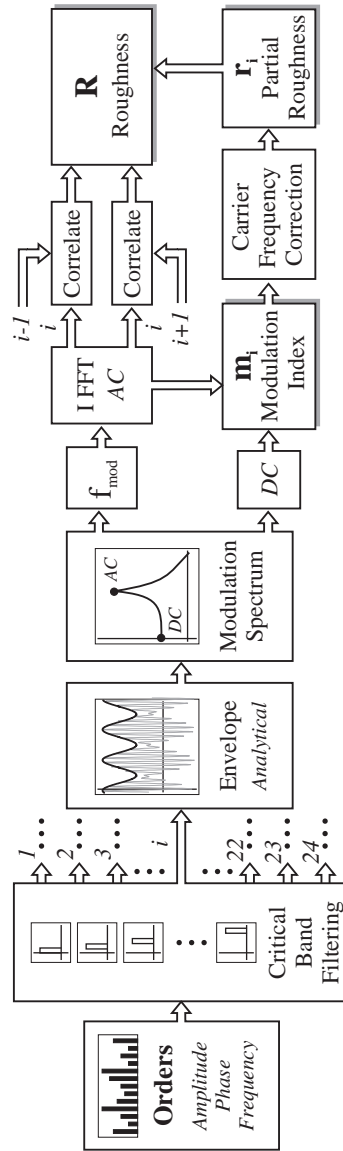


FIGURE 8: Order-based Roughness calculation flow chart

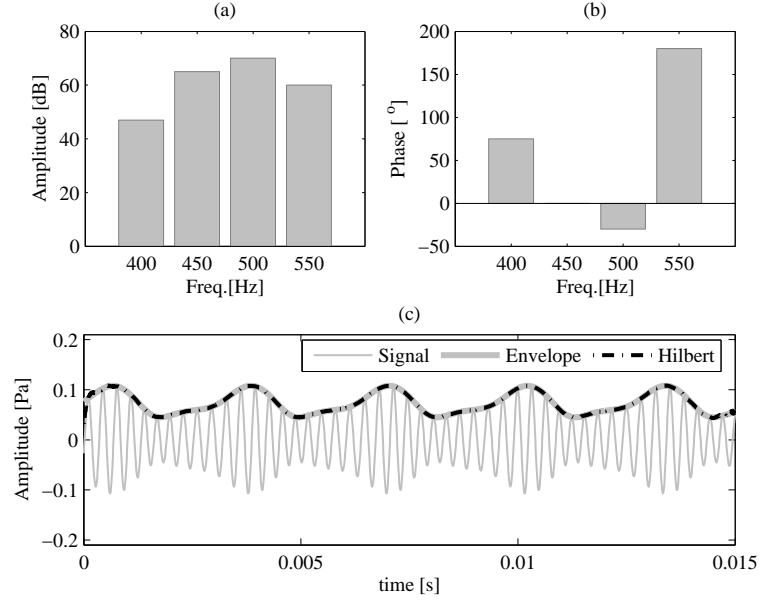


FIGURE 9: Engine Sound: Orders (a) amplitude, (b) phase and (c) time-domain signal with envelopes

Given the amplitude A_i for each order i :

$$DC^2 = A_1^2 + A_2^2 + A_3^2 + A_4^2 \quad (10)$$

In this example, the envelope is composed of three *AC* sub-envelopes with modulation frequencies of 50Hz, 100Hz and 150Hz, respectively.

$$\begin{aligned} AC_1^2(t) &= 2A_1A_2 \cos(2\pi(\theta_2 - \theta_1)t + (\varphi_2 - \varphi_1)) \\ &+ 2A_2A_3 \cos(2\pi(\theta_3 - \theta_2)t + (\varphi_3 - \varphi_2)) \\ &+ 2A_3A_4 \cos(2\pi(\theta_4 - \theta_3)t + (\varphi_4 - \varphi_3)) \end{aligned} \quad (11)$$

$$\begin{aligned} AC_2^2(t) &= 2A_1A_3 \cos(2\pi(\theta_3 - \theta_1)t + (\varphi_3 - \varphi_1)) \\ &+ 2A_2A_4 \cos(2\pi(\theta_4 - \theta_2)t + (\varphi_4 - \varphi_2)) \end{aligned} \quad (12)$$

$$AC_1^2(t) = 2A_1A_4 \cos(2\pi(\theta_4 - \theta_1)t + (\varphi_4 - \varphi_1)) \quad (13)$$

where θ_i and φ_i are the order frequency and phase angle, respectively.

Figure 9(c) compares the calculated envelope with the one obtained in the classical way by applying the Hilbert Transform to the critical band sound signal. The analytical approach clearly results in a similar envelope, but with a processing speed which is up to ten times faster [29].

(III) Modulation Index, Partial and Total Roughness: The remaining steps of the order-based algorithm are exactly the same as those in the classical approach [23].

For each Bark band, a modulation index m_i is calculated from the sound envelope which is then transformed into a partial roughness value r_i by applying psycho-acoustic weighting functions. The correlations between adjacent critical bands are finally taken into account to calculate the total roughness R from the partial roughness values (Fig. 8).

4. Results

In spite of the great number of publications on noise control, there are few papers available describing the listeners perception to such control actions. Some edited sound samples are compared with the original records in [31,32] in order to assess what the effect of a hypothetical active control would have on SQ metrics. Gonzalez *et al.* [25] correlate comfort predictor metrics with jury test for an ANC system assembled in a room where synthesized and recorded engine sounds were used. More recently, an adaptive scheme for ASQC has been presented [33], which effectively reshapes residual noise in ducts, thus directly affecting SQ.

The results obtained with the proposed experimental scheme regards the application of an actual control system to a vehicle cabin mock-up excited with engine sound. The SQ equivalent engine model used here considers 20 orders (0.5, 1, 1.5, ..., 10) and refers to a 4-cylinder inline engine operating in two conditions: 50km/h in 4th gear (1634rpm) and 90km/h in 5th gear (2694rpm). Due to the SQ

equivalence, besides validating the modelling procedure, rather general conclusions can be drawn from these results.

Figure 10 shows comparisons of the passive and active Specific Loudness perceived by the driver and the back passenger for 50km/h. Figure 11 shows the same comparisons for 80km/h. Plots on the left-hand side result from measured data while those on the right-hand side are the corresponding simulations. Simulation and measurement results agree well, both in the level and the shape of the Specific Loudness contours.

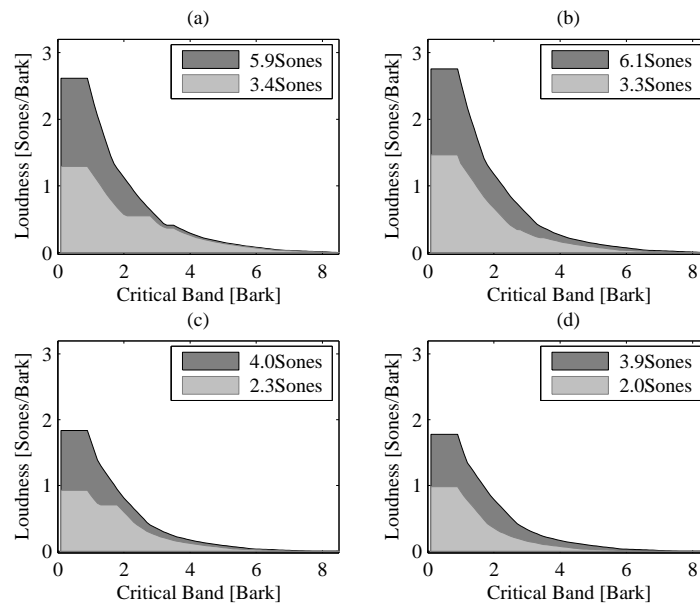


FIGURE 10: Engine sound Loudness @ 50km/h, passive (dark) and active (light): Driver (a) experimental and (b) simulated; Passenger (c) experimental and (d) simulated

The results presented in Fig. 10(a) and (c) reveal an attenuation of 42% on Zwicker Loudness; the simulated results predicted a slightly higher attenuation of 45% for the driver and 48% for the passenger. The results for 80km/h also present good agreement between measured and simulated data, besides some overestimation of the control action around 2Bark. Due to the latter mismatch, the overall reduction is

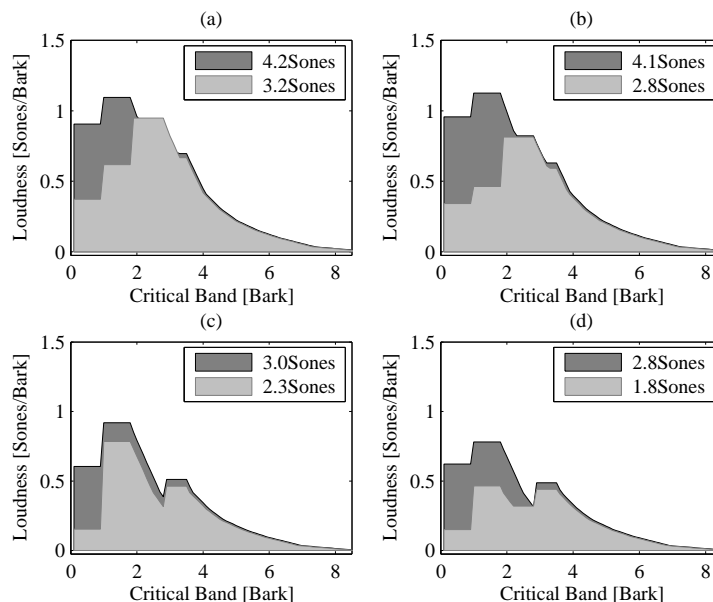


FIGURE 11: Engine sound Loudness @ 80km/h, passive (dark) and active (light): Driver (a) experimental and (b) simulated; Passenger (c) experimental and (d) simulated

somewhat overestimated by the simulation; the measured data show a 23% reduction for both, driver and passenger, while the simulated results present 31% and 35%, respectively.

The presented simulation procedure allows the analysis of the controller global effects, which can be visualized in 3D colourmaps as depicted in Figs. 12 and 13. Figure 12(a) shows the Zwicker Loudness values for 50km/h on passive configuration, as Fig. 12(b) shows the active configuration. The colour scale is kept the same for both plots, which allows the contrast between passive and active results, revealing that, despite the control action being local, the Loudness attenuation can be global.

Similar conclusions can be drawn from Fig. 13, which shows the results for 80km/h. Figure 13(a) shows the Zwicker Loudness for the passive configuration and Fig. 13(b) shows the active. While for 50km/h (Fig. 12) the first longitudinal mode of the cavity seems to play an

important role, the resulting pressure field at 80km/h is rather more complicated. Even then, the Loudness attenuation is again global.

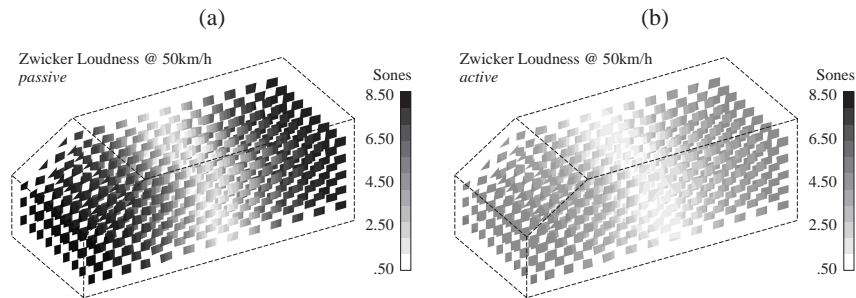


FIGURE 12: 3D Zwicker Loudness colormap @ 50km/h: (a) passive and (b) active

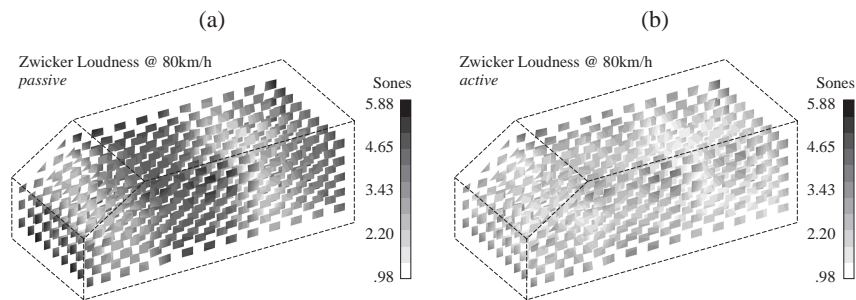


FIGURE 13: 3D Zwicker Loudness colormap @ 80km/h: (a) passive and (b) active

The proposed modelling procedure allows time-domain simulation, but since the order-based roughness algorithm (described in Section 3.2) is more efficient, a frequency-domain analysis of the sound field in the PC is sufficient to generate the colormaps shown in Figs. 14 and 15.

Figure 14(a) and (b) show the passive and active roughness on the PC, respectively. As expected, the roughness values are slightly increased. This is due to the attenuation of some order amplitudes, which can unmask orders in their vicinities, allowing modulation and, therefore, increasing roughness. Again, in the case of 50km/h, the first

longitudinal mode of the PC plays an important role; in the passive configuration, the higher pressure values prevent modulations everywhere but close to its nodal-plane in the middle of the cavity. As this mode is damped by the active control, its influence region diminishes allowing a broader rough region. It is important to notice that there is no significant increase on the maximum roughness value (0.075Asper), it is only the region with some significant partial (or specific) roughness that increases.

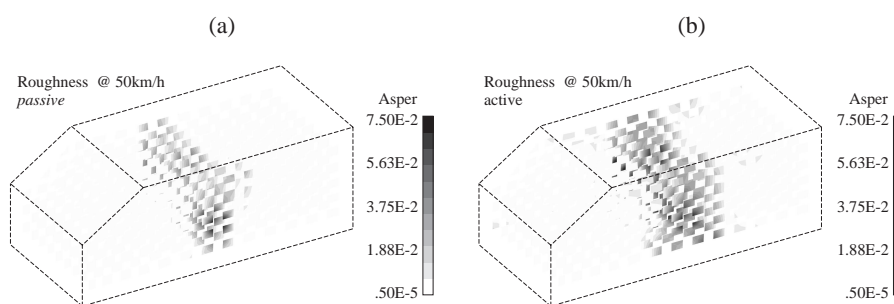


FIGURE 14: 3D Roughness colormap @ 50km/h: (a) passive and (b) active

Figures 15(a) and (b) show the passive and active roughness for 80km/h, respectively. Again, the effect of the controller is more noticeable in the overall spread of higher roughness values than in an increase of the maximum roughness observed before, in this case 0.25Asper . Even if it is not that straightforward to associate this pattern with a single mode shape, it is noticeable that regions presenting a higher roughness have increased.

Concerning the appreciation of the active control action, it is important to note that the reduction in Loudness is much more noticeable than the changes in roughness. However, besides being responsible for the feeling of power and sportiveness, roughness is usually associated with unpleasantness. In this way, future control algorithms should take roughness into account. Anyway, it is considered that the effect of such ASAC system has improved the perception of the engine sound for the occupants.

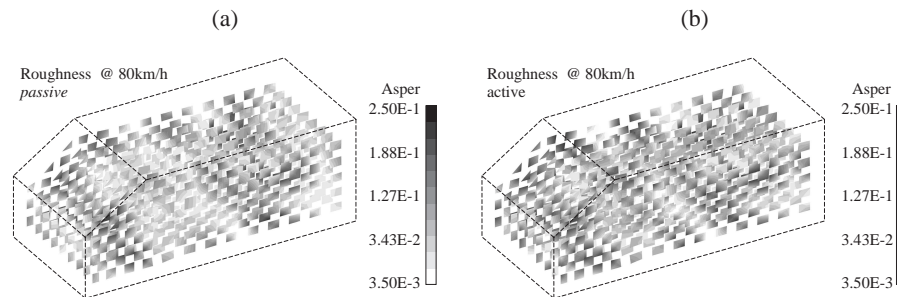


FIGURE 15: 3D Roughness colormap @ 80km/h: (a) passive and (b) active

5. Conclusions

This paper describes a modelling procedure for ASAC, which allows the use of standard vibro-acoustic FE models in the control design. The modelling procedure is experimentally validated, with a vehicle mock-up, for both passive and active configurations.

The proposed experimental setup is acoustically excited using a SQ equivalent engine simulator, typically employed in auralization. The use of such scheme allows repeatable measurements with engine-like excitation signals, furnishing results that can be directly correlated to automotive applications.

The selected control strategy, collocated velocity feedback, presents satisfactory results for global noise reduction in the passenger compartment. The results for Loudness attenuation are presented in terms of Specific and Zwicker Loudness, the latter being linearly related to the human sensation of volume. The results indicate that the effect of the controller is not just noticed locally by the occupants, but is improved rather globally.

Finally, the simulation scheme and analysis tools presented here, such as the 3D SQ plots, enables the quantitative assessment of important design parameters, helping the decision making process in an early design phase. The feasibility of these analyses rely on the compact state-space representation of the FE model and the fast algorithms used to calculate SQ metrics.

The way to improve roughness is through order balancing. The desired order profiles (amplitude and phase vs. rpm) can be defined with

the aid of SQ equivalent models. Though, the control strategy must be capable of order balancing. Therefore, a next step in this study will investigate other control strategies, such as adaptive feedforward controllers and their inclusion in the real-time engine simulator framework, for an eventual fully numerical ASQC design platform.

Acknowledgements

The research of Leopoldo P. R. de Oliveira is supported in the framework of a bilateral agreement between KU Leuven and University of São Paulo. The research presented in this paper was performed as part of the Marie Curie RTN project: A Computer Aided Engineering Approach for Smart Structures Design (MC-RTN-2006-035559).

Bibliography

- [1] B. Pluymers, B. van Hal, D. Vandepitte, W. Desmet, Trefftz-Based Methods for Time-Harmonic Acoustics, *Arch Comput Methods Eng* (2007) 14: 343381, doi:10.1007/s11831-007-9010-x
- [2] Z. Junhong, H. Jun, CAE process to simulate and optimise engine noise and vibration, *Mechanical Systems and Signal Processing*, 20 (2006) 1400-1409.
- [3] S. Donders, R. Hadjit, M. Brughmans, L. Hermans, W. Desmet, A wave-based substructuring approach for fast vehicle body optimization, *International Journal on Vehicle Design* (2007) 43(1-4) 100-115.
- [4] T. Mori, A. Takaoka, M. Maunder, Achieving a vehicle level sound quality target by a cascade to system level noise and vibration targets, SAE Paper No. 850965.
- [5] D. Berckmans, K. Janssens, H. Van der Auweraer, P. Sas, W. Desmet, Model-based synthesis of aircraft noise to quantify human perception of sound quality and annoyance, *Journal of Sound and Vibration* 311 (2008) 1175-1195.
- [6] S. Hurlebaus, L. Gaul, Smart structure dynamics, *Mechanical Systems and Signal Processing*, 20 (2006) 255-281.

- [7] H. Van der Auweraer, K. Janssens, L. de Oliveira, M. da Silva, W. Desmet, Virtual prototyping for sound quality design of automobiles, *Sound and Vibration*, April (2007) 26-30.
- [8] K. Janssens, P. Van de Ponsele, M. Adams, The integration of sound quality equivalent models in a real-time virtual car sound environment. *Proceedings of DAGA Conference*, 18-20 March, 2003, Aachen, Germany, 6p.
- [9] J. Swevers, C. Lauwerys, B. Vandersmissen, M. Maes, K. Reybrouck, P.Sas, A model-free control structure for the on-line tuning of the semi-active suspension of a passenger car, *Mechanical Systems and Signal Processing*, 21 (2007) 1422-1436
- [10] A. Preumont, *Vibration Control of Active Structures: An Introduction*, 2nd edition, Kluwer Academic Publishers, 2002.
- [11] K. Henriouille, P. Sas, Experimental validation of a collocated PVDF volume velocity sensor/actuator pair, *Journal of Sound and Vibration* 265 (2003) 489-506.
- [12] F. Kerber, S. Hurlebaus, B.M. Beadle, U. Stöbener, Control concepts for an active vibration isolation system, *Mechanical Systems and Signal Processing*, 21 (2007) 3042-3059.
- [13] T. Bein, J. Bö, S. Herold, D. Mayer, T. Melz, M. Thomaier, Smart Interfaces and Semi-Active Vibration Absorber for Noise Reduction in Vehicle Structures, *Aerospace Science and Technology*, 2007, doi:10.1016/j.ast.2007.10.008
- [14] P. Sas, C. Bao, F. Augustynowicz, W. Desmet, Active control of sound transmission through a double panel partition, *Journal of Sound and Vibration*, (1995) 180(4) 609-625.
- [15] W. Desmet, B. Pluymers, P. Sas, Vibro-acoustic analysis procedures for the evaluation of the sound insulation characteristics of agricultural machinery cabins, *Journal of Sound and Vibration*, 266 (2003) 407-441.
- [16] W. Desmet, D. Vandepitte, Finite element method in acoustics, *Seminar on Advanced Techniques in Applied and Numerical Acoustics - ISAAC17*, Leuven - Belgium, September 2006, pp. 1-48.

-
- [17] Sysnoise rev. 5.5 User's Manual, LMS International, Leuven, Belgium, 2000.
- [18] J. Luo, H.C. Gea, Modal Sensitivity analysis of coupled acoustic-structural systems, *Journal of Vibration and Acoustics* 119 (1997) 545-550.
- [19] L.P.R. de Oliveira, M.M. da Silva, H. Van Brussel, P. Sas, W. Desmet, Concurrent mechatronic design approach for active control of cavity noise, *Journal of Sound and Vibration* (2008), doi:10.1016/j.jsv.2008.01.009
- [20] P.A. Nelson, S.J. Elliott, *Active control of sound* Academic Press Limited, London - UK, 1993.
- [21] R. Williamns, M. Allman-Ward, P. Jennings, M. Batel, Using an interactive NVH simulator to compute and understand customer opinions about vehicle sound quality, *Symposium on International Automotive Technology*, 2007, Pune, India, SAE Paper No. 2007-26-036.
- [22] H. Fastl, Recent developments in sound quality evaluation, *Keynote Lecture from the Forum Acusticum 2005*, Budapest, Hungary, 1647-1653.2
- [23] E. Zwicker, H. Fastl, *Psychoacoustics: Facts and Models*, Springer Series in Information Sciences, Heidelberg, 1999, Ed.2.
- [24] B. Brassow, M. Clapper, Powertrain sound quality development of the Ford GT, SAE Paper No. 2005-02-2480.
- [25] A. Gonzalez, M. Ferrer, M. de Diego, G. Piñero, J.J. Garcia-Bonito, Sound quality of low-frequency and car engine noises after active noise control, *Journal of Sound and Vibration*, 265 (2003) 663-679.
- [26] International Organization for Standardization, Method for Calculating Loudness Level, ISO-532B, 1975.
- [27] H. Van der Auweraer, K. Wyckaert, Sound Quality: Perception, Analysis and Engineering, *International Seminar on Advanced and Numerical Acoustics - ISAAC 16*, 2006, Leuven, Belgium, 28pp.

- [28] P. Daniel, R. Weber, Psychoacoustical Roughness: Implementation of an Optimized Model, *ACUSTICA - acta acustica*, 83 (1997) 113-123.
- [29] K. Janssens, S. Ahrens, A. Bertand, J. Lanslots, P. Van de Ponselee, A. Vecchio, H. Van der Auweraer, An On-line Order-based Roughness Algorithm, *SAE Noise and Vibration Conference*, 2007, USA, SAE Paper No. 07NVC-173.
- [30] K. Tsuge, K. Kanamaru, T. Kido, N. Masuda, A Study of Noise in Vehicle Passenger Compartment during Acceleration, *SAE Noise and Vibration Conference*, 1985, USA, SAE Paper No. 850965.
- [31] G. Mangiante, Limitations on the performance of active noise control systems due to subjective effects. *J. Acoust. Soc. Am.*, 115(5) (2004) 2498
- [32] G. Canvet, G. Mangiante, Psychoacoustic assessment of active noise control, *Proceedings of ACTIVE 04*, Septembre 20-22, 2004, Williamsburg, USA, pp.1-10
- [33] S.M. Kuo, A. Gupta, S. Mallu, Development of adaptive algorithm for active sound quality control, *Journal of Sound and Vibration*, 299 (2007) 12-21..

Chapter 5

Active control of engine noise transmitted into cavities: simulation, experimental validation and sound quality assessment

Leopoldo P.R. de Oliveira
Paul Sas
Wim Desmet
Karl Janssens
Peter Gajdatsy
Herman Van Der Auweraer

Paper presented at the Acoustics'08 Conference in July 2008 - Paris, France:

L.P.R. de Oliveira, P. Sas, W. Desmet, K. Janssens, P. Gajdatsy, H. Van der Auweraer, Active control of engine noise transmitted into cavities: simulation, experimental validation and sound quality assessment, *Proceedings of Acoustics08*, Paris - FRANCE (2008), 10pp.

L.P.R. de Oliveira, P. Sas, W. Desmet, K. Janssens, P. Gajdatsy, H. Van der Auweraer, Active control of engine noise transmitted into cavities: simulation, experimental validation and sound quality assessment, *J. Acoust. Soc. Am.* (2008) 123(5) 3872.

Tables 2 and 4 have been formatted according to Table 3. For sake of completeness and to allow the comparison with the feedforward control strategy, the results related to the feedback controller, previously published in *Active sound quality control of engine induced cavity noise* (Chapter 4), are repeated here.

Abstract

Active control has been proposed as a possible solution to cope with low frequency noise reduction in vehicles. Active noise control systems tend to be designed with a target on the sound pressure level reduction. However, the perceived control efficiency for the occupants can be more accurately assessed if psychoacoustic metrics are taken into account. The aim of this paper is to evaluate, numerically and experimentally, the effect of (i) a collocated velocity feedback controller and (ii) an adaptive feedforward controller on the engine sound quality in a vehicle mockup. The simulation scheme is described and experimentally validated. The engine excitation is provided by a sound quality equivalent engine simulator, running on a real-time platform that delivers harmonic excitation in function of the driving condition. The controller performance is evaluated in terms of sound quality metrics such as Roughness, Zwicker- and Specific-Loudness. As a result of the control action, Loudness is significantly reduced while Roughness can either be increased or decreased, depending on the role of the controlled order in the modulation mechanism. Eventually, engine sound quality is improved overall.

1. Introduction

The successful development of new products relies on the capability of assessing the performance of conceptual design alternatives in an early design phase. In recent years, major progress was made hereto, based on the extensive use of virtual prototyping, particularly in the automotive industry. The novelty in this framework is to account for the human perception when defining product performance criteria [1,2].

Additionally, active control has shown the potential to enhance system dynamic performance which allows lighter and improved products. Research done in the last years on smart materials and control concepts has led to practical applications with promising results for the automotive industry [3]. However, to make the step to the design of active sound quality control (ASQC), the control schemes, along with appropriate simulation procedures, need to become an integral part of the product development process [4,5]. In other words, this requires: (i) the product performance metrics to be based on human perception attributes and (ii) the simulation models to support the specific aspects related to smart structures (active systems, actuators, sensors and control logic).

In order to demonstrate the proposed simulation procedure and evaluate the effect of active control on the perceived sound quality (SQ), a vibro-acoustic cabin mock-up is selected (Fig.1). It consists of a simplified car cavity with rigid acoustic boundary conditions. The passenger compartment (PC) and the engine compartment (EC) are connected through a flexible firewall which allows noise generated in the EC to be transmitted to the PC. A sound source placed in the EC works as a primary disturbance source. The primary source is driven by a real-time engine simulator, capable of delivering a harmonic excitation based on the engine orders' amplitude and phase [6]. Two control strategies have been evaluated: (i) an ASAC scheme involving a collocated velocity feedback controller with a structural sensor/actuator pair (SAP) and (ii) an adaptive feedforward controller with a structural secondary actuator and an acoustic error sensor.

The control strategies are presented in Section 2. In Section 3, the simulation procedure is described. The experimental validation and the results obtained with both controllers, in terms of Roughness [7],

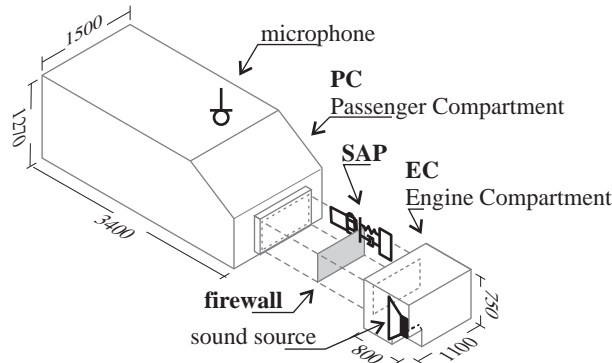


FIGURE 1: Vehicle mock-up

Specific-Loudness and Zwicker-Loudness [8,9] are treated in Section 4. Finally, some general conclusions are addressed in Section 5.

2. Control Strategies

As mentioned before, two distinct control strategies are considered in this paper, a collocated velocity feedback and an adaptive feedforward control.

The collocated velocity feedback consists of a linear time invariant controller based on structural sensors and actuators, tuned according to the acoustic pressure measured on the PC. This controller acts like an active damper by introducing a force proportional to the measured velocity signal (Fig.2). This method is suitable for broadband disturbance and is, theoretically, inherently stable. The use of a digital integrator requires a high-pass filter to avoid drift.

The adaptive feedforward strategy is based on a modified version of the Fx-LMS [10]. This scheme was proposed to increase the convergence speed of the standard Fx-LMS, which is achieved by compensating for the secondary path dynamics. As it can be seen in Fig. 3, the error signal used for the LMS update is the signal coming from the error microphone diminished by the estimate of the secondary path contribution ($F_s \times \hat{\mathbf{S}}$). In this way, the Fx-LMS behaves closer to a purely LMS algorithm.

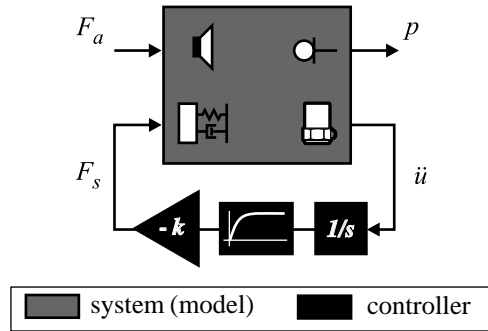


FIGURE 2: Feedback control

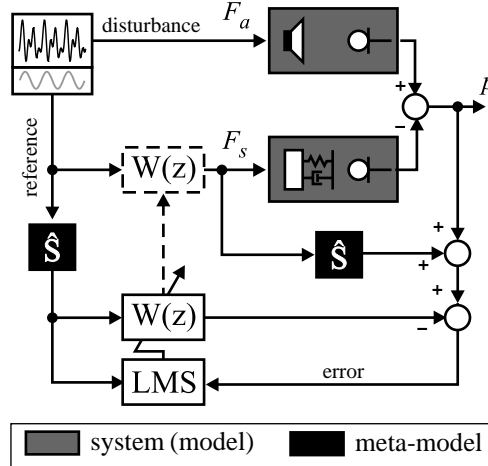


FIGURE 3: Adaptive feedforward control

3. ASAC simulation scheme

The modelling procedure presented here is a general framework in which different control strategies can be implemented, revealing the functionality of such an approach to the assessment of conceptual design performance [1,5,11].

One of the key aspects in this modelling approach resides in deriving reasonably sized models that integrate the structural and acoustic components along with the control algorithm. In order to fulfil this requirement, a fully coupled finite element (FE) model of the vibro-acoustic system is written as a modal state-space (SS) model (Eq.1). As a result of using the coupled vibro-acoustic modal base, any combination of structural and acoustic inputs/outputs can be used for the control design, e.g., an acoustic source in the EC, structural sensors and actuators on the firewall and microphones on the PC.

$$\begin{Bmatrix} \dot{\mathbf{q}} \\ \ddot{\mathbf{q}} \end{Bmatrix} = \begin{bmatrix} \mathbf{0} & \mathbf{I} \\ -\mathbf{\Omega}^2 & -\mathbf{\Gamma} \end{bmatrix} \begin{Bmatrix} \mathbf{q} \\ \dot{\mathbf{q}} \end{Bmatrix} + \begin{bmatrix} \mathbf{0} \\ \mathbf{\Phi}_L^T \mathbf{B} \end{bmatrix} \begin{Bmatrix} \mathbf{F}_{si} \\ \mathbf{F}_{ai} \end{Bmatrix} \quad (1)$$

$$\begin{Bmatrix} \mathbf{u}_o \\ \mathbf{p}_o \end{Bmatrix} = \begin{bmatrix} \mathbf{C} \mathbf{\Phi}_R & \mathbf{0} \end{bmatrix} \begin{Bmatrix} \mathbf{q} \\ \dot{\mathbf{q}} \end{Bmatrix} \quad (2)$$

where \mathbf{q} is the vector of modal amplitudes of the Eulerian vibro-acoustic model in displacement \mathbf{u} and pressure \mathbf{p} ; \mathbf{B} and \mathbf{C} are Boolean matrices that select input and output DoFs, respectively; \mathbf{F} is the load vector, $\mathbf{\Phi}_L$ and $\mathbf{\Phi}_R$ are the left and right-eigenvector which hold the following properties:

$$\mathbf{\Phi}_L^T \begin{bmatrix} \mathbf{M}_s & \mathbf{0} \\ -\rho_0 \mathbf{K}_c^T & \mathbf{K}_a \end{bmatrix} \mathbf{\Phi}_R = \mathbf{I} \quad (3)$$

$$\mathbf{\Phi}_L^T \begin{bmatrix} \mathbf{K}_s & \mathbf{K}_c \\ \mathbf{0} & \mathbf{K}_a \end{bmatrix} \mathbf{\Phi}_R = \mathbf{\Omega}^2 \quad (4)$$

$$\mathbf{\Phi}_L^T \begin{bmatrix} \mathbf{D}_s & \mathbf{0} \\ \mathbf{0} & \mathbf{D}_a \end{bmatrix} \mathbf{\Phi}_R = \mathbf{\Gamma} \quad (5)$$

where ρ_0 is the air density, the index a refers to acoustic and s to structural DoFs, \mathbf{K} , \mathbf{D} and \mathbf{M} are the stiffness, damping and mass matrices, respectively, and \mathbf{K}_c is the vibro-acoustic coupling matrix; \mathbf{I} is the identity matrix, $\mathbf{\Omega}$ is the matrix of natural frequencies and $\mathbf{\Gamma}$ is the modal damping matrix. For a more detailed description of the state-space model, the reader is referred to [11].

The original FE model, consisting of the firewall and the cavities, contains 24192 DoFs (23196 unconstrained acoustic and 1026 unconstrained structural). Applying the aforementioned modal reduction, it has been reduced to a SS model with $2 \times N$ DoFs, related to the N kept modes, with force and volume velocity as inputs and displacement and pressure as outputs. The modal base was built with modes ranging from 0 to 400Hz, resulting in $N = 107$.

The numerical validity of the reduced model is illustrated by comparing FRFs from the original FE model with the reduced SS model (Fig. 4). The system inputs are volume velocity applied in the EC (acoustic input) and force applied on the firewall (structural input); and the outputs are pressure measured in the PC (acoustic output) and displacement measured on the firewall (structural output). The

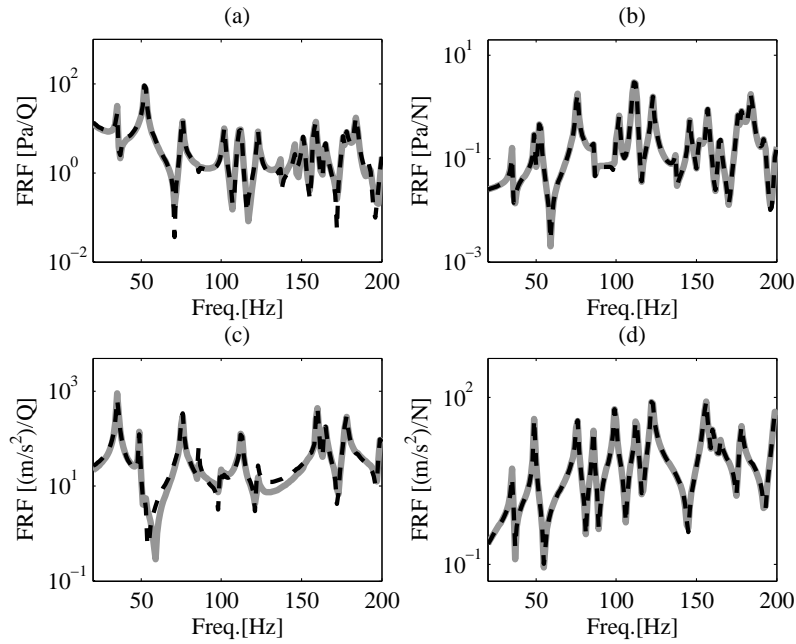


FIGURE 4: Comparison between (---) FE and (—) SS FRFs: (a) Acoustic/Acoustic, (b) Acoustic/Structural, (c) Structural/Acoustic and (d) Structural/Structural

good correlation between the SS and the FE model validates the model reduction procedure.

For the adaptive feedforward simulations, a meta-model is needed to represent S as a FIR filter. As depicted in Fig. 5, this meta-model can be obtained with an LMS-based off-line secondary path estimation [12]. After convergence, $W(z)$ should resemble the secondary path transfer function.

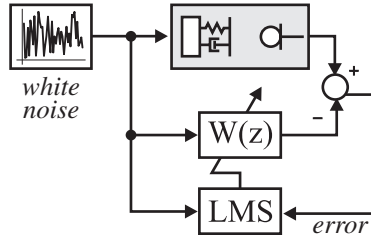


FIGURE 5: Off-line secondary path estimation

4. Experimental Validation

In Figure 6, the FRFs derived from the reduced SS model are compared with the FRFs measured on the cabin mock-up. These FRFs include the transfer paths to the driver's microphone from both inputs: primary acoustic source and secondary structural actuator. The vibro-acoustic system has been excited with white noise. The FRFs are measured with an Hv estimator, while input and output signals are filtered with Hanning windows.

For the adaptive controller, the reference for the FRFs should be the voltage signal sent to either the shaker (V_S) or the acoustic source (V_P). Fig.7 shows a comparison of such FRFs and the Fourier transform of the FIR filters identified as in Fig.5.

In both cases (Figs. 6 and 7) comparisons present a good agreement. Few discrepancies arise, a.o., from the lack of accuracy in determining the exact place of the disturbance source, sensor/actuator pair and microphones and from assuming the disturbance source as an ideal point source. Such mismatches are expected and believed not to harm the accuracy of the results, as previous analyses have shown [1,5,11].

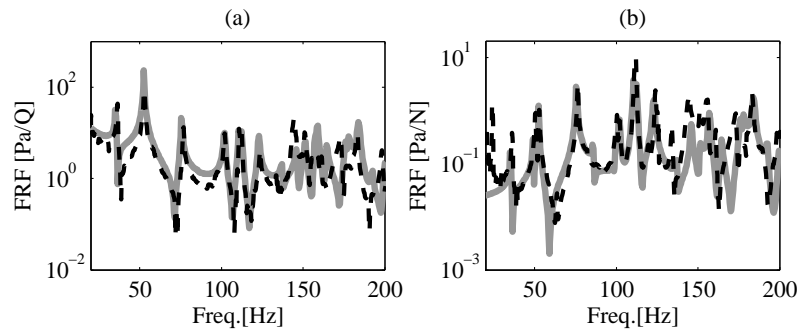


FIGURE 6: Comparison of (- - -) experimental and (—) numerical FRFs: (a) acoustic input and (b) structural input

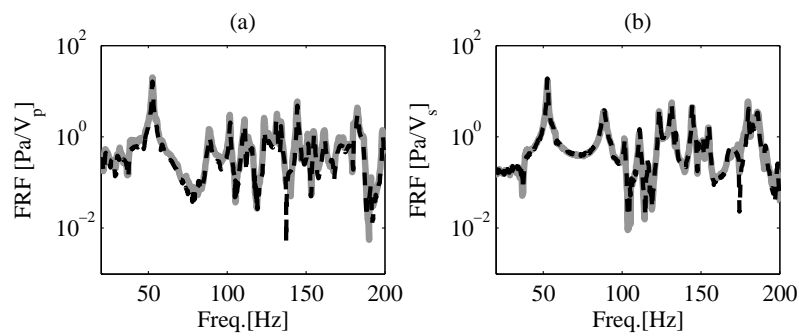


FIGURE 7: Comparison of (- - -) FRFs and (—) FFT of identified FIR filters: (a) primary and (b) secondary paths

Moreover, in order to have an engine-like excitation, which allows meaningful SQ measurements, a real-time engine simulator was used [6]. SQ-equivalent engine models are used in product development, as it enables one to experience and assess the NVH of a virtual (or real) vehicle under various driving conditions [6,13]. The novelty here is the use of such device as a source of excitation. In this case, the engine sound, which is a function of the driving condition (engine speed, gear, throttle and brake positions, etc.) is fed to the acoustic source in the EC. Results obtained as such, benefit from this SQ-equivalence and,

therefore, allow the correlation with real engine sounds.

Henceforth, two driving conditions are analyzed, namely 50km/h (1634rpm) and 80km/h (2694rpm). The excitation consists of 20 complex orders (0.5, 1.0, 1.5, ..., 10), from which the amplitudes are depicted in Fig.8.

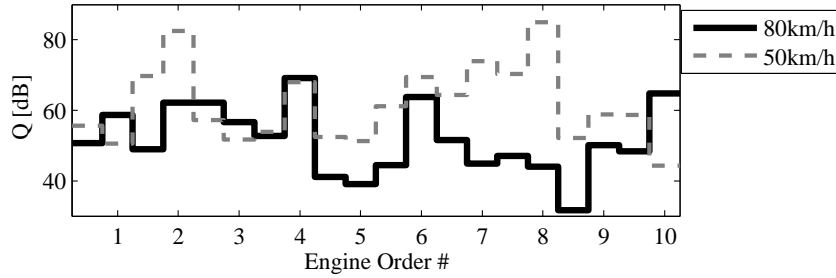


FIGURE 8: Order amplitudes for two driving conditions

The measured excitation can be used as disturbance input in the simulations to obtain the passive and active responses that can be compared to the measured ones. Due to the SQ-equivalence of the excitation, SQ metrics can be calculated from the resulting pressure signals, from which rather general conclusions can be drawn.

4.1 Feedback control

For the feedback controller setup, the feedback gain k (Fig. 2) is optimized to minimize the sound pressure level measured at the driver's head position [11]. The order amplitudes for the passive and active system can be seen in Fig. 9. As it can be seen, some orders are damped and some slightly amplified. Overall, the sound pressure level (SPL) is reduced by 7dB.

Figure 10 shows comparisons of the passive and active Specific Loudness perceived by the driver for 50km/h and 80km/h driving conditions. The corresponding Zwicker Loudness is presented in Table 1. In this way it is possible to affirm that the reduction in SPL can be clearly perceived by the occupants.

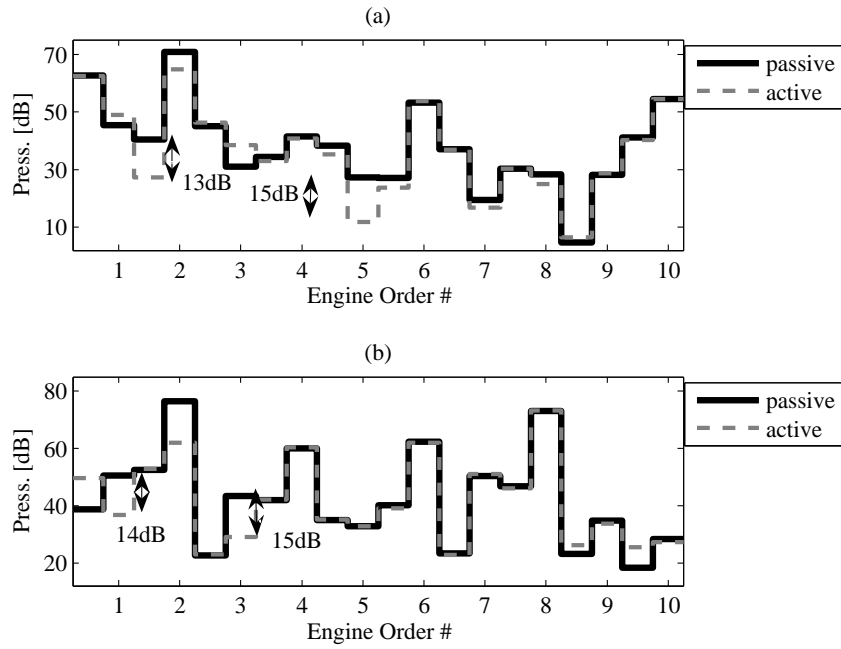


FIGURE 9: Order amplitudes for feedback control and two driving conditions, (a) 50km/h and (b) 80 km/h

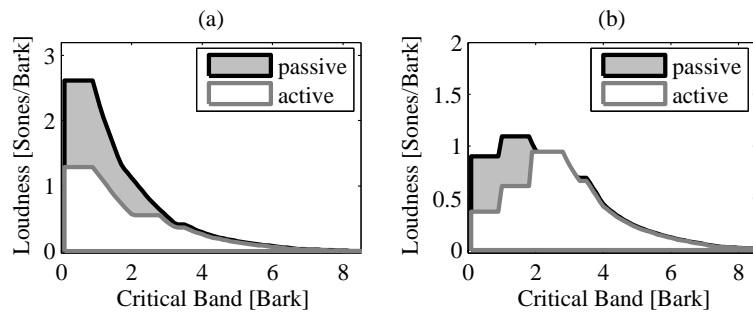


FIGURE 10: Specific Loudness (a) @ 50km/h and (b) @ 80km/h

TABLE 1: Zwicker Loudness [Sones]

	experimental		simulated	
	50km/h	80km/h	50km/h	80km/h
passive	5.9	4.2	6.1	4.1
active	3.4	2.3	3.3	1.8

As a result of the feedback control, Roughness can be slightly increased. This is due to the attenuation of some order amplitudes, which can unmask orders in their vicinities, allowing modulation and, therefore, increasing roughness. Previous simulation results [1] show that this feedback controller increases Roughness in some regions, though not affecting the maximum Roughness value.

Table 2 presents the values obtained for both driving conditions. In general, Roughness at the driver's head position is increased, but still remains quite bellow the maximum value encountered in the cavity. In fact the values are rather low, which indicates that Roughness should not be of much concern to the interior SQ at those driving conditions.

TABLE 2: Roughness at driver's head position [Asper]

	50km/h	80km/h
passive	4.8×10^{-3}	2.5×10^{-2}
active	2.5×10^{-2}	3.6×10^{-2}

4.2 Adaptive feedforward control

To implement the adaptive feedforward control, the FIR filter \hat{S} is estimated as depicted in Fig. 5. The frequency sample for the real-time DSP is 2kHz. The frequency of 10th order at 80km/h is 450Hz, well below the DSP Nyquist frequency.

The reference signal consists of a sine wave with the same frequency of the targeted order, which yields an adaptive notch-filter [12]. This is an interesting feature for the intended future application of such con-

trollers, *i.e.*, order balancing. In order to independently tune different orders' amplitudes, similar controllers could be connected in parallel since each narrowband action would not interfere with each other. Also, due to the narrow band of the control action, it is affordable to use a short filter $W(z)$, in this case a order-10 FIR filter.

Figure 11 shows the 2^{nd} order cuts for the passive, standard Fx-LMS and modified Fx-LMS. These simulation results show that the modified Fx-LMS considerably increases the convergence speed. After 500 iterations (.25s @ 2kHz frequency sample) the modified Fx-LMS has reduced 15dB while the standard algorithm only 5dB.

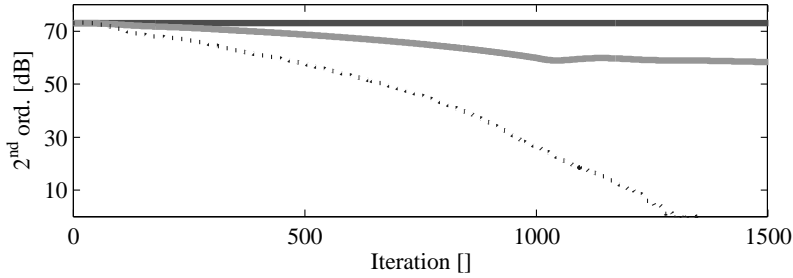


FIGURE 11: Second order cuts for (solid black) passive, (solid gray) standard Fx-LMS and (dotted black) modified Fx-LMS.

Figure 12 shows the experimental order amplitudes measured by the driver's microphone with controller on and off for both driving conditions. The 2^{nd} order is targeted in both cases and the reduction obtained specifically for this order is 34dB for 50km/h and 51dB for 80km/h.

When it comes to the SQ analysis, some discrepancies between the results for feedback and feedforward should be stressed. The feedback measurements have a slightly lower frequency range. Although comparisons for 50km/h can be done, results related to 80km/h should be analyzed separately for each control strategy.

The Specific Loudness plots for 50km/h and 80km/h are shown in Fig. 13. As it can be seen, even if the controller is targeting just a single order, the effect on the perceived loudness is quite noticeable. The Zwicker Loudness for passive and active systems (Table 3) reveals a reduction of 45% in the perceived volume.

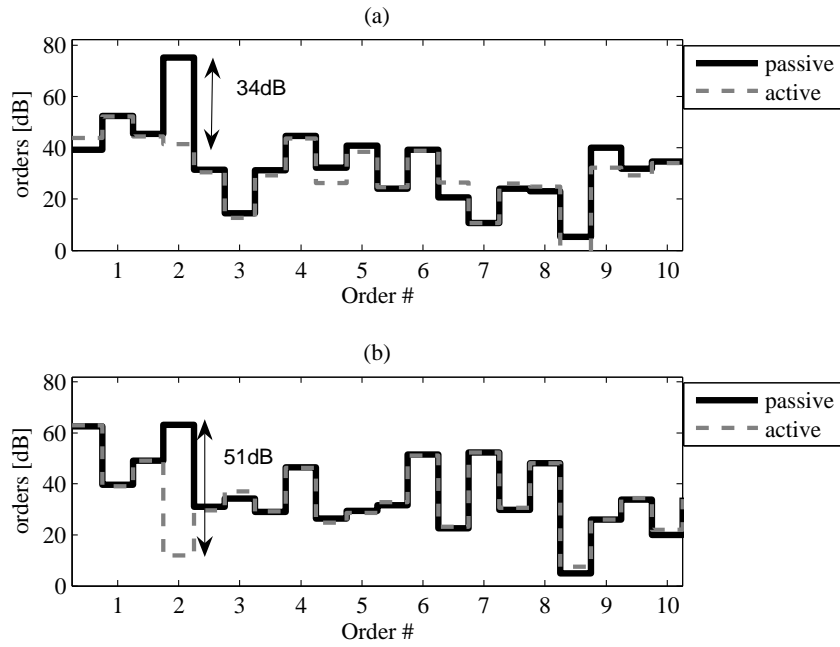


FIGURE 12: Order amplitudes for feedforward control and two driving conditions, (a) 50km/h and (b) 80 km/h

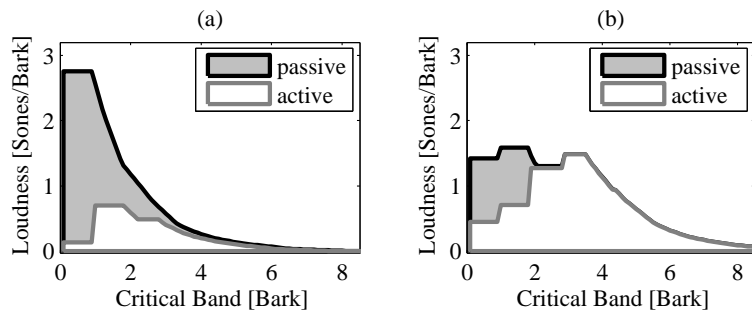


FIGURE 13: Specific Loudness (a) @ 50km/h and (b) @ 80km/h

TABLE 3: Zwicker Loudness [Sones]

	50km/h	80km/h
passive	6.1	7.5
active	1.9	5.8

When reducing the amplitude of an order, Roughness can be affected in two ways: (i) if that is a dominant order, by reducing it, modulating orders can be unmasked and Roughness increases, or (ii) if that is one of the modulating orders, Roughness is decreased. At 50km/h, there is booming of the second order, such that the controller gives rise to Roughness (Table 4). On the other hand, at 80km/h, the second order contributes to the modulation, hence Roughness is reduced.

TABLE 4: Roughness at driver's head position [Asper]

	50km/h	80km/h
passive	3.4×10^{-3}	2.3×10^{-2}
active	3.3×10^{-2}	1.7×10^{-2}

5. Conclusions and Future Work

This paper describes a modeling procedure for ASAC, which allows the use of standard vibro-acoustic FE models in the control design. The modeling procedure is experimentally validated with a vehicle mock-up.

The proposed experimental setup is acoustically excited by a SQ-equivalent engine simulator, typically employed in auralization. The use of such scheme allows repeatable measurements with engine-like excitation signals, furnishing results that can be directly correlated to automotive applications.

The results for Loudness attenuation are presented in terms of Specific and Zwicker Loudness, the latter being linearly related to the human sensation of volume. The results indicate that the controllers are

quite effective with respect to the occupants perception of the sound field. While the feedback control provides an efficient broadband reduction that could be targeted to road or wind-noise, independent order control (with varying rpm) can only be achieved by an adaptive scheme. The presented adaptive feedforward control converges fast which indicates it could cope with varying rpm within the transient regime, though such conditions have not yet been evaluated.

While Loudness is always improved, the only way to improve Roughness is through order balancing. The only control strategy presented here which is capable of coping with this is the adaptive feedforward. In that way, the desired order profiles (amplitude and phase vs. rpm) can be defined with the aid of SQ-equivalent models and further used to define target values for the feedforward controller.

A next step in this study will investigate more efficient convergence algorithms in order to cope with fast varying engine speeds. Also, the inclusion of such adaptive feedforward controllers in the real-time engine simulator is under study, towards a fully numerical ASQC design platform.

Acknowledgements

The research of Leopoldo P. R. de Oliveira is supported in the framework of a bilateral agreement between KU Leuven and University of São Paulo. The research presented in this paper was performed as part of the Marie Curie RTN project: A Computer Aided Engineering Approach for Smart Structures Design (MC-RTN-2006-035559).

References

- [1] L.P.R. de Oliveira, *et al.*, Active sound quality control of engine induced cavity noise, *Mechanical Systems and Signal Processing* (2008), doi:10.1016/j.ymsp. 2008.04.005
- [2] D. Berckmans, *et al.*, Model based synthesis of aircraft noise to quantify human perception of sound quality and annoyance, *Journal of Sound and Vibration* 311 (2008) 1175-1195.
- [3] S. Hurlebaus, L. Gaul, Smart structure dynamics, *Mechanical Systems and Signal Processing* 20 (2006) 255-281.

- [4] S.M. Kuo, A. Gupta, S. Mallu, Development of adaptive algorithm for active sound quality control, *Journal of Sound and Vibration* 299 (2007) 12-21.
- [5] H. Van der Auweraer, *et al.*, Virtual prototyping for sound quality design of automobiles, *Sound and Vibration* April (2007) 26-30.
- [6] K. Janssens, P. Van de Ponsele, M. Adams, The integration of sound quality equivalent models in a real-time virtual car sound environment. *Proceedings of DAGA Conference, 18-20 March, 2003, Aachen, Germany*, 6p.
- [7] K. Janssens, *et al.*, An On-line Order-based Roughness Algorithm, *SAE Noise and Vibration Conference, 2007, USA*, SAE Paper No.07NVC-173.
- [8] E. Zwicker, H. Fastl, *Psychoacoustics: Facts and Models*, Springer Series in Information Sciences, Heidelberg, 1999, Ed.2.
- [9] *International Organization for Standardization*, Method for Calculating Loudness Level, ISO-532B, 1975.
- [10] C. Bao, Adaptive algorithms for active noise control and their applications, *PhD Thesis*, Katholieke Universiteit Leuven, Mechanical Engineering Department - PMA, 1994.
- [11] L.P.R. de Oliveira, *et al.*, Concurrent mechatronic design approach for active control of cavity noise, *Journal of Sound and Vibration* (2008), doi:10.1016/j.jsv.2008.01.009
- [12] S.M Kuo, D.R. Morgan, *Active Noise Control Systems: Algorithms and DSP implementation*, John Wiley and Sons, Inc. - New York (1996).
- [13] R. Williams, *et al.*, Using an interactive NVH simulator to compute and understand customer opinions about vehicle sound quality, *Symposium on International Automotive Technology*, 2007, Pune, INDIA, SAE Paper No.2007-26-036.

Chapter 6

NEX-LMS: a novel adaptive control scheme for sound quality control

Leopoldo P.R. de Oliveira
Bert Stallaert
Karl Janssens
Herman Van der Auweraer
Paul Sas
Wim Desmet

Paper submitted to Mechanical Systems and Signal Processing on December the 2nd 2008:

Leopoldo P.R. de Oliveira, Bert Stallaert, Karl Janssens, Herman Van der Auweraer, Paul Sas, Wim Desmet, NEX-LMS: a novel adaptive control scheme for sound quality control, *Mechanical Systems and Signal Processing - under review*.

Abstract

This paper presents a novel adaptive control scheme, with improved convergence rate, for the equalization of harmonic disturbances such as engine noise. First, modifications for convergence improvement of the standard filtered-X LMS control scheme are described. Equalization capabilities are then implemented, allowing the independent tuning of different harmonics, which enables sound quality design. The control scheme principle is first demonstrated with a simple secondary path model, and then, experimentally validated with the aid of a vehicle mockup which is excited with engine noise. The engine excitation is provided by a real-time sound quality equivalent engine simulator. Stationary and transient engine excitation are used for control performance assessment. The results reveal that the proposed controller is capable of large order-level reductions for stationary excitation, which allows a comfortable margin for equalization. The same holds for slow run-ups, thanks to the improved convergence rate. This margin, however, gets narrower with shorter transients.

1. Introduction

Interior noise in a vehicle is an important element in the customer perception of the overall vehicle's quality [1-9]. The interior noise is made up of contributions from many sources: some only contribute to the overall loudness and annoyance (*e.g.*, uncorrelated road or wind noise), while others reveal important information on the operation of the vehicle and can invoke a desired emotional response [10], as it is the case with engine noise, targeted in this paper.

The engine-related interior sound quality design is of major importance for vehicle sound branding, as it underlines its image (*e.g.*, sportiveness, refinement, luxury, etc.) [4,11]. In this context, sound branding brings an extra motivation for the use of active control, as it would enable easy and inexpensive adaptations to local markets, of products based on global platforms, meeting distinct customer expectations with the same hardware [4]. Moreover, such control systems can be implemented without compromising other engine/vehicle design attributes, *e.g.* emissions, fuel consumption, exterior noise, etc. [11]. These two aspects, easy local-marked adaptation and decoupled design parameters, would simplify the NVH development process and make it a potential field of application for active control.

Demonstrations of the viability of active control in cavity noise applications, including automotive interior noise reduction, have been described by several authors in the past few years [12-18]. Usually, in these applications, the objective is to reduce the noise generated by the primary source(s) as much as possible. The novelty in this framework is to account for the human perception when defining performance criteria, either to evaluate or to drive the design of active solutions [11,19-23]. In this context, sound quality specialists could prescribe the ideal (or the brand signature) engine sound in terms of its order-level vs. RPM profiles, which would be achieved by means of active sound quality control (ASQC).

This paper focuses on the use of ASQC to match prescribed engine order-level vs. RPM profiles. The control strategy is based on the feedforward filtered x-LMS algorithm (Fx-LMS) [24-27], to which modifications are proposed in order to improve the convergence rate and allow order-level equalization. This control strategy is described

in Section 2. The test setup and the real-time implementation of the controller are described in Section 3. Section 4 presents the experimental results. Finally, some general conclusions are addressed in Section 5.

2. Novel adaptive algorithm for sound quality control: NEX-LMS

The aim of the proposed control scheme is to achieve a pre-defined order-level vs. RPM profile, thus achieving a desired sound quality target in an authentic ASQC manner. Besides converging to some pre-defined amplitudes, the controller must cope with varying engine speeds. Therefore, the controller has to be capable of tracking changes on the disturbance, converging as fast as possible to the desired output value. To this end, an adaptive feedforward strategy is proposed, which is a modified version of the standard FX-LMS algorithm. The first modifications aim at improving the convergence rate of the adaptive scheme, in order to cope with changing RPMs during normal engine operation. Afterwards, equalization capabilities are implemented to allow the tuning of order-levels according to the RPM. In this section, each component of the proposed ASQC scheme is described, starting from the standard adaptation algorithm and the implemented improvements. Finally, the equalization feature is addressed.

The core of the control scheme is an adaptive digital filter. One of its simplest representations is depicted in Fig. 1(a). It consists of two distinct elements: an adaptive algorithm and a digital filter (W). The former adjusts the coefficients of the latter, usually a finite impulse response filter (FIR) as in Eq.(1), to perform the desired signal processing [26].

$$\mathbf{w}(n) \equiv [w_0(n) \ w_1(n) \ \cdots \ w_{(L-1)}(n)]^T \quad (1)$$

where $\mathbf{w}(n)$ is the vectorial representation at the instant n of the filter W with L coefficients w .

The most commonly used performance criteria for digital filter adaptation are those based on mean square error (MSE). The minimization of the MSE, $\xi(n) \equiv E[e^2(n)]$, is usually achieved by a steepest-descent method. Eventually, this results in the well-known least mean square (LMS) algorithm (Fig. 1a) for updating the coefficients of W :

$$\mathbf{w}(n+1) = \mathbf{w}(n) + \mu \mathbf{x}(n)e(n) \quad (2)$$

where μ is the convergence coefficient, $\mathbf{x}(n)$ is the reference signal and $e(n)$ the instantaneous error, *i.e.*, the difference between the disturbance signal $d(n)$ and the controller output signal $y(n)$. In active control of noise, $d(n)$ is usually the unwanted outcome of the process, *e.g.*, the noise coming from the engine (primary source) through the primary path.

Figure 1(b) shows the performance surface for the LMS adaptive system with filter W of length $L = 2$, as a function of the filter coefficients $[w_0; w_1]$. An adaptation path, from an arbitrary starting point to the global optimum, is also illustrated. For this example, the disturbance signal $d(n)$ consists of a sine-wave of frequency 800Hz and power $P_d = 10V_{RMS}$ while the reference signal $x(n)$ is a sine-wave of the same frequency as $d(n)$ and power $P_x = 1V_{RMS}$. By using a sine-wave as a reference signal, the controller acts like an adaptive notch filter, acting solely at the frequency of $x(n)$ [26]. The higher μ , the faster the algorithm reaches the optimum filter coefficients, but too high values of μ can destabilize the system. If μ falls into the interval $0 < \mu < 2/(LP_x)$ the system should converge, however, in practice [26] the following boundaries are typically used:

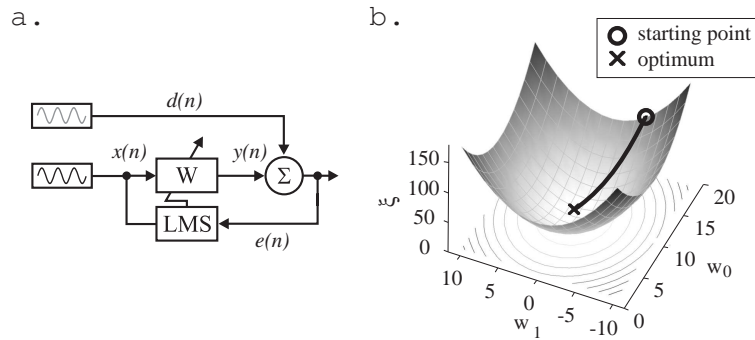


FIGURE 1: LMS adaptive system: (a) block diagram and (b) performance surface with $L = 2$

$$\frac{.01}{LP_x} < \mu < \frac{.1}{LP_x} \quad (3)$$

In real-life applications, the output of the filter W is fed to the secondary actuator (speaker or control shaker), therefore, it is influenced by the secondary path dynamics (S in Fig. 2a) before it becomes the physical quantity $y(n)$ that superposes with the primary disturbance. S consists of reconstruction filters, power amplifier, secondary actuator dynamics etc. The adaptive filter coefficients must converge to the appropriate values despite the presence of S , which in any case will affect the controller performance as it can be seen in Fig. 2(b). There, and for the following examples, a secondary path model with two poles, at 200Hz and 450Hz, is used. On this plot, each line shows the evolution of the error in time, for different disturbance frequencies, some of them are highlighted. The adaptive algorithm uses a fixed μ , such that the controller is stable for the whole frequency range; as follows, fast convergence is only reached near the secondary path resonances.

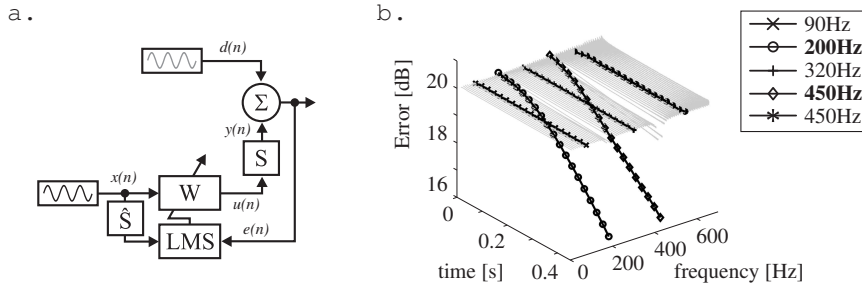


FIGURE 2: Filtered-x LMS adaptive system: (a) block diagram (b) evolution of error in time for different disturbance frequencies (some highlighted)

Improvement in convergence speed of the standard Fx-LMS (Fig. 3a) is achieved, initially, by modifying the structure of the standard controller as suggested in [28] and recently revisited in [29] (Fig. 3b). There, the gradient descent method behaves as the standard LMS algorithm (highlighted area in Fig. 3b), thus with convergence rate comparable with standard LMS schemes. Since the signal $d'(n)$ used in the modified version is an estimate of the primary disturbance signal $d(n)$, the effect of the secondary path dynamics is diminished. Moreover, this

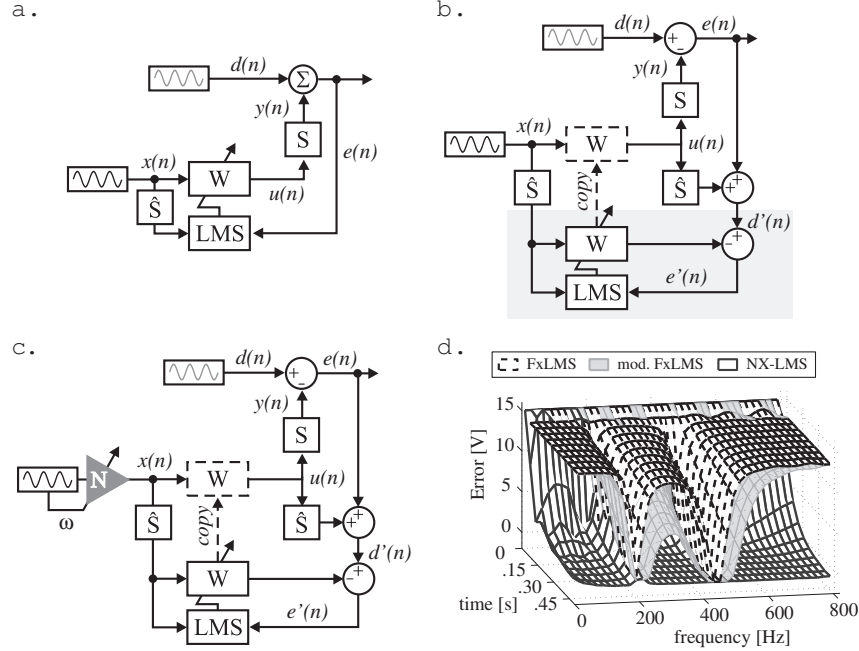


FIGURE 3: Adaptive controller schemes: (a) Fx-LMS, (b) modified Fx-LMS, (c) NX-LMS and (d) evolution of error in time for different disturbance frequencies

modified version retains the robustness of the conventional Fx-LMS for eventual errors on the secondary path modelling [28], *i.e.*, the phase angle of the model \hat{S} should be within $\pm 90^\circ$ from the secondary path S [24].

In addition to the aforementioned modifications to the Fx-LMS algorithm, the proposed adaptive scheme features a normalization filter in the form of the scheduled gain N (Fig. 3c). The role of N is to compensate for the secondary path dynamics such that the filtered signal $\hat{S}\mathbf{x}$ has the same power throughout the frequency band of interest (recall Eq.3); in this way, performance is optimized for a fixed μ . Taking \mathbf{x} as a constant amplitude sinusoid, it is intuitive that for each disturbance frequency ω , $N(\omega) = 1/|\hat{S}(\omega)|$; although for practical applications, this value is kept within a safety margin:

$$\frac{.01}{|\hat{S}(\omega)|} < N(\omega) < \frac{.1}{|\hat{S}(\omega)|} \quad (4)$$

Figure 3(d) compares the convergence for the three adaptive algorithms: Fx-LMS, modified Fx-LMS and the NX-LMS considering the same secondary path dynamics as before. As it can be seen, the three algorithms have similar performance close to 200Hz and 450Hz. The modified version improves the convergence for off-resonance frequencies and eventually, the normalized version (NX-LMS) outperforms the modified Fx-LMS, extending the fast convergence to the whole frequency band.

Finally, the last requirement for the proposed adaptive scheme is equalization, in other words, driving the resulting error to a desired value rather than to zero. It means that the adaptive system should be able to reduce the disturbance down to the minimum achievable at some frequencies, as well as amplify it if desired. This equalization feature is provided by the gain β (Fig. 4a) similarly to the one proposed in [30] and revisited in [21,31]. The difference here is that, thanks to the use of the estimated primary disturbance $d'(n)$, the equalization needs to be applied only once, after the filter W . As a result, the effective secondary excitation $y^*(n)$ is the scaled version of the one on the modified Fx-LMS, *i.e.*, $y^*(n) = \beta y(n)$. This proposed control scheme is referred to as NEX-LMS hereafter.

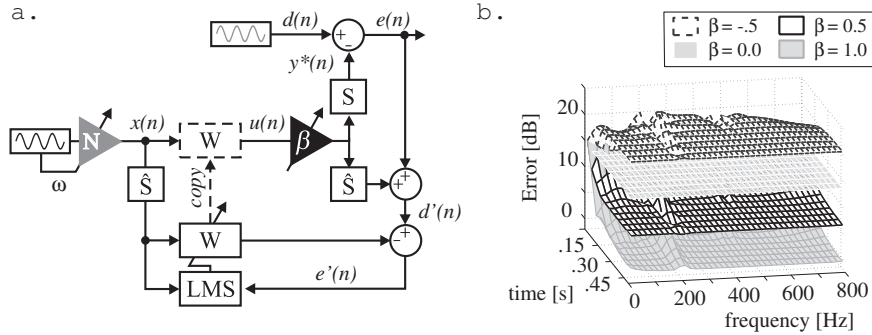


FIGURE 4: NEX-LMS: (a) block diagram and (b) evolution of error in time for different values of β

Due to the equalization, the resulting error signal $e(n)$ is given by Eq.(5), where after convergence, $y(n)$ should tend to $d(n)$ yielding Eq.(6). In this way, the residual error amplitude can be controlled by adjusting β . This system behaves symmetrically w.r.t. $\beta = 1$. Within the interval $0 < \beta < 1$, the system presents a residual error which is between the passive ($\beta = 0$) and maximum performance ($\beta = 1$). The same holds for $1 < \beta < 2$, although with opposite phase. Outside these ranges, *i.e.*, $\beta < 0$ or $\beta > 2$, the system amplifies the original disturbance. Fig. 4(b) shows how the NEX-LMS can change the residual error according to the value of β : when $\beta = 1.0$ the result is the same as the one in Fig. 3(d), for $\beta = 0.0$ the residual noise is the unchanged primary disturbance and for $\beta = 0.5$ and $\beta = -0.5$ the residual error is an equalization, either reduction or amplification of the primary noise.

$$e(n) = d(n) - y^*(n) = d(n) - \beta y(n) \quad (5)$$

$$e(n) \approx (1 - \beta)d(n) \quad (6)$$

Furthermore, $\beta(\omega)$ can be described as a scheduled gain, such that the residual error is shaped according to a pre-defined amplitude vs. ω profile, or in the case of engine noise, order-level vs. RPM.

Finally, the NEX-LMS features a fast converging adaptive algorithm based on the normalization of the reference signal and equalization capabilities, elements necessary for an adaptive engine sound quality controller.

3. Controller implementation

The proposed control scheme is demonstrated on a vehicle cabin mock-up, which has been used in previous works [14,20] (Fig. 5). It consists of a simplified car cavity with rigid acoustic boundary conditions. The passenger compartment (PC) and the engine compartment (EC) are connected through a flexible firewall which allows noise generated in the EC to be transmitted to the PC.

The primary disturbance is provided by a calibrated acoustic source (*LMS-QSource*) placed in the EC (Fig. 5b). It is driven by a real-time engine simulator (*LMS Virtual Car Sound - VCS*), which delivers harmonic excitation based on the engine orders' amplitude and phase.

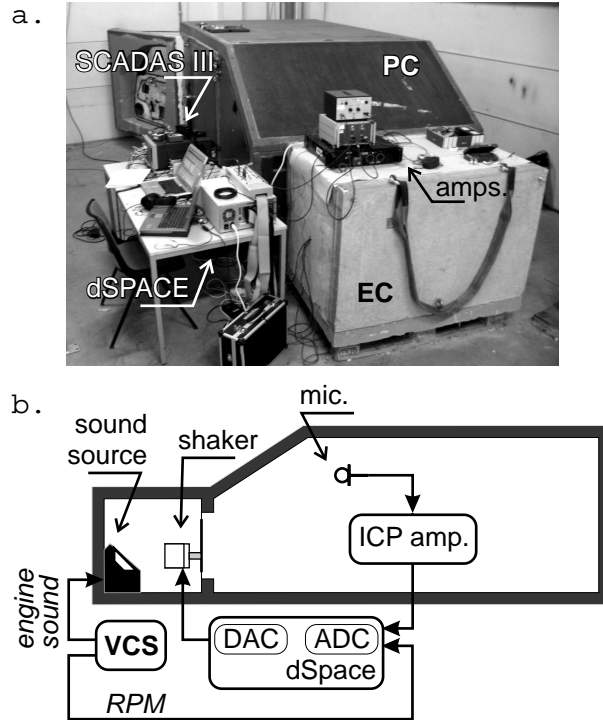


FIGURE 5: Experimental setup: (a) picture and (b) schematic view

Such sound quality equivalent engine models are used in product development, as it enables one to experience and assess the NVH of a virtual or hybrid (numerical + measured) vehicle under various driving conditions [32,33]. The novelty here is the use of such device as a source of excitation. In this case, the engine sound, which is a function of the driving condition (engine speed, gear, throttle and brake positions, etc.) is fed to the acoustic source in the EC. Results obtained as such, benefit from this sound quality equivalence and, therefore, allow the correlation with real engine sounds. Also, according to Fig. 5, VCS provides the engine RPM to the adaptive controller, which would be provided by the CAN-bus in a real vehicle implementation. The use of the CAN-bus (or a tacho) as a reference signal for the adaptive controller, in contrast with an acoustic signal, prevents it from having

a feedback path from the secondary actuator to the reference sensor, which could lead to instability and slower convergence [26].

The secondary actuator is an electrodynamic shaker (*LDS V201/3*). The microphone used as error sensor is a *B&K 4188*. The controller is implemented in a modular 1006 *dSPACE* system running at 2000Hz sample frequency throughout the measurements. Time and frequency domain data are recorded with a *SCADAS III* running *LMS Test.Lab*.

For the practical implementation of the adaptive feedforward control, the FIR filter \hat{S} is estimated off-line, with a LMS adaptive algorithm [26]. The process consists of exciting the secondary path with white noise (or a band pass noise in the frequency band of interest) while providing the same signal as a reference to a conventional LMS algorithm (as the one in Fig. 1a). After convergence, the filter W in that scheme will resemble the secondary path impulse response. This filter can then be used as \hat{S} in the NEX-LMS scheme. A comparison of the measured and estimated secondary paths is depicted in Fig. 6. The solid line refers to the FRF measured with the *SCADAS III* while the dotted line is the frequency domain representation of the identi-

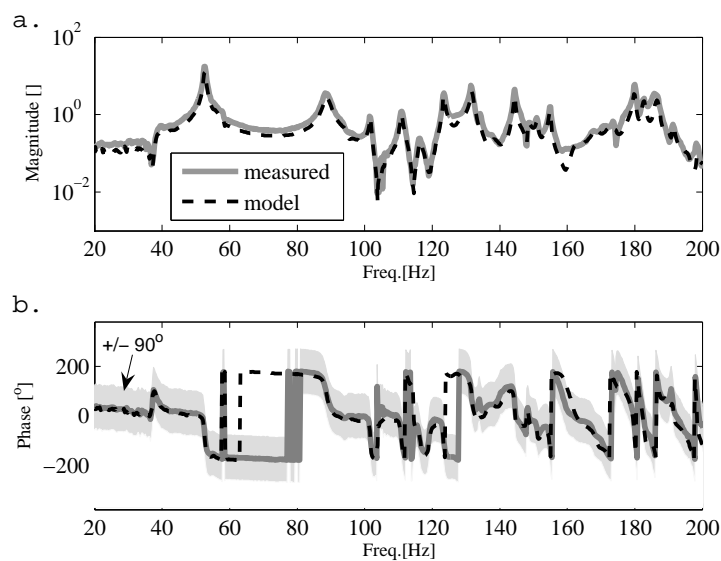


FIGURE 6: Identified model validation: (a) magnitude and (b) phase

fied FIR filter \hat{S} . The FRF is taken between the voltage output from the microphone and the voltage input to the shaker amplifier. The highlighted area in the phase plot relates to the $\pm 90^\circ$ [24] robustness margin around the reference (measured FRF).

This system is lightly damped, due to the rigid acoustic boundaries. As a result, it takes longer for the impulse response to fade out. Therefore, the selected FIR filter \hat{S} is 8000 samples long (4s @ 2kHz). The use of a sinusoid reference allows a shorter W , which is 10 samples long in this application. As shown above and indicated in [21], the normalization filter $N(\omega)$ is obtained by the inverse of $|\hat{S}|$ and implemented as a lookup table linked to the engine RPM. The equalization filter $\beta(\omega)$ is implemented in the same way, *i.e.*, values are set for a range of RPMs and presented as a lookup table linked to the engine RPM. Given the primary disturbance $d(\omega)$ and the residual error after convergence $e_r(\omega)$, the $\beta(\omega)$ that results in the desired residual error $e_d(\omega)$ can be obtained by linear interpolation (Fig. 7):

$$\beta(\omega) = \frac{d(\omega) - e_d(\omega)}{d(\omega) - e_r(\omega)} \quad (7)$$

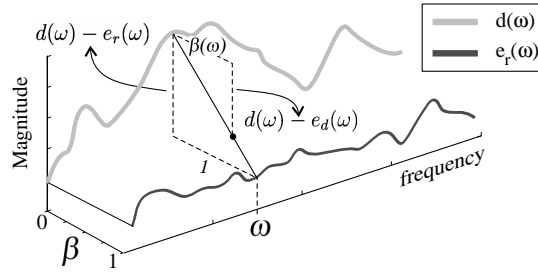


FIGURE 7: Method for obtaining $\beta(\omega)$

If $e_r(\omega)$ is not known beforehand, a simplified version of Eq.(7) can be used, where the residual error is assumed to be zero (Eq.8). This initial estimation can be used as a hot-start for an iterative optimization, or an *in situ* fine tuning of $\beta(\omega)$.

$$\beta(\omega) = 1 - \frac{e_d(\omega)}{d(\omega)} \quad (8)$$

4. Results

This section presents the experimental results obtained with the aforementioned setup. Initially, the behaviour of the NEX-LMS is assessed for stationary driving conditions (constant RPMs). The focus is on its capability of reducing a certain order-level as fast as possible, without affecting the neighbouring orders. In a further step, the performance of the controller in transient conditions is evaluated, where the equalization is tested during run-ups.

The colourmaps in Fig. 8 show the amplitude of different engine orders in time domain as the controller is turned on. Different RPMs are shown as well as the control of different orders. Figs. 8(a) and (b) refer to the same RPM, but different target orders, namely, 2^{nd} and 4^{th} . Figs. 8(c) and (d) are again related to the 2^{nd} order, but different RPMs. In any of these cases, the target order is significantly reduced while keeping the other orders undisturbed, which is one of the requirements for such a controller. In this way, it would be possible to add similar controllers in parallel, targeting different orders in a decentralized architecture, with minimum cross-interference.

The improved convergence features allow the use of this controller during transient disturbance. In order to evaluate its performance in this condition, three run-ups from 1000 to 3000RPM were used, lasting 32s (long), 16s (medium) and 8s (short), respectively.

Figure 9 shows, the passive (light gray) and the NEX-LMS (dashed black) 2^{nd} order cut for the long run-up. For the NEX-LMS, β is set to keep the 2^{nd} order as close as possible to constant (25dB) throughout the run-up. This shall be treated as the reference case, as this is the longest run-up, hence the one that allows more time for the controller to adapt to changes in the disturbance. The two additional curves demonstrate experimentally, the aforementioned symmetry of β around 1. As it can be seen, with half of the output ($\beta = 0.5 \therefore y^*(n) = 0.5y(n)$), reductions from 10dB to 35dB are achieved throughout the run-up.

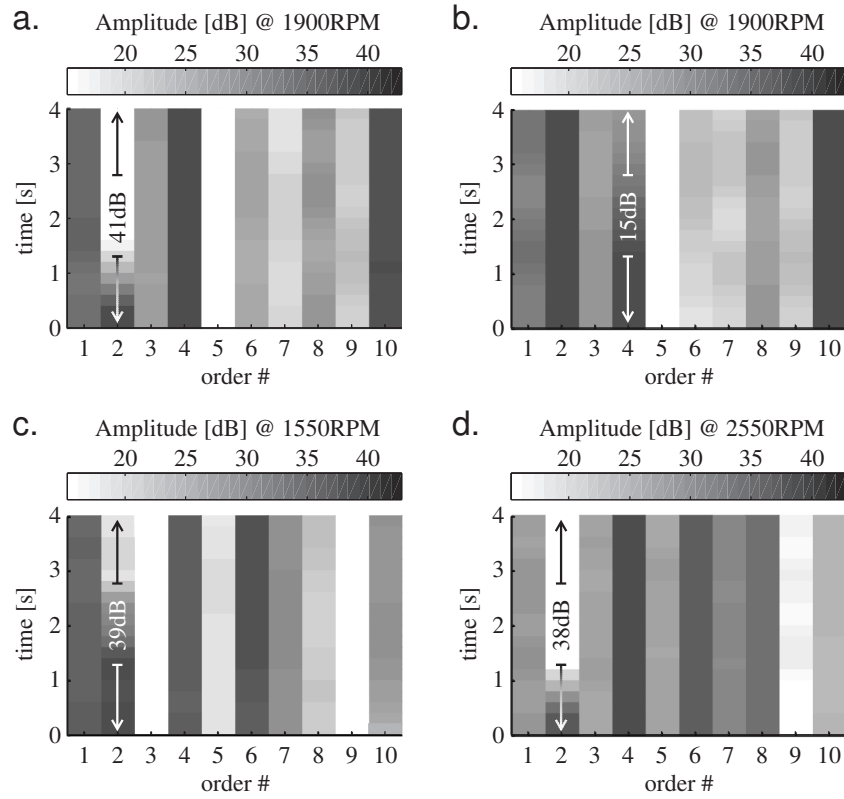


FIGURE 8: Evolution of order-levels in time for different RPMs and tracking orders

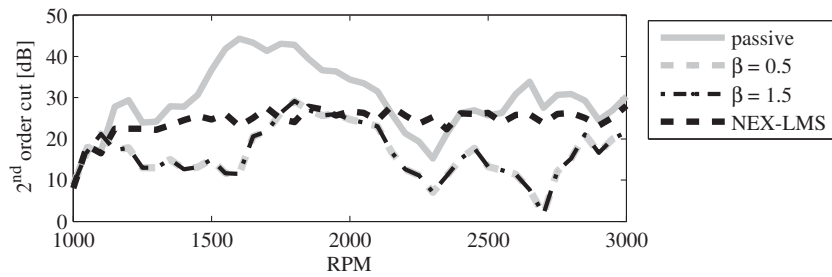


FIGURE 9: 2nd order cut for long run-up: passive system, NEX-LMS and constant values of β

The performance for the medium run-up is shown in Fig. 10. Together with the passive and NEX-LMS, the non-equalized (NX-LMS) performance is also shown. The latter is, actually, the lower bound (minimum level achievable) for a 16s run-up. As it can be seen, the performance around 1600RPM is the most affected. The main reason for the loss of performance is the faster change on the disturbance, which makes it more challenging for the controller to follow and adapt.

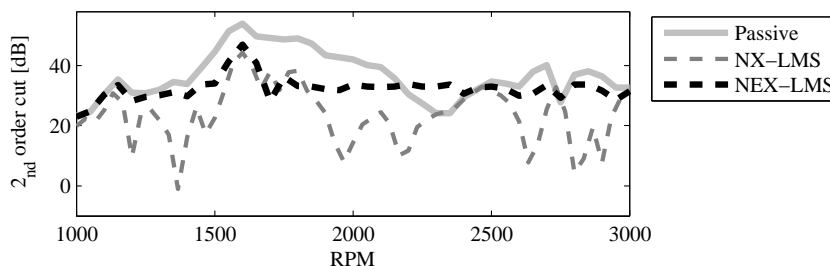


FIGURE 10: 2^{nd} order cut for medium run-up: passive system, NX-LMS and NEX-LMS

It is worth observing that part of this loss is not directly associated with the order cut itself, but rather with leakage from the neighbouring resonance. As the system is lightly damped, when a certain order excites an acoustic resonance (which is the case of the 2^{nd} order at 1560RPM - 52Hz for this cavity) the resulting booming noise echoes while the engine RPM is changing. The controller will follow the engine order and, as a result, this resonance will remain uncontrolled. This phenomenon is clear in Fig. 11, where time-frequency colourmaps are shown for the passive and active system. Around 5s, the first cavity resonance is excited and, immediately afterwards, the resonating cavity influences the order cut estimation, resulting in an overestimation of its level.

For an even shorter run-up (8s), performance decreases, as it is shown in Fig. 12. The maximum achievable reduction illustrated by the NX-LMS is much closer to the passive order cut than before and reveals that the room for equalization gets narrower with faster run-ups. Still, for the selected amplitude, besides the booming at 1600RPM, the 2^{nd} order cut remains fairly flat. As for the booming, de Oliveira et al. (2008) shows that one of the possible solutions is a linear time invariant

feedback controller, that could work in conjunction with the proposed adaptive NEX-LMS.

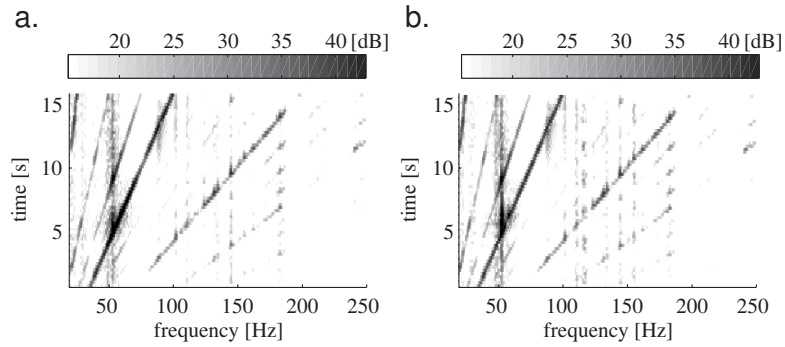


FIGURE 11: Medium run-up time-frequency plot: (a) passive and (b) NEX-LMS

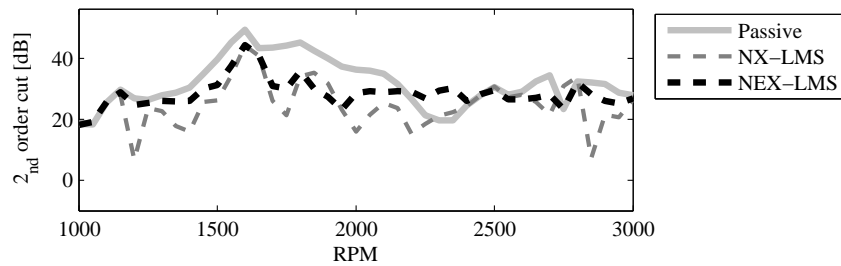


FIGURE 12: 2^{nd} order cut for short run-up: passive system, NX-LMS and NEX-LMS

5. Conclusions

This paper presents a novel adaptive scheme, NEX-LMS, for the equalization of harmonic noise components with improved convergence. It features a fast converging adaptive algorithm, based on the filtered x-LMS algorithm with normalized reference signal and equalization capabilities, elements necessary for adaptive sound quality controllers.

The proposed controller is experimentally validated on a vehicle mock-up which is acoustically excited by a sound quality equivalent engine simulator. The use of such scheme allows repeatable measurements with engine-like excitation signals, furnishing results that can be directly correlated to automotive applications.

The results are presented for stationary RPMs as well as for run-ups. They indicate that the controller is effective, reaching up to 38dB reduction. Also, it was possible to independently control an order, which is an interesting feature for order balancing applications. In order to independently tune multiple orders, similar controllers can be connected in parallel since each narrowband action does not interfere with each other. The improved convergence of the NEX-LMS controller allows to cope with varying engine speeds. The controller has been tested against three run-ups with different lengths (32s, 16s and 8s). As expected, the range of equalization is narrowed for faster run-ups, nevertheless, reductions up to 20dB can still be observed for the faster run-up.

Next steps in this study will address the control of more points inside de cavity, *e.g.* with a multi-channel adaptive scheme. In addition, the use of the proposed NEX-LMS for controlling roughness will be investigated. For that, not only amplitude but also phase has to be taken into account. The desired order-level profiles (amplitude and phase vs. RPM) could, again, be defined with the aid of sound quality-equivalent models and used to define target values for such a controller.

Acknowledgements

The research of Leopoldo P. R. de Oliveira is supported in the framework of a bilateral agreement between KU Leuven and University of São Paulo. The research of B. Stallaert is financed by a scholarship of the Institute for the Promotion of Innovation through Science and Technology in Flanders (IWT Vlaanderen). The work presented in this paper was performed as part of the Marie Curie RTN project: A Computer Aided Engineering Approach for Smart Structures Design (MC-RTN-2006-035559).

Bibliography

- [1] B. Schulte-Fortkamp, Vehicle interior noise - a product of interactive expertise, *Proceedings of NOISE-CON 2008*, 28-30 July, 2008, Dearborn -USA, 6p.
- [2] M.H. Fouladi, M.J.M. Nor, A.K. Ariffin, Spectral analysis methods for vehicle interior vibro-acoustics identification, *Mechanical Systems and Signal Processing* 23 (2009) 489-500.
- [3] D. Berckmans, K. Janssens, H. Van der Auweraer, P. Sas, W. Desmet, Model-based synthesis of aircraft noise to quantify human perception of sound quality and annoyance, *Journal of Sound and Vibration* 311 (2008) 1175-1195.
- [4] T. Abe, Up-front NVH Engineering - Vision, Challenges and Enablers, *Keynote Lecture ISMA2008: International Conference on Noise and Vibration Engineering*, Sep.15-17, Leuven BELGIUM (2008).
- [5] G. Vandernoot, P. Van Der Linden, P. Mas, C. Locqueteau, E. Leborgne, Predictive modeling of audio quality inside car cabins, *Proceedings of ISMA2008: International Conference on Noise and Vibration Engineering*, Sep.15-17, Leuven BELGIUM (2008), 3097-3112.
- [6] T.C. Giorjão, E.L. de Albuquerque, A.L. Cherman, Noise sources balancing on vehicle development to improve customer satisfaction, *Proceedings of ISMA2006: International Conference on Noise and Vibration Engineering*, Sep.18-20, Leuven BELGIUM (2006), 4309-4316
- [7] R. Sottek, W. Krebber, G.R. Stanley, Tools and methods for product sound design of vehicles, SAE Paper No.2005-01-2513.
- [8] G. Eisele, K. Wolff, N. Alt, M. Hüser, Application of vehicle interior noise simulation (VINS) for NVH analysis of a passenger car, SAE Paper No.2005-01-2514.
- [9] T. Mori, A. Takaoka, M. Maunder, Achieving a vehicle level sound quality target by a cascade to system level noise and vibration targets, SAE Paper No.2005-10-2394.

- [10] B. Brassow, M. Clapper, Powertrain sound quality development of the Ford GT, SAE Paper No.2005-02-2480.
- [11] M. Kronast, V. Mellin, C. Carme, A sound quality active noise profiling system for a passenger testvehicle, *Proceedings of Euronoise 2006*, Tampere FINLAND (2006), 6pp.
- [12] N. Alujević, P. Gardonio, K.D. Frampton, Experiments on a Smart Double Panel with Active Dampers for the Control of Sound Transmission, *Proceedings of ISMA2008: International Conference on Noise and Vibration Engineering*, Sep.15-17, Leuven BELGIUM (2008), 5-18.
- [13] B. Stallaert, G. Pinte, S. Devos, W. Symens, J. Swevers, P. Sas, Filtered-x LMS vs repetitive control for active structural acoustic control of periodic disturbances, *Proceedings of ISMA2008: International Conference on Noise and Vibration Engineering*, Sep.15-17, Leuven BELGIUM (2008), 79-87.
- [14] L.P.R. de Oliveira, M.M. da Silva, H. Van Brussel, P. Sas, W. Desmet, Concurrent mechatronic design approach for active control of cavity noise, *Journal of Sound and Vibration* 314 (2008) 507-525.
- [15] F. Kerber, S. Hurlebaus, B.M. Beadle, U. Stöbener, Control concepts for an active vibration isolation system, *Mechanical Systems and Signal Processing* 21 (2007) 3042-3059.
- [16] S. Hurlebaus, L. Gaul, Smart structure dynamics, *Mechanical Systems and Signal Processing* 20 (2006) 255-281.
- [17] H. Van der Auweraer, L. de Oliveira, M. da Silva, S. Herold, J. Mohring, A. Deraemaeker, A Virtual Prototyping Approach to the Design of Smart Structures Applications, *Proceedings of ISMA2006: International Conference on Noise and Vibration Engineering*, Sep.18-20, Leuven BELGIUM (2006), 273-284.
- [18] L.P.R. de Oliveira, A. Deraemaeker, J. Mohring, H. Van der Auweraer, P. Sas, W. Desmet, A CAE modeling approach for the analysis of vibroacoustic systems with distributed ASAC control, *Proceedings of ISMA2006: International Conference on Noise and Vibration Engineering*, Sep.18-20, Leuven BELGIUM (2006), 321-336.

-
- [19] S.M Kuo, R.K. Yenduri, A. Gupta, Frequency-domain delayless active sound quality control algorithm, *Journal of Sound and Vibration*, 318 (2008) 715-724.
- [20] L.P.R. de Oliveira, K. Janssens, P. Gajdatsy, H. Van der Auweraer, P. S. Varoto, P. Sas, W. Desmet, Active sound quality control of engine induced cavity noise, *Mechanical Systems and Signal Processing* 23 (2009) 476-488.
- [21] S.M. Kuo, A. Gupta, S. Mallu, Development of adaptive algorithm for active sound quality control, *Journal of Sound and Vibration* 299 (2007) 12-21.
- [22] H. Van der Auweraer, K. Janssens, L. de Oliveira, M. da Silva, W. Desmet, Virtual Prototyping for Sound Quality Design of Automobiles, *Sound and Vibration* 41(4) (2007) 26-31.
- [23] A. Gonzalez, M. Ferrer, M. de Diego, G. Piñero, J.J. Garcia-Bonito, Sound quality of low-frequency and car engine noises after active noise control, *Journal of Sound and Vibration*, 265 (2003) 663-679.
- [24] D.R. Morgan, An analysis of multiple correlation cancellation loops with a filter in the auxiliary path" *IEEE Trans. Acoust., Speech, Signal Processing*, ASSP-28, Aug.(1980), 454-467.
- [25] P.A. Nelson, S.J. Elliot, *Active Control of Sound*, Academic Press, (1992).
- [26] S.M Kuo, D.R. Morgan, *Active Noise Control Systems: Algorithms and DSP implementation*, John Wiley and Sons, Inc. - New York (1996).
- [27] G. Barrault, J.C.M. Bermudez, A. Lenzi, New analytical model for the filtered-x least mean squares algorithm verified through active noise control experiment, *Mechanical Systems and Signal Processing* 21 (2007) 1839-1852.
- [28] C. Bao, P. Sas, H. Van Brussel, A novel filtered-x LMS algorithm for active noise control, *Journal A* 34(1) (1993) 89-94.
- [29] X. Sun, G. Meng, LMS algorithm for active noise control with improved gradient estimate, *Mechanical Systems and Signal Processing* 20 (2006) 920-938.

- [30] S.M. Kuo, M.J. Ji, X.H. Jiang, Development and experiment of narrowband active noise equalizer, *Noise Control Engineering Journal* 41(3) (1993) 281-288.
- [31] M. de Diego, A. Gonzalez, M. Ferrer, G. Piñero, Multichannel active noise control system for local spectral reshaping of multifrequency noise, *Journal of Sound and Vibration* 274 (2004) 249-271.
- [32] K. Janssens, P. Van de Ponsele, M. Adams, The integration of sound quality equivalent models in a real-time virtual car sound environment, *Proceedings of DAGA Conference*, 18-20 March, Aachen GERMANY (2003), 6pp.
- [33] R. Williamns, M. Allman-Ward, P. Jennings, M. Batel, Using an interactive NVH simulator to compute and understand customer opinions about vehicle sound quality, SAE Paper No.2007-26-036.

Chapter 7

Conclusions and future developments

This thesis is devoted to the study and improvement of both modelling procedures and control strategies, with the broader aim of improving products' sound quality by means of active control. In order to achieve this goal, changes in two aspects on the present product development process are needed: (i) narrowing the gap between passive system and control design and (ii) take, as much as possible, the objective and subjective nature of human perception into consideration when designing or evaluating the performance of smart-systems.

The following sections present the thesis' main achievements, general conclusions and suggestions for future work.

7.1 Main achievements

- a simulation procedure for active control systems including the vibro-acoustic plant, sensor/actuator dynamics and the control algorithm,
- the use of the proposed simulation procedure for the concurrent optimisation of a ASAC system,
- experimental validation of the simulation procedure for passive and active optimal ASAC system,
- sound quality assessment of optimal ASAC system,

- 3D sound quality colourmaps as an evaluation tool for active (or passive) system modification,
- a novel adaptive sound quality control system: NEX-LMS.

7.2 General conclusions

With the broader objective of narrowing the gap between the passive system and active control design, a simulation scheme is proposed, which is based on standard FE/FE vibro-acoustic modal models. The resulting coupled system is formulated as a state-space model which is suitable for control design and compact enough for optimization as discussed in Chapters 2 and 3 (de Oliveira et al., 2008, 2007b) .

The proposed simulation scheme forms the basis for the concurrent mechatronic design presented in Chapter 3 (de Oliveira et al., 2008), which considers structural and control parameters simultaneously. The compact and accurate representation of the vibro-acoustic system in the state-space form, allowed the calculation of the pareto plots, shown in Fig. 16. Each of these plots requires a substantial amount of calculations, which was only feasible due to the efficiency of the simulation scheme.

The accuracy of the modelling procedure was validated in two steps: first by correlating the direct FE and the reduced SS passive models and, secondly, with an experimental validation campaign, in which passive and optimum active systems were confronted.

The added value of such an approach is made clear, when the global optimal design outperforms the solution suggested by a traditional sequential design, i.e., the optimum active system performs better than the optimal passive system with an optimized controller. The use of the velocity feedback control strategy (active damping) allows an intuitive analysis of the optimizations results: the optimal passive system resulted from the most “uncoupled” combination of structure and cavities (resonance frequencies apart from each other and incompatible mode shapes). Since the control can only introduce damping to the system, the resultant global damping archived by acting on the weakly coupled modes of the firewall are minimum, as observed in Chap. 2. In contrast, the results presented in Chap. 3 reveal that by using a non-optimal structure, which efficiently couples with the acoustic cavities, one can significantly affect the acoustic response by using only

structural sensors and actuators.

In Chapter 4 (de Oliveira et al., 2009), the optimal controller (derived previously) is assessed in terms of sound quality improvement. In order to do that, *LMS Virtual Car Sound*, which is typically used for real-time auralization, is used as a SQ-equivalent disturbance source. In this way, it provides repeatable measurements with engine-like excitation signals that allow a directly correlation to automotive SQ applications. The control performance is evaluated in terms of Zwicker loudness and Roughness. 3D SQ colourmaps are introduced as tools for the evaluation of the control performance inside the passenger compartment, and provide a quantitative assessment of the global effect the controller had on the cavity.

Quantitative results from the feedback and a modified Fx-LMS feedforward controllers are compared in Chapter 5 (de Oliveira et al., 2008). While the feedback control provides efficient broadband reduction, it is clear that independent order control (with varying RPM) can only be achieved by an adaptive scheme. Since the feedback controller is acting in a broadband, it could be targeted to reduce road or wind-noise, while booming or order balance should be tackled with an adaptive feedforward scheme.

Chapter 6 presents a novel adaptive scheme for the equalization of harmonic noise components with improved convergence. It features a fast converging adaptive algorithm, based on the Fx-LMS algorithm with normalized reference signal and equalization capabilities, elements necessary for adaptive sound quality controllers. As for the feedback control, this control strategy is experimentally validated on a vehicle mock-up, with the aid of SQ-equivalent engine noise simulator.

Reductions of up to 38dB were reached for stationary RPMs. It is also verified that the control scheme is capable of independently controlling a single order. This feature is particularly important for the proposed application, where similar controllers could be connected in parallel to equalize multiple orders. The improved convergence of the NEX-LMS scheme allows the control of orders while varying engine speed. The controller has been tested against three run-ups with different durations (32s, 16s and 8s). As expected, the range of equalization is narrowed for faster run-ups, nevertheless, reductions up to 20dB can still be observed for the faster run-up.

7.3 Future developments

As mentioned before, two main research tracks can be identified in this thesis: (i) narrowing the gap between passive system and control design and (ii) including the objective and subjective nature of human perception into control design and evaluation. Those are rather broad and recent research fields, that motivates new research/technology activities. While (i) can gain a great deal of improvement with virtual prototyping, by extending or combining existing solutions to include the necessary features for smart-materials and control design, either at component- or system-level; (ii) needs a good understanding of the most relevant metrics for each application, standardisation and even, the development of new metrics (as it is the case with vibration-quality).

More specifically, the following topics could complete or be a natural continuation of this thesis.

Piezoelectric elements: Given the potential of piezoelectric materials for active control purposes, a natural step further would involve the use of such distributed sensing and actuation on the proposed modelling/optimization methodology. Depending on the selection of software, a technological issue might rise, as a standard solid FE piezoelectric formulation would lead to very dense meshes that could hinder the optimization step.

Improvements to the NEX-LMS: To the present, there is no record of an active control strategy that can improve roughness. Mostly what is evaluated is loudness. The proposed NEX-LMS controller can tackle the order tracking and the amplitude equalization, but in the event of a undesired modulation, triggered by the unmasking of orders neighboring the controlled one, not much can be done, besides adding another controller to those orders. In other words, the present control strategies (presented here and found in literature) do not tackle the orders' phase relation. Modifications to the present control scheme or completely new concepts could be pursued in order to cope with that. Another natural evolution of the proposed adaptive scheme is its extension to a MIMO formulation.

Inclusion of control algorithms in real-time auralization: The inclusion of feedback and adaptive feedforward controllers in the

real-time NVH simulator is of interest as it would enable the assessment of the controller action by the designer, an expert panel or for a jury test. It would represent, in this way, a valuable tool for the design of active solutions.

The mid-frequency range: In vibro-acoustic CAE, there is a mid-frequency range which is too high for element-based techniques (such as FEM or BEM) and do not offer the necessary modal density for energy based methods (such as SEA). A deterministic technique, based on the indirect Trefftz approach (wave based method - Desmet, 1998) has been proposed to tackle this issue. This state-of-the-art simulation tools could be used to furnish the necessary vibro-acoustic models for the control design, or be extended to enable frequency-domain control design in a multi-physics approach.

Validation in a real vehicle: The implementation of the proposed control scheme in a real vehicle poses some technological tasks (e.g., the development and packaging of sensors and actuators) but can also be interesting from a research perspective, as it rises questions related to the perceived control efficiency, e.g., under the presence of multiple disturbance sources (aerodynamic, tyre/road, etc.); the quality of the the system identification process for a more complex (maybe non-linear) system; the importance of variability (or uncertainty) for the control performance/desing, etc.

Optimization including passive solutions: The assessment of the trade-offs between passive and active control in a concurrent optimization. In this way, the real trade-offs could be assessed, in contrast with the standard design procedure, in which passive solutions are exercised to their limit and active control is included in the very end, for trouble shutting. In the same context, hybrid solutions could be assessed concurrently.

Active control for aeroacoustic disturbances: As engine noise is reduced (actively or passively), other sources become more evident, which is the case aeroacoustic noise. That is a challenging field of research from many perspectives: the disturbance has a broad frequency band and no reference signal may be available with time enough for adaptation; aerospace is known for being

weight sensitive, the volume to be controlled is big, what leads to high modal density, etc.

Active control for musical instruments: Music and musical instruments are recurrent research topics among acousticians, often challenging our ability in explaining (or deciphering) what was developed during centuries of intuitive and empiric labour. It is also an attractive subject for young researchers and can furnish good examples for courses on vibration and vibro-acoustics. Therefore, the use of active and/or passive design to improve the sound quality of musical instruments can be a valuable research topic.

Active noise control and new automotive technologies: An mentioned in Section 1.2.3, the introduction of new technologies, recently driven by tighter legislations on carbon-fuel emissions, lead to, e.g., hybrid cars, variable engine displacement, etc. Each of these new concepts pose challenges to vehicle NVH. The noise and vibration issues related to variable engine displacement are clearer, the engine mounts cannot be optimized for both driving conditions, which can lead to excessive vibration and structural born noise, not to mentions the sound quality aspect. On hybrids, external and internal noise can be an issue. Pedestrians are used to the sound of a regular car approaching, and hybrids can be rather silent. Active control can also provide the means to control engine noise in hybrids, such that the occupants are kept regardless of driving mode, either by having a more silent interior or the constant perception of a familiar combustion engine.

Bibliography

- Abe, T. (2008). Up-front NVH engineering - vision, challenges and enablers. In *ISMA2008: International Conference on Noise and Vibration Engineering - Keynote Lecture*, Leuven BELGIUM.
- Alujević, N., P. Gardonio, and K. D. Frampton (2008). Experiments on a smart double panel with active dampers for the control of sound transmission. In *Proceedings of ISMA2008: International Conference on Noise and Vibration Engineering*, Leuven BELGIUM, pp. 5–18.
- Bao, C., P. Sas, and H. Van Brussel (1991). Active control of engine-induced noise inside cars. In *Proceedings of Inter-Noise '91*, Sydney AUSTRALIA, pp. 525–528.
- Bao, C., P. Sas, and H. Van Brussel (1993). A novel filtered-x LMS algorithm for active noise control. *Journal A* 34(1), 89–94.
- Barrault, G., J. C. M. Bermudez, and A. Lenzi (2007). New analytical model for the filtered-x least mean squares algorithm verified through active noise control experiment. *Mechanical Systems and Signal Processing* 21(4), 1839–1852.
- Barrault, G., J. C. M. Bermudez, and A. Lenzi (2007). New analytical model for the filtered-x least mean squares algorithm verified through active noise control experiment. *Mechanical Systems and Signal Processing* 21(2007), 1839–1852.
- Bein, T., J. Bö, S. Herold, D. Mayer, T. Melz, and M. Thomaier (2007). Smart interfaces and semi-active vibration absorber for noise reduction in vehicle structures. *Aerospace Science and Technology*, doi:10.1016/j.ast.2007.10.008.

- Berckmans, D., K. Janssens, H. Van der Auweraer, P. Sas, and W. Desmet (2008). Model-based synthesis of aircraft noise to quantify human perception of sound quality and annoyance. *Journal of Sound and Vibration* 311(2008), 1175–1195.
- Boonen, R. (2003). *Development of an active exhaust silencer with acoustical characterization of internal combustion engines*. Leuven BELGIUM: PhD thesis, K.U.Leuven.
- Braess, H. H. and U. Seiffert (2005). *Handbook of automotive engineering*. Warrendale USA: Society of Automotive Engineering - SAE.
- Brassow, B. and M. Clapper (2005). Powertrain sound quality development of the Ford GT. SAE Paper No. 2005-02-2480.
- CALM II Network (2004). Research for a quieter europe in 2020. *European Commission - Research Directory*, www.calm-network.com.
- Canévet, G. and G. Mangiante (2004). Psychoacoustic assessment of active noise control. In *Proceedings of Active 04*, Williamsburg USA, pp. 1–10.
- Carme, C. (1987). Absorption acoustique active dans les cavites. In *Doctor Thesis, Universite D'Aix-Marseille II*, France.
- Costin, M. H. and D. R. Elzinga (1989). Active reduction of low-frequency tire impact noise using digital feedback control. *IEEE Control Systems Magazine* 9(5), 3–6.
- Coyette, J. P. and Y. Dubois-Pèlerin (1994). An efficient coupling procedure for handling large size interior structural-acoustic problems. In *Proceedings of ISMA 19: International Conference on Noise and Vibration Engineering*, Leuven BELGIUM, pp. 729–738.
- Cunefare, K. A. and S. De Rosa (1999). An improved state-space method for coupled fluid-structure interaction analysis. *J. Acoust. Soc. Am.* 105(1999), 206–210.
- da Silva, M., O. Bröls, B. Paijmans, W. Desmet, and H. Van Brussel (2008). Computer-aided integrated design for mechatronic systems with varying dynamics. In *H. Ulbrich & L. Ginzinger (eds.) Motion and Vibration Control, Selected Papers from MOVIC 2008*, Springer, NETHERLANDS, pp. 53–62.

- da Silva, M., W. Desmet, and H. Van Brussel (2008). Design of mechatronic systems with configuration-dependent dynamics: simulation and optimization. *IEEE/ASME Trans. on Mechatronics* 13(6), 638–646.
- Daniel, P. and R. Weber (1997). Psychoacoustical roughness: Implementation of an optimized model. *ACUSTICA - acta acustica* 83, 113–123.
- De Fonseca, P., P. Sas, and H. Van Brussel (1999). A comparative study of methods for optimising sensor and actuator locations in active control applications. *Journal of Sound and Vibration* 21(4), 651–679.
- de Oliveira, L. P. R., M. M. da Silva, H. Van Brussel, P. Sas, and W. Desmet (2008). Concurrent mechatronic design approach for active control of cavity noise. *Journal of Sound and Vibration* 314(2008), 507–525.
- de Oliveira, L. P. R., A. Deraemaeker, J. Mohring, H. Van der Auweraer, P. Sas, and W. Desmet (2006). A CAE modeling approach for the analysis of vibroacoustic systems with distributed ASAC control. In *Proceedings of ISMA2006: International Conference on Noise and Vibration Engineering*, Leuven BELGIUM, pp. 321–336.
- de Oliveira, L. P. R., K. Janssens, P. Gajdatsy, H. Van der Auweraer, P. S. Varoto, P. Sas, and W. Desmet (2009). Active sound quality control of engine induced cavity noise. *Mechanical Systems and Signal Processing* 23(2), 476–488.
- de Oliveira, L. P. R., P. Sas, W. Desmet, K. Janssens, P. Gajdatsy, and H. Van der Auweraer (2008). Active control of engine noise transmitted into cavities: simulation, experimental validation and sound quality assessment. *J. Acoust. Soc. Am.* 123(5), 3872.
- de Oliveira, L. P. R., B. Stallaert, W. Desmet, J. Swevers, and P. Sas (2006). Optimisation strategies for decentralized ASAC. In *Proceedings of Forum Acusticum 2005*, Budapest HUNGARY, pp. 875–880.
- de Oliveira, L. P. R., B. Stallaert, K. Janssens, H. Van der Auweraer, P. Sas, and W. Desmet (2009). NEX-LMS: a novel adaptive control scheme for sound quality control. *Mechanical Systems and Signal Processing*.

- de Oliveira, L. P. R., P. S. Varoto, P. Sas, and W. Desmet (2007a). A state-space approach for ASAC simulation. In *Proceedings of the XII International Symposium on Dynamic Problems of Mechanics - DINAME 2007*, Ilhabela BRAZIL, pp. 1–10.
- de Oliveira, L. P. R., P. S. Varoto, P. Sas, and W. Desmet (2007b). A state-space modeling approach for active structural acoustic control. *Journal of Shock and Vibration* (2009), In Press.
- De Rosa, S., G. Pezzullo, L. Lecce, and F. Marulo (1994). Structural acoustic calculations in the low frequency range. *AIAA Journal of Aircraft* 31(6), 1387–1394.
- De Rosa, S., A. Sollo, F. Franco, and K. A. Cunefare (2001). Structural-acoustic optimisation of a partial fuselage with a standard finite element code. In *7th AIAA/CEAS Aeroacoustics Conference and Exhibit; Collection of Technical Papers. Vol. 1 (A01-30800 07-71)*, Maastricht NETHERLANDS, May 28-30, pp. AIAA-2001-2114.
- Dehandschutter, W. (1997). *The reduction of structure-born noise by active control of vibration*. Leuven BELGIUM: PhD thesis, K.U.Leuven.
- Dehandschutter, W. and P. Sas (1998). Active control of structure-borne road noise using vibration actuators. *Journal of Vibration and Acoustics* 120(2), 517–523.
- Desmet, W. (1998). *A wave based prediction technique for coupled vibroacoustic analysis*. Leuven BELGIUM: PhD thesis, K.U.Leuven.
- Desmet, W., B. Pluymers, and P. Sas (2003). Vibro-acoustic analysis procedures for the evaluation of the sound insulation characteristics of agricultural machinery cabins. *Journal of Sound and Vibration* 266(2003), 407–441.
- Desmet, W. and D. Vandepitte (2004). Finite element method in acoustics. In *ISAAC 16 - Seminar on Advanced Techniques in Applied and Numerical Acoustics*, Leuven BELGIUM.
- Diego, M., A. Gonzalez, M. Ferrer, and G. Piñero (2004). Multichannel active noise control system for local spectral reshaping of multifrequency noise. *Journal of Sound and Vibration* 274, 249–271.

- Donders, S., R. Hadjit, M. Brughmans, L. Hermans, and W. Desmet (2007). A wave-based substructuring approach for fast vehicle body optimization. *International Journal on Vehicle Design* 43(1-4), 100–115.
- Eisele, G., K. Wolff, N. Alt, and M. Hüser (2005). Application of vehicle interior noise simulation (VINS) for NVH analysis of a passenger car. SAE Paper No. 2005-01-2514.
- El-Masri, N., M. Tournour, and C. McCulloch (2002). Meshing procedure for vibro-acoustic models. In *Proceedings of ISMA2002: International Conference on Noise and Vibration Engineering*, Leuven BELGIUM, pp. 2151–2157.
- Elliott, S. J. (1990). In-flight experiments on the active control of propeller-induced cabin noise. *Journal of Sound and Vibration* 140(2), 219–238.
- Elliott, S. J. (1994). Active control of structure-born noise. *Journal of Sound and Vibration* 177(5), 651–673.
- Elliott, S. J. and P. A. Nelson (1993). Active noise control: Low-frequency techniques for suppressing acoustic noise leap forward with signal processing. *IEEE Signal Processing Magazine* October 1993, 12–35.
- Elliott, S. J., I. M. Stothers, P. A. Nelson, A. M. McDonald, D. C. Quinn, and S. T. (1988). The active control of engine noise inside cars. In *InterNoise 88*, Avignon FRANCE, September (1988), pp. 987–990.
- Elliott, S. J. and T. J. Sutton (1996). Performance of feedforward and feedback systems for active control. *IEEE Transaction on speech and audio processing* 4(3), 214–223.
- Everstine, G. C. (1981a). Structural acoustic analogies for scalar field problems. *International Journal of Numerical Methods in Engineering* 17(3), 471–476.
- Everstine, G. C. (1981b). A symmetric potential formulation for fluid-structure interactions. *Journal of Sound and Vibration* 79(1981), 157–160.

- Fastl, H. (2002). Sound design of machines from a musical perspective. In *Proceedings of Sound Quality Symposium*, Dearborn, USA, pp. 1–10.
- Fastl, H. (2005). Recent developments in sound quality evaluation. In *Keynote Lecture from the Forum Acusticum 2005*, Budapest HUNGARY, pp. 1647–1653.
- Felice, M. J. (2008). Driving next generation powertrain refinement through virtual design. In *The International LMS Engineering Simulation Conference 2008*, Paris FRANCE.
- Fohr, F., C. Carme, J. L. Peube, P. Vignassa, and F. LeBrazidec (2002). Active exhaust line for truck diesel engine. In *Proceedings of ACTIVE 02*, Southampton UK, pp. 327332.
- Fouladi, M. H., M. J. M. Nor, and A. K. Ariffin (2008). Spectral analysis methods for vehicle interior vibro-acoustics identification. *Mechanical Systems and Signal Processing*, doi:10.1016/j.ymssp.2008.04.001.
- Fridrich, R. J. (2005). Music analogy: an alternative strategy for sound quality requirements. SAE Paper No. 2005-01-2477.
- Gan, W. S. and S. M. Kuo (2007). An integrated audio and active noise control headsets. *IEEE Transactions on Consumer Electronics* 48(2), 243–247.
- Giordano, J. A. and G. H. Koopmann (1995). State-space boundary element-finite element coupling for fluid-structure interaction analysis. *J. Acoust. Soc. Am.* 98, 363–372.
- Giorjão, T. C., E. L. de Albuquerque, and A. L. Cherman (2006). Noise sources balancing on vehicle development to improve customer satisfaction. In *Proceedings of ISMA2006: International Conference on Noise and Vibration Engineering*, Leuven BELGIUM, pp. 4309–4316.
- Glasberg, B. and B. Moore (2002). A model of loudness applicable to time-varying sounds. *Journal of the Audio Engineering Society* 50(5), 331–342.

- Gobbi, M., F. Levi, and G. Mastinu (2006). Multi-objective stochastic optimisation of the suspension system of road vehicles. *Journal of Sound and Vibration* 298(2006), 1055–1072.
- Gonzalez, A., M. Ferrer, M. Diego, G. Piñero, and J. J. Garcia-Bonito (2003). Sound quality of low-frequency and car engine noises after active noise control. *Journal of Sound and Vibration* 265, 663–679.
- Guicking, D. (1996). Active control of vibration and sound - an overview of the patent literature. In *Proceedings of ISMA 21: International Conference on Noise and Vibration Engineering*, Leuven BELGIUM, pp. 199–220.
- Happian-Smith, J. (2002). *An introduction to modern vehicle design*. Warrendale USA: Society of Automotive Engineering - SAE.
- Henriouille, K. (2001). *Distributed actuators and sensors for active noise control*. Leuven BELGIUM: PhD thesis, K.U.Leuven.
- Henriouille, K. and P. Sas (2003). Experimental validation of a collocated pvdf volume velocity sensor/actuator pair. *Journal of Sound and Vibration* 265, 489–506.
- Herold, S., H. Atzrodt, D. Mayer, and M. Thomaier (2005). Integration of different approaches to simulate active structures for automotive applications. In *Proceedings of Forum Acusticum 2005*, Budapest HUNGARY, pp. 909–914.
- Hufenbach, W., M. Dannemann, F. Kolbe, T. Labuhn, and R. Klug (2008). Silent aircraft toilets - different concepts for reducing the sound emission. In *Proceedings of ISMA2008: International Conference on Noise and Vibration Engineering*, Leuven BELGIUM, pp. 2293–2302.
- Hurlebaus, S. and L. Gaul (2006). Smart structure dynamics. *Mechanical Systems and Signal Processing* 20(2006), 255–281.
- ISO226 (2003). *Normal equal-loudness-level contours, Ed.2*. International Organization for Standardization.
- ISO532B (1975). *Method for Calculating Loudness Level*. International Organization for Standardization.

- Janssens, K., S. Ahrens, A. Bertand, J. Lanslots, P. Van de Ponsele, A. Vecchio, and H. Van der Auweraer (2007). An on-line order-based roughness algorithm. SAE Paper No. 07NVC-173.
- Janssens, K., P. V. de Ponsele, and M. Adams (2003). The integration of sound quality equivalent models in a real-time virtual car sound environment. In *Proceedings of DAGA Conference*, Aachen GERMANY, pp. 1–6.
- Janssens, K., A. Vecchio, P. Mas, H. Van der Auweraer, and P. Van de Ponsele (2004). Sound quality evaluation of structural design changes in a virtual car sound environment. In *Proceedings Institute of Acoustics 26(2)*.
- Jay, G. C. (2007). Sound/vibration quality engineering: Part I - introduction and the SVQ engineering process. *S V Sound and Vibration 41(4)*, 16–25.
- Jones, R. W., B. L. Olsen, and B. R. Mace (2007). Comparison of convergence characteristics of adaptive iir and fir filters for active noise control in a duct. *Applied Acoustics 68(7)*, 729–738.
- Junhong, Z. and H. Jun (2006). CAE process to simulate and optimise engine noise and vibration. *Mechanical Systems and Signal Processing 20(2006)*, 1400–1409.
- Jurč, R. and O. Jiříček (2005). Differences of sound quality evaluations of vacuum cleaners, computer fans and hair dryers. In *Proceeding of Forum Acusticum 2005*, Budapest HUNGARY, pp. L165–L168.
- Kerber, F., S. Hurlebaus, B. M. Beadle, and U. Stöbener (2007). Control concepts for an active vibration isolation system. *Mechanical Systems and Signal Processing 21(2007)*, 3042–3059.
- Kido, K. (1975). Reduction of noise by use of additional sound sources. In *Proceedings of Inter-Noise '75*, Sendai JAPAN, pp. 647–650.
- Kochan, K., T. Kletschkowski, D. Sachau, and H. Breitbach (2008). Active noise control in a semi-closed aircraft cabin. In *Proceedings of ISMA2008: International Conference on Noise and Vibration Engineering*, Leuven BELGIUM, pp. 35–50.

- Kronast, M. (2007). Development of an active noise control system for a passenger vehicle. In *Workshop on Model Reduction and Control, May 2007*, Kaiserslautern GERMANY.
- Kronast, M., V. Mellin, and C. Carme (2006). A sound quality active noise profiling system for a passenger test vehicle. In *Proceedings of Euronoise 2006*, Tampere FINLAND, pp. 1–6.
- Kuo, S. M., A. Gupta, and S. Mallu (2007). Development of adaptive algorithm for active sound quality control. *Journal of Sound and Vibration* 299(2007), 12–21.
- Kuo, S. M., M. J. Ji, and X. H. Jiang (1993). Development and experiment of narrowband active noise equalizer. *Noise Control Engineering Journal* 1(3), 281–288.
- Kuo, S. M., M. J. Ji, and X. H. Jiang (1995). Development and analysis of a narrowband active noise equalizer. *IEEE Transactions on Speech and Audio Processing* 3(3), 217–222.
- Kuo, S. M. and S. Mallu (2005). Adaptive active sound quality control algorithm. In *Proceedings of 2005 International Symposium on Intelligent Signal Processing and Communication Systems*, Hong Kong, 13–16 Dec., pp. 737–740.
- Kuo, S. M. and D. R. Morgan (1996). *Active Noise Control Systems: Algorithms and DSP implementation*. New York (USA): John Wiley and Sons, Inc.
- Kuo, S. M., R. K. Yenduri, and A. Gupta (2008). Frequency-domain delayless active sound quality control algorithm. *Journal of Sound and Vibration* 318(2008), 715–724.
- Lang, G. (2001). Understanding the physics of electrodynamic shaker performance. *S V Sound and Vibration* 35(10), 1–9.
- Lee, S. K. (2008). Objective evaluation of interior sound quality in passenger cars during acceleration. *Journal of Sound and Vibration* 310, 149–168.
- Li, S. (2005). A state-space coupling method for fluid-structure interaction analysis of plates. *J. Acoust. Soc. Am.* 118(2005), 800–805.

- Liu, W., Z. Hou, and M. A. Demetriou (2006). A computational scheme for the optimal sensor/actuator placement of flexible structures using spatial h2 measures. *Mechanical Systems and Signal Processing* 20, 881–895.
- LMS.Sysnoise (2000). *rev. 5.5 User's Manual*. Leuven BELGIUM: LMS International.
- Lueg, P. (1932). Process of silencing sound oscillations. *US Patent No. 2043416*.
- Luo, J. and H. C. Gea. Modal sensitivity analysis of coupled acoustic-structural systems. *Journal of Vibration and Acoustics* 119(1997), 545–550.
- Mabe, J. (2008). Variable area jet nozzle for noise reduction using shape memory alloy actuators. *J. Acoust. Soc. Am.* 123, 3871.
- Mackay, A. and S. Kenchington (2004). Active control of noise and vibration a review of automotive applications. In *Proceedings of Active 04*, Williamsburg USA, pp. 1–11.
- Maguire, D. J. (2008). *Active muffler technology demonstration - meeting for product commercialization assessment by NVHT*. K.U.Leuven (PMA).
- Maia, N. M. M. and J. M. M. Silva (1997). *Theoretical and Experimental Modal Analysis*. New York, USA: John Wiley and Sons Inc.
- Mangiante, G. (2004). Limitations on the performance of active noise control systems due to subjective effects. *J. Acoust. Soc. Am* 115(5), 2498.
- Mangiante, G. and G. Canevet (2007). Noise annoyance reduction using active control. *J. Acoust. Soc. Am* 121, 3179.
- Martin, V., A. Cummings, and C. Gronier (2004). Discrimination of coupled structural/acoustic duct modes by active control: principles and experimental results. *Journal of Sound and Vibration* 274(3-5), 583–603.
- McConnell, K. G. and P. S. Varoto (2008). *Vibration Testing: Theory and Practice*. New York, USA: Wiley, 2nd edition.

- Mohammed, J. I. and S. J. Elliott (2005). Active control of fully coupled structural-acoustic systems. In *Proceeding of Inter-Noise 2005*, Rio de Janeiro BRAZIL, pp. 1–10.
- Morgan, D. R. (1980). An analysis of multiple correlation cancellation loops with a filter in the auxiliary path. *IEEE Trans. Acoust., Speech, Signal Processing ASSP-28*(Aug.1980), 454–467.
- Mori, T., A. Takaoka, and M. Maunder (2005). Achieving a vehicle level sound quality target by a cascade to system level noise and vibration targets. SAE Paper No.850965.
- MSC.Nastran (2004). *Reference Manual*. (USA): MSC Software.
- Nehl, J., C. Steffens, and C. Nussman (2006). Virtual NVH powertrain development. In *Proceedings of Euronoise 2006*, Tampere FINLAND, pp. 1–7.
- Nelson, P. A. and S. J. Elliot (1992). *Active Control of Sound*. Academic Press.
- Olbrechts, T., P. Sas, and D. Vandepitte (1997). FRF measurement errors caused by the use of inertia mass shakers. In *Proceedings of the 15 International Modal Analysis Conference - IMAC XV*, Orlando USA, pp. 188–194.
- Olson, H. F. (1953). Electric sound absorber. *J. Acoust. Soc. Am.* 25, 1130–1136.
- Olson, H. F. (1956). Electronic control of noise, vibration and reverberation. *J. Acoust. Soc. Am.* 28(5), 966.
- Olson, L. G. and K. J. Bathe (1985). Analysis of fluid-structure interactions: a direct symmetric coupled formulation based on the fluid velocity potential. *Computers & Structures* 21(1985), 21–32.
- Olsson, C. (2006). Analysis of fluid-structure interactions: a direct symmetric coupled formulation based on the fluid velocity potential. *Journal of Sound and Vibration* 294, 162–176.
- Oswald, L. J. (1984). Reduction of diesel-engine noise inside passenger compartments using active, adaptive noise control. *Noise control engineering journal* 23(3), 110.

- Paillard, B., C. T. Le Donh, A. Berry, and J. Nicolas (1995). Accelerating the convergence of the filtered-x lms algorithm through transform-domain optimisation. *Mechanical Systems and Signal Processing* 9(4), 445–464.
- Pan, G. and D. A. Bies (1987). The effect of fluid structure coupling on the sound waves in an enclosure: theoretical part. *J. Acoust. Soc. Am.* 2(1987), 691–706.
- Park, C., C. Fuller, and M. Kidner (2002). Evaluation and demonstration of advanced active noise control in a passenger automobile. In *Proceedings of ACTIVE 02*, Southampton UK, pp. 275–284.
- Park, C. G., C. Fuller, J. P. Carneal, V. Collin, J. T. Long, R. E. Powell, and J. L. Schmidt (2004). On-road demonstration of noise control in a passenger automobile - part 2. In *Proceedings of ACTIVE 04*, Williamsburg USA, pp. 1–12.
- Penne, F. (2004). Shaping the sound of the next-generation BMW. In *Proceedings of ISMA2004: International Conference on Noise and Vibration Engineering*, Leuven BELGIUM, pp. 25–39.
- Plunt, J. and M. Hellström (2006). Impact sound quality of consumer products evaluation by sound quality-metrics and wavelet time-frequency analysis. In *Proceedings of Euronoise 2006*, Tampere FINLAND, pp. 1–6.
- Pluymers, B., B. Van Hal, D. Vandepitte, and W. Desmet (2007). Trefftz-based methods for time-harmonic acoustics. *Arch. Comput. Methods Eng.* 14(4), 343–381.
- Preumont, A. (2002). *Vibration Control of Active Structures: An Introduction*. AH Dordrecht NETHERLANDS: Kluwer Academic Publishers.
- Rao, D. (1987). Electrodynamic interaction between a resonating structure and an exciter. In *Proceedings of the 5th International Modal Analysis Conference - V IMAC*, pp. 1142–1150.
- Rees, L. E. and S. J. Elliott (2006). Adaptive algorithms for active sound-profiling. *IEEE Transactions on Speech and Audio Processing* 14(2), 711–719.

- Ross, C. F. (1982). An adaptive digital filter for broadband sound control. *J. Sound and Vib.* 80(3), 381–389.
- Saha, P. (2007). Is automotive sound quality just in the ear of the beholder? *S V Sound and Vibration* 41(4), Editorial.
- Sano, H., T. Yamashita, and M. Nakamura (2002). Recent applications of active noise and vibration control to automobiles. In *Proceedings of Active 02*, Southampton UK, pp. 29–42.
- Sas, P. (2004). Introduction to technical acoustics. In *ISAAC 16 - Seminar on Advanced Techniques in Applied and Numerical Acoustics*, Leuven BELGIUM.
- Sas, P., C. Bao, F. Augusztinovicz, and W. Desmet (1995). Active control of sound transmission through a double panel partition. *Journal of Sound and Vibration* 180(4), 609–625.
- Sas, P. and L. Van Laere (1988). Principles and applications of active noise cancellation. In *Proceedings of NOISE-CON 88, USA*, pp. 279–284.
- Scheuren, J. (2004). Engineering applications of active sound and vibration control. In *Proceedings of Active 04*, Williamsburg USA, pp. 1–19.
- Schulte-Fortkamp, B. (2008). Vehicle interior noise - a product of interactive expertise. In *Proceedings of NOISE-CON 2008*, 8-30 July, Dearborn USA, pp. 1–6.
- Shin, S. H., J. G. Ih, T. Hashimoto, and S. Hatano (2008). Sound quality evaluation of the booming sensation for passenger cars. *Applied Acoustics*, doi:10.1016/j.apacoust.2008.03.009.
- Simshauser, E. D. and M. E. Hawley (1955). Noise-cancelling headset - an active ear defender. *J. Acoust. Soc. Am.* 27(1), 207.
- Sommerfeldt, S. D. and T. O. Samuels (2001). Incorporation of loudness measures in active noise control. *J. Acoust. Soc. Am.* 109(2), 591–599.
- Sottek, R., W. Krebber, and G. R. Stanley (2005). Tools and methods for product sound design of vehicles. SAE Paper No.2005-01-2513.

- Stallaert, B., G. Pinte, S. Devos, W. Symens, J. Swevers, and P. Sas (2008). Filtered-x LMS vs. repetitive control for active structural acoustic control of periodic disturbances. In *Proceedings of ISMA2008: International Conference on Noise and Vibration Engineering*, Leuven BELGIUM, pp. 79–87.
- Stöbener, U. and L. Gaul (2001). Active vibration control of a car body based in experimentally evaluated modal parameters. *Mechanical Systems and Signal Processing* 15(1), 173–188.
- Sun, X. and G. Meng (2006). LMS algorithm for active noise control with improved gradient estimate. *Mechanical Systems and Signal Processing* 20(2006), 920–938.
- Swevers, J., C. Lauwerys, B. Vandersmissen, M. Maes, K. Reybrouck, and P. Sas (2007). A model-free control structure for the on-line tuning of the semi-active suspension of a passenger car. *Mechanical Systems and Signal Processing* 21(2007), 1422–1436.
- Tomlinson, G. R. (1979). Force distortion in resonance testing of structures with electrodynamic vibration exciters. *Journal of Sound and Vibration* 63(1979), 337–350.
- Tsuge, K., K. Kanamaru, T. Kido, and N. Masuda (1985). A study of noise in vehicle passenger compartment during acceleration. SAE Paper No. 850965.
- Unholtz, K. (1961). *Shock and Vibration Handbook*, Chapter v.2, pp. 25.1–25.74. McGraw-Hill Book Co., New York, , ed.1,.
- Van Amerongen, J. and P. Breedveld (2003). Modelling of physical systems for the design and control of mechatronic systems. *Annual Reviews in Control* 27(2003), 87–117.
- Van Brussel, H., P. Sas, I. Németh, D. P., and P. Van den Braembussche (2001). Towards a mechatronic compiler. *IEEE/ASME Transactions on Mechatronics* 6(1), 90–105.
- Van der Auweraer, H., L. de Oliveira, M. da Silva, S. H. J. Mohring, and A. Deraemaeker (2006). A virtual prototyping approach to the design of smart structures applications. In *Proceedings of ISMA2006: International Conference on Noise and Vibration Engineering*, Leuven BELGIUM, pp. 273–284.

- Van der Auweraer, H., K. Janssens, L. de Oliveira, M. da Silva, and W. Desmet (2007). Virtual prototyping for sound quality design of automobiles. *S V Sound and Vibration* 41(4), 26–31.
- Van der Auweraer, H., M. Tournour, K. Wyckaert, and K. De Langhe (2005). Vibro-acoustic CAE from an industrial application perspective. SAE Paper No. 2005-26-050.
- Van der Auweraer, H. and K. Wyckaert (2004). Sound quality: Perception, analysis and engineering. In *ISAAC 16 - Seminar on Advanced Techniques in Applied and Numerical Acoustics*, Leuven BELGIUM.
- Vandernoot, G., P. Van Der Linden, P. Mas, C. Locqueteau, and E. Leborgne (2008). Predictive modeling of audio quality inside car cabins. In *Proceedings of ISMA2008: International Conference on Noise and Vibration Engineering*, Leuven BELGIUM, pp. 3097–3112.
- Vandeurzen, U. and J. Leuridan (2008). The next revolution in simulation, beyond 3D CAE: the multi-functional system mock-up redefines the product development process. In *The International LMS Engineering Simulation Conference 2008*, Paris FRANCE.
- Varoto, P. S. and L. P. R. de Oliveira (2002a). Interaction between a vibration exciter and the structure under test. *S V Sound and Vibration* 3(10), 20–26.
- Varoto, P. S. and L. P. R. de Oliveira (2002b). On the force drop-off phenomenon in shaker testing in experimental modal analysis. *Journal of Shock and Vibration* 9, 165–175.
- Vastfjäll, D., M. A. Gulböl, M. Kleiner, and T. Garling (2002). Affective evaluation of and reactions to exterior and interior vehicle auditory quality. *Journal of Sound and Vibration* 255(3), 501–518.
- Whitten, R. P. (1972). Community response to aircraft noise. In *Proceedings of the IEEE Electronics and Aerospace Systems Convention 72*, Washington DC, USA, pp. 180–183.
- Williams, J. S. and G. C. Steyer (1995). Experimental noise path analysis for problem identification in automobiles. In *Proceedings of the 13 International Modal Analysis Conference - IMAC XIII*, Nashville USA, pp. 442–447.

- Williams, R., M. Allman-Ward, P. Jennings, and M. Batel (2007). Using an interactive NVH simulator to compute and understand customer opinions about vehicle sound quality. SAE Paper No.2007-26-036.
- Xianmin, Z., L. Jianwei, and S. Yunwen (2007). Simultaneous optimal structure and control design of flexible linkage mechanism for noise attenuation. *Journal of Sound and Vibration* 299(2007), 1124–1133.
- Zhou, Y. L., Q. Z. Zhang, X. D. Li, and W. S. Gan (2008). On the use of an spsa-based model-free feedback controller in active noise control for periodic disturbances in a duct. *Journal of Sound and Vibration* 317(3-5), 456–472.
- Zwicker, E. and H. Fastl (1999). *Psychoacoustics: Facts and Models*. HeidelbergGermany: Springer-Verlag.

Curriculum Vitae

Personal data

Leopoldo Pisanelli Rodrigues de Oliveira, *Prof.Dr.*

Address: Departamento de Engenharia Mecânica
Escola de Engenharia de São Carlos - USP
Av. Trabalhador Sancarlense, 400
13566-590 São Carlos - SP, Brazil

E-mail: leopro@sc.usp.br

Place and date of birth: São Carlos, August 3rd 1977

Nationality: Brazilian

Education

- **2004-2008:** Ph.D. student at the Department of Mechanical Engineering, Katholieke Universiteit Leuven; funded by KU Leuven.
- **March 2007:** Doctoral degree in Mechanical Engineering, Engineering School of São Carlos - University of São Paulo, Brazil.
OLIVEIRA, L.P.R., (2007). Active noise control in vehicles and its impact on sound quality, Doctoral Thesis, EESC-USP, 162p.
- **April 2003:** Masters degree in Mechanical Engineering, Engineering School of São Carlos - University of São Paulo, Brazil.
OLIVEIRA, L.P.R., (2003). The interaction between electrodynamic shakers and the structure under test in multiple excitation tests, Master Thesis, EESC-USP, 112p.
- **1996-2000:** degree in Mechanical Engineering from the Department of Mechanical Engineering, University of São Paulo, Brazil.
- **1993-1995:** High-school: Colégio Nossa Senhora Auxiliadora, Ribeirão Preto-SP, Brazil.

List of publications

International peer reviewed journal articles

- [1] L.P.R. de Oliveira, B. Stallaert, K. Janssens, H. Van der Auweraer, P. Sas, W. Desmet, “NEX-LMS: a novel adaptive control scheme for sound quality control”, *Mechanical Systems and Signal Processing*, Under Review.
- [2] L.P.R. de Oliveira, P.S. Varoto, P. Sas, W. Desmet, “A state-space modelling approach for active structural acoustic control”, *Journal of Shock and Vibration*, In Press.
- [3] L.P.R. de Oliveira, K. Janssens, H. Van der Auweraer, P.S. Varoto, P. Sas, W. Desmet, “Active Sound Quality Control of Engine Cavity Noise”, *Mechanical Systems and Signal Processing*, doi:10.1016/j.ymssp.2008.04.005.
- [4] L.P.R. de Oliveira, P. Sas, W. Desmet, K. Janssens, P. Gajdatsy, H. Van der Auweraer, “Active control of engine noise transmitted into cavities: simulation, experimental validation and sound quality assessment”, *J. Acoust. Soc. Am.*, Vol.123, No.5, Pt.2, pp.3872, (2008).
- [5] L.P.R. de Oliveira, M.M. da Silva, P. Sas, W. Desmet and H. Van Brussel, “Concurrent mechatronic design approach for active control of cavity noise”, *Journal of Sound and Vibration (JSV)*, 314 (2008) 507-525.
- [6] L.P.R. de Oliveira, B. Stallaert, P. Sas, “Optimisation strategies for decentralized ASAC”, *Journal of the European Acoustic Association (EAA) - International Journal on Acoustics, Acta Acustica united with Acustica*, Vol. 91 (Suppl. 1), pp.S60, (2005).

- [7] H. Van der Auweraer, K. Janssens, L.P.R. de Oliveira, M.M. da Silva and W. Desmet, "Virtual prototyping for sound quality design of automobiles", *S V Sound and Vibration* 41(4), 26-30, (2007).
- [8] P.S. Varoto, L.P.R. Oliveira, "On the force drop off phenomenon in shaker testing in experimental modal analysis", *Shock and Vibration* 9 (4-5 SPEC.), 165-175, (2002).
- [9] P.S. Varoto, L.P.R. Oliveira, "Interaction Between a Vibration Exciter and the Structure Under Test", *S V Sound and Vibration* 36 (10), 20-26, (2002).
- [10] L.P.R. Oliveira, W.L. Marar, "Geometria de mecanismos", *Revista de Iniciação Científica da USP*, v.2, p.49-52, (2000).

Full papers in proceedings of international conferences

- [1] L.P.R. de Oliveira, W. Desmet, P. Sas, K. Janssens, H. Van der Auweraer, "Adaptive control schemes for engine sound quality improvement", *International Conference on Noise and Vibration Engineering - ISMA 2008*, p.3085-3096., Leuven - Belgium, (2008).
- [2] L.P.R. de Oliveira, P. Sas, W. Desmet, K. Janssens, P. Gajdatsy, H. Van der Auweraer, "Active control of engine noise transmitted into cavities: simulation, experimental validation and sound quality assessment", *Proceedings of Acoustics'08*, 10pp., Paris - France, (2008).
- [3] L.P.R. de Oliveira, P. Sas, W. Desmet, K. Janssens, P. Gajdatsy, H. Van der Auweraer, "Active sound quality control of engine noise transmitted into cavities", *ASME Sound Quality Symposium - SQS 2008*, 10pp., Dearborn, Michigan, July 31, (2008).
- [4] F. Haase, M. Kauba, D. Mayer, H. van der Auweraer, Peter G., L.P.R. de Oliveira, M.M. da Silva, P. Sas, A. Deraemaeker, "Active Vibration Control of an Automotive Firewall for Interior Noise Reduction", *Adaptronic Congress 2008*, 8pp., Berlin - Germany, 20 - 21 May (2008).

- [5] T. Cardone, R. d'Ippolito, S. Donders, H. Van der Auweraer, L.P.R. de Oliveira, M.M. da Silva, "Robustness Assessment and Optimization of a Simplified Smart Structure Model for Structural Acoustic Control", *Proceedings of the Leuven Symposium on Applied Mechanics in Engineering - LSAME.08*, 12pp., Leuven - Belgium (2008).
- [6] L.P.R. Oliveira, P.S Varoto, P. Sas, W. Desmet, P. Mas, H. Van der Auweraer, "The Impact of Active Noise Control on the Perceived Sound Quality", *Proceedings of the 19th International Congress of Mechanical Engineering - COBEM 2007*, 10pp., Brasilia - Brazil, (2007).
- [7] H. Van der Auweraer, K. Janssens, A. Vecchio, L.P.R. de Oliveira, M.M. da Silva, W. Desmet, "Optimisation of ANVC Systems Design Using an Integrated Simulation Approach", *Proceedings of the Adaptronic Congress 2007*, 10pp., Gttingen - Germany, 23-24 May, (2007).
- [8] H. Van der Auweraer, P. Mas, L.P.R. de Oliveira, M.M. da Silva and W. Desmet, "Simulation-Based Optimization of an Active Noise and Vibration Control Solution", *Proceedings of IMAC XXV, Orlando, (Florida, USA)*, 10pp., February 19-22, (2007).
- [9] L.P.R. Oliveira, P.S. Varoto, P. Sas, W. Desmet, "A state-space approach for ASAC simulation", *Proceedings of the XII International Symposium on Dynamic Problems of Mechanics - DINAME 2007*, 10pp., Ilhabela-SP, Brazil, (2007).
- [10] H. Van der Auweraer, P. Mas, P. Segaert, L.P.R. de Oliveira, M.M. da Silva and W. Desmet, "CAE-based Design of Active Noise Control Solutions", *Proceedings of 10th Symposium on International Automotive Technology - SIAT 2007, Pune (India)*, SAE Paper No. 2007-26-032, January 17-20, (2007).
- [11] H. Van der Auweraer, S. Herold, J. Mohring, L. de Oliveira, M. da Silva and A. Deraemaeker, "CAE approach to the design of smart structures applications", *Proceedings of the 6th European Conference on Noise Control - EURONOISE 2006, Tampere (Finland)*, p.1-6, May 10 - June 1, (2006).

- [12] H. Van der Auweraer, S. Herold, J. Mohring, L. de Oliveira, M. da Silva and G. Pinte, "Virtual prototyping of active noise and vibration solutions", *Proceedings of the Transportation Research Arena - TRA 2006, Göteborg (Sweden)*, p.1-10, June 12-16, (2006).
- [13] L.P.R Oliveira, A. Deraemareker, J. Mohing, W. Desmet, P. Sas, "A CAE modeling approach for the analysis of vibroacoustic systems with distributed ASAC control", *Proceedings of the International Conference on Noise and Vibration Engineering - ISMA 2006*, p.321-336., September 18-20, Leuven - Belgium, (2006).
- [14] H. Van der Auweraer, L. de Oliveira, M. da Silva, S. Herold, J. Mohring and A. Deraemaeker, "A virtual prototyping approach to the design of smart structures applications", *Proceedings of the International Conference on Noise and Vibration Engineering - ISMA 2006, Leuven (Belgium)*, p.273-284., September 18-20, Leuven - Belgium, (2006).
- [15] H. Van der Auweraer, K. Janssens, L. de Oliveira, M. da Silva and W. Desmet, "Sound synthesis approach for sound quality design of ANVC applications", *Proceedings of the 35th International Congress and Exposition on Noise Control Engineering - INTERNOISE 2006, Honolulu (Hawaii, USA)*, p.1-10., December 3-6, (2006).
- [16] P.S. Varoto, M. Lofrano, T.R. Cicogna, L.P.R. Oliveira, K.G. McConnell, "Moment mobility FRF measurement techniques", *Proceedings of IMAC-XXIV*, p.371-383., St. Louis, Missouri-USA, (2006).
- [17] L.P.R. Oliveira, B. Stallaert, W. Desmet, J. Swevers, P. Sas, "Optimisation Strategies for Decentralized ASAC", *Proceedings of Forum Acusticum 2005*, p.875-880., Budapest - Hungary, (2005).
- [18] P.G.B. Nbrega, J.B. Hanai, L.P.R. Oliveira, M.A. Ferreira, P.S. Varoto, "Dynamic experimental investigation of column base connections for precast concrete structures", *Proceedings of IV International ACI/CANMET Conferende on Quality of Concrete Structures and Recent Advances in Concrete Material and Testing, ISBN 85-98576-08-5*, p.524-539., September 6-7, Olinda - Brazil, (2005).

- [19] L.P.R. Oliveira, P.S. Varoto, "Improving data quality in shaker testing", *Proceedings of X International Symposium on Dynamic Problems of Mechanics - DINAME 2003*, p.135-140., Ubatuba - Brazil, (2003).
- [20] L.P.R. Oliveira, M.M. da Silva and P.S. Varoto, "Experimental Modal Analysis Approaches for High Quality Tests", *Proceedings of SAE Congress Brazil, São Paulo (Brazil)*, SP. SAE Paper 2003-01-3679, (2003).
- [21] M.M. da Silva, L.P.R. Oliveira, L.G.S. Ericsson, A. Costa Neto and P.S. Varoto, "An experimental investigation on the modal characteristics of an off-road competition vehicle chassis", *Proceedings of SAE Congress Brazil, São Paulo (Brazil)*, SAE Paper 2003-01-3689., (2003).
- [22] P. S. Varoto, L.P.R. Oliveira, "Interao entre mecanismos de excitao e a estrutura sob estudo em anlise modal experimental", *Série Arquimedes: Anais do DINCON 2003*, v. 2, p.2174-2199., São José dos Campos - SP, Brasil, (2003).
- [23] M.M. da Silva, L.P.R. Oliveira, L.G.S. Ericsson, A. Costa Neto and P.S. Varoto, "An experimental investigation on the modal characteristics of an off-road competition vehicle chassis", *Proceedings of the XXIV CILAMCE - CILAMCE 2003, Ouro Preto (Brazil)*, p.1-10., October 29-31, Ouro Preto - Brazil, (2003).
- [24] C.M. Barbieri, L.P.R. Oliveira, J.M. Alves, P.S. Varoto, "Assessment of fracture healing using vibration analysis: a sheep animal model", *Proceedings of EMBEC'02 - 2nd European Medical and Biological Engineering Conference*, 5pp., Vienna - Austria, (2002).
- [25] L.P.R. Oliveira, P.S. Varoto, M. Lofrano, "Techniques for the estimation of the angular FRF in modal testing", *Proceedings of International Conference on Structural Dynamic Modelling*, v.1, 10pp., Funchal - Portugal, (2002).
- [26] L.P.R. Oliveira, P.S. Varoto, "The Effects of Armature Rotation on Data Quality in Base Driven Shaker Testing", *Proceedings of*

- the International Conference on Noise and Vibration Engineering - ISMA 27*, p.911-918., September 16-18, Leuven - Belgium, (2002).
- [27] W.F. Mamed, P.S. Varoto, L.P.R. Oliveira, "Vibroacoustic modal testing of a vehicle cabin", *Proceedings of the International Conference on Noise and Vibration Engineering - ISMA 27*, p.2085-2092., September 16-18, Leuven - Belgium, (2002).
- [28] W.F. Mamed, L.P.R. Oliveira, P.S. Varoto, "On the identification of acoustic modal and response mode for reactive filters", *Proceedings of II Congresso Nacional de Engenharia Mecânica - CONEM2002*, 10pp, João Pessoa - Brasil, (2002).
- [29] L.P.R. Oliveira, M. Lofrano, P.S. Varoto, "On the estimation of angular FRF in modal testing", *Proceedings of II Congresso Nacional de Engenharia Mecânica - CONEM2002*, 10pp., João Pessoa - Brasil, (2002).
- [30] F.D. Marques, P.S. Varoto, G.R. Benini, L.P.R. Oliveira, "An Investigation on the Modal Characteristics of an Aircraft Wing Structure", *Proceedings of the IX International Symposium on Dynamic Problems of Mechanics - DINAME 2001*, v.9, p.465-469., Florianópolis - Brasil, (2001).
- [31] P.S. Varoto, L.P.R. Oliveira, "On the force drop off phenomenon in shaker testing in experimental modal analysis", *Proceedings of XVI Congresso Brasileiro de Engenharia Mecânica - COBEM 2001*, p.249-258., Uberlândia-MG, Brazil, (2001).
- [32] P.S. Varoto, L.P.R. Oliveira, "On the interaction between the vibration exciter and the structure under test in vibration testing", *Proceedings of XIX International Modal Analysis Conference - IMAC2001*, p.640-647., Kissimmee USA, (2001).